

EXAMINATION OF DNA METHYLATION AND CHROMATIN
STRUCTURE AT THE HUMAN HYPOXANTHINE
PHOSPHORIBOSYLTRANSFERASE LOCUS

By

CHIEN CHEN

A DISSERTATION PRESENTED TO THE GRADUATE SCHOOL OF THE
UNIVERSITY OF FLORIDA IN PARTIAL FULFILLMENT OF THE
REQUIREMENTS FOR THE DEGREE OF DOCTOR OF PHILOSOPHY

UNIVERSITY OF FLORIDA
2000

ACKNOWLEDGEMENTS

The work described in this dissertation was performed in the laboratory of Dr. Thomas P. Yang at the University of Florida, College of Medicine. I would like to thank Dr. Yang for his advice and support in this endeavor, both scientific and otherwise. I would also like to thank the members of my thesis committee, Dr. Henry Baker, Dr. Rob Ferl, Dr. Michael Kilberg and Dr. Philip Laipis, for their advice and suggestions with regard to the experiments described herein and also for their advice about graduate education in general. In addition, I would like to thank Dr. Jorg Bungert for his generous contribution of materials for the *in vitro* chromatin reconstitution assays and for his technical advice with regard to these experiments. I would like to thank Kelly Leach in the Bungert lab for substantial assistance with the protocol for *in vitro* reconstitution of chromatin templates. I would like to thank all the members of the Yang lab both past and present for their scientific advice and moral support over these many years, particularly Dr. Michael Litt, Sue Lee Kang, Daniel Catalaa and Dr. Jyoti Khadake. Last but not least, I would like to thank my parents, Tsong Yuan Chen and Shu Mei Chen, and my siblings, Don Hui Chen and Hou Chen, for their love and support, which has allowed me to focus on this endeavor.

TABLE OF CONTENTS

ACKNOWLEDGEMENT.....	ii
ABSTRACT.....	v
CHAPTERS	
1. REVIEW OF LITERATURE.....	1
The Human Hypoxanthine Phosphoribosyltransferase Gene.....	1
X Chromosome Inactivation.....	2
DNA Methylation in Mammals.....	13
Chromatin Structure.....	24
2. MATERIALS AND METHODS.....	28
Cell Lines.....	28
5-aza-deoxycytidine (5aCdr) Treatment and Isolation of Single Cell-Derived Clones.....	28
5-aza-deoxycytidine Reactivation Studies.....	29
Trichostatin A (TSA) Treatment of Cells.....	30
Genomic DNA Preparation.....	30
RNA Preparation.....	31
Detection of <i>HPRT</i> mRNA by Reverse Transcriptase PCR (RT-PCR).....	32
Hydrazine Treatment of DNA for Methylation Analysis.....	32
<i>In Vivo</i> DNase I Treatment of Cells for DNase I <i>in vivo</i> Footprinting.....	33
<i>In Vitro</i> DNase I treatment of naked DNA.....	34
LMPCR amplification.....	34
Single-Stranded Probe Synthesis for LMPCR analysis.....	39
<i>In Vivo</i> DNase I Treatment of Cells for DNase I General Sensitivity and Hypersensitivity Analysis.....	40
MNase Treatment of Cells <i>In Vivo</i>	41
MNase Treatment of Genomic DNA <i>In Vitro</i>	41
Southern Blot Analysis of the <i>HPRT</i> Promoter by Indirect End-labeling...	42
Probe Synthesis by Random Priming.....	43
DNA Methylation of Plasmid Templates <i>In Vitro</i>	43
Reconstitution of Nucleosomes onto the <i>HPRT</i> Promoter <i>In Vitro</i>	44
Assessment of Translational Phasing of Nucleosomes on <i>In Vitro</i> Reconstituted Chromatin by MNase Digestion and Southern Analysis.....	45

3. EVIDENCE THAT SILENCING OF THE <i>HPRT</i> PROMOTER BY DNA METHYLATION IS MEDIATED BY CRITICAL CPG SITES.....	47
Introduction.....	47
Results.....	49
Discussion.....	67
4. EXAMINATION OF THE TRANSLATIONAL AND ROTATIONAL POSITIONING OF NUCLEOSOMES ON THE ACTIVE AND INACTIVE <i>HPRT</i> PROMOTER.....	72
Introduction.....	72
Results.....	73
Discussion.....	96
5. CONCLUSIONS AND FUTURE DIRECTIONS.....	107
Summary of the Methylation Analysis of the <i>HPRT</i> Promoter.....	107
Future Studies on DNA Methylation at the <i>HPRT</i> Gene.....	108
Summary of Nucleosome Phasing at the <i>HPRT</i> Promoter <i>In Vivo</i>	111
Future Studies to Examine the Role of Nucleosomal Organization in the Transcriptional Regulation of the <i>HPRT</i> Gene.....	112
APPENDIX A METHYLATION PATTERNS OF EACH OF THE 61 CLONES THAT FAILED TO REACTIVATE THE <i>HPRT</i> GENE AFTER 5ACDR TREATMENT.....	115
Methylation Pattern of the Upper Strand.....	116
Methylation Pattern of the Lower Strand.....	120
APPENDIX B ADDITIONAL PROTOCOLS.....	124
Assessment of Rotational Phasing on <i>In Vitro</i> Reconstituted Chromatin by High-Resolution DNase I Cleavage Analysis.....	124
Small Scale Preparation of BAC DNA.....	125
Large Scale Preparation of BAC DNA.....	126
REFERENCES.....	128
BIOGRAPHICAL SKETCH.....	147

Abstract of Dissertation Presented to the Graduate School of the University of Florida in
Partial Fulfillment of the Requirements for the Degree of Doctor of Philosophy

EXAMINATION OF DNA METHYLATION AND CHROMATIN STRUCTURE AT
THE HUMAN HYPOXANTHINE PHOSPHORIBOSYLTRANSFERASE LOCUS

By

Chien Chen

December 2000

Chair: Thomas P. Yang

Major Department: Biochemistry and Molecular Biology

X chromosome inactivation mediates the differential expression of genes on the active and inactive X chromosomes in each female somatic cell. To understand the mechanisms that maintain X chromosome inactivation, I have examined the role that DNA methylation and chromatin structure in the promoter play in the transcriptional repression of the human hypoxanthine phosphoribosyltransferase gene (*HPRT*). Transcriptional repression of the *HPRT* gene strongly correlates with methylation at 3 critical sites near the major transcription initiation sites of the promoter. Partial promoter demethylation at non-critical sites does not increase the *HPRT* reactivation frequency of clones re-treated with the demethylating agent, 5-aza-deoxycytidine, suggesting that critical site methylation contributes disproportionately to transcriptional silencing. Direct inhibition of transcription factor binding is unlikely to be primarily responsible for this repression since the critical methylation sites do not coincide with transcription factor binding sites identified by either DNase I or DMS *in vivo* footprinting. Histone

deacetylation is also unlikely to be the principal mechanism of methylation-mediated transcriptional repression since trichostatin A treatment does not reactivate the inactive *HPRT* allele, even when the promoter is partially demethylated. However, differential methylation may mediate the differential chromatin structure of the promoter between the active and inactive *HPRT* alleles. The active *HPRT* promoter is assembled into an array of translationally phased nucleosomes, which is interrupted over approximately 350 bp including the minimal promoter, the multiple transcription initiation sites and all of the transcription factor binding sites identified by *in vivo* footprinting. This 350 bp region appears devoid of nucleosomes based on its hypersensitivity to both DNase I and MNase and the similarity of its high-resolution DNase I cleavage pattern to naked DNA. In contrast, the inactive *HPRT* promoter is assembled into randomly positioned nucleosomes that are rotationally phased over at least 210 bp covering a cluster of 5 GC boxes and the multiple transcription initiation sites. The potential role of methylation in determining the rotational orientation of nucleosomes and the effect of rotational phasing on transcription are discussed.

CHAPTER 1 REVIEW OF LITERATURE

To better understand the mechanisms involved in maintaining transcriptional silencing of the human hypoxanthine phosphoribosyltransferase gene on the inactive X chromosome, I have examined the roles of DNA methylation and chromatin structure in this process. To provide a sufficient background for this discussion, I present a brief overview of the current literature regarding the human hypoxanthine phosphoribosyltransferase gene, X chromosome inactivation, DNA methylation, and chromatin structure.

The Human Hypoxanthine Phosphoribosyltransferase Gene

The human hypoxanthine phosphoribosyltransferase gene (*HPRT*) encodes a protein involved in the salvage pathway of guanine and hypoxanthine nitrogen bases. A defect in this protein results in Lesch Nyhans syndrome in males and, sometimes, gouty arthritis in females (107). The *HPRT* gene is located at Xq26.1 - q26.2 on the human X chromosome and is subject to X inactivation. It spans approximately 42 Kb and is split into 9 exons. It is constitutively expressed in all tissues although its expression is highest in the brain. Like other “housekeeping” genes, it has a TATA-less promoter that is GC rich and contains several consensus binding sites for the transcription factor Sp1. Like many genes with TATA-less promoters, the *HPRT* gene has multiple sites of transcription initiation (93, 151). The active and inactive alleles of the *HPRT* gene, on the

active and inactive X-chromosomes respectively, exhibit several differences. Differential methylation is observed, with the promoter of the active allele completely unmethylated whereas the promoter of the inactive allele is densely methylated except at the 5 consensus Sp1 binding sites that are unmethylated on both active and inactive alleles (75). Also, the active and inactive alleles of the *HPRT* gene exhibit differential accessibility as determined by DNase I general sensitivity (117) and differential factor binding as determined by dimethyl sulfate *in vivo* footprinting (77). The active allele is more accessible and binds transcription factors *in vivo* whereas the inactive allele is relatively more inaccessible and is devoid of transcription factor binding. The *HPRT* gene is a convenient model system for examining the maintenance of X chromosome inactivation because its expression can be either selected for or against in cell culture using HAT (hypoxanthine, aminopterin, thymidine) or 6-thioguanine (2-amino-6-mercaptopurine) respectively.

X Chromosome Inactivation

X chromosome inactivation is the mechanism by which eutherian mammals compensate for the dosage imbalance of genes on the X chromosome between males, which have a single X chromosome, and females, which have two X chromosomes. During X chromosome inactivation, one of the two X chromosomes in each female somatic cell is randomly chosen for transcriptional silencing, resulting in a single active X chromosome in each cell (126). Prior to X inactivation, genes on both female X-chromosomes are expressed (51). However, early in embryogenesis, at about 5.5 d.p.c. (days post coitum) in mice, X chromosome inactivation initiates in the embryo proper, as

marked by a drop in the expression of various X-linked genes. By 10.5 d.p.c., all somatic tissues have completed X inactivation (188). As a result female mammals are chimeric with respect to the expression of genes on the X chromosome (126).

The process of X chromosome inactivation may be subdivided into 3 distinct steps: initiation, spreading and maintenance (70). Initiation involves three distinct processes, counting, choosing and silencing. Counting is the process by which the cell determines how many X-chromosomes are present and compares it to the ploidy of the cell. For each diploid genome, one X chromosome remains active while all other X-chromosomes are inactivated (62). It is unclear how counting occurs but it is thought to require both an X-linked and an autosomal component (135). Once the cell has determined how many X-chromosomes should remain active, it has to choose which X chromosome(s) to keep active (62). While choosing is typically random in normal somatic cells, in mice a region known as the Xce can modify the probability of a X chromosome being chosen. The relative “strength” of the individual Xce alleles on each X chromosome determines the level of skewing of X chromosome inactivation in cis (3). No equivalent region has been identified in humans. After the active X chromosome is chosen, all other X-chromosomes in each cell must be silenced. Although these processes are closely interrelated, they are genetically distinct.

X chromosome inactivation is thought to initiate at the X inactivation center (XIC) located at Xq13.2, based on translocation studies (30). In addition to being required for silencing, the XIC is thought to contain the X-linked components of both counting and choosing since ring X-chromosomes lacking the XIC are neither counted nor inactivated (41, 136, 209). A gene known as the X inactive specific transcript or *XIST*

has been identified within the minimal XIC and is thought to be a vital silencing component of the XIC. *XIST/Xist* is the only gene known that is expressed exclusively from the inactive X chromosome in somatic cells (25, 28). It encodes a transcript that has several unusual properties. The *XIST/Xist* RNA is very large (approximately 17kb and 15kb respectively (26, 29)), has no extended conserved open reading frame and is not thought to be translated or to leave the nucleus. In interphase somatic cells, *XIST/Xist* RNA is found coating the inactive X chromosome (25, 29). Prior to X inactivation, an unstable *Xist* transcript is expressed and localized in cis to the XIC on both X-chromosomes. During X chromosome inactivation, a stable transcript accumulates in cis on the inactive X-chromosome but not on the active X chromosome, which eventually ceases to express *Xist* altogether (84). The accumulation of *Xist* on the inactive X chromosome, which is thought to mediate the initiation and spreading of X inactivation in early embryogenesis, involves transcript stabilization rather than differential transcription of the two alleles (180). Consistent with the idea that *Xist* stabilization is responsible for X inactivation, Wutz and Jaenisch (212) have recently shown that induction of a inducible transgenic *Xist* RNA which, unlike endogenous *Xist*, is stable in undifferentiated cells results in untimely X inactivation and cell death.

It has been suggested that promoter switching at the *Xist* locus from the P0 promoter, which generates an “unstable” transcript, to the P1 promoter, which generates a “stable” transcript, mediates *Xist* RNA stabilization and is therefore responsible for initiating X chromosome inactivation (180). However, this hypothesis is controversial. Warshawky et al. have recently shown that the putative “stable” promoter P1 can initiate transcription of *Xist* in both differentiated and undifferentiated cells. Furthermore, the P1-

initiated transcript is unstable in undifferentiated cells but stable in differentiated cells (204). In addition, a transgene carrying the “stable” P1 promoter but lacking the “unstable” P0 promoter is capable of initiating inactivation (105). Interestingly, Warshawsky et al. were unable to find the P0 initiated transcript and argue that it is an artifact of an antisense transcript, *Tsix* (204).

The *Xist* locus appears to be a necessary cis silencing component of the XIC. Knockout of the mouse *Xist* gene on one X chromosome results in failure to initiate X chromosome inactivation in cis (129, 157). Conversely, ectopic expression of *Xist* transgenes confers inactive X-chromosome-like properties to autosomes in cis (71, 103, 105, 106). However, while *Xist* expression and stabilization in cis are thought to be necessary for X inactivation, they are apparently not sufficient. Clemson et al. (39) have recently demonstrated that stabilization and localization of *Xist* RNA on the active mouse X chromosome by 5-aza-cytidine reactivation is not sufficient to inactivate the X chromosome. This suggests that an unidentified developmentally regulated factor expressed in early embryogenesis is required to mediate X inactivation by *Xist* stabilization. The window during which *Xist* stabilization can mediate X inactivation appears to be quite short. Wutz and Jaenisch have shown that an inducible *Xist* transgene can only induce X inactivation during ES cell differentiation (212). Within 4 days of differentiation, induction of the transgene could not cause X inactivation as measured by cell death. Clemson et al. (39) have also shown an uncoupling of *Xist* stabilization and localization in mouse/human hybrids. Since *XIST* RNA is stable but its localization is aberrant in rodent/human hybrid cell lines, *XIST* localization apparently requires a

species-specific autosomal factor(s) which is different from that necessary for stabilization.

In addition to silencing, *XIST/Xist* also appears to be involved in the choice component of X chromosome inactivation. Plenge et al. have identified in the human *XIST* promoter a point mutation that dramatically skews X chromosome inactivation in favor of inactivating the mutant allele (163). Surprisingly, the expression of *XIST* is actually lower on the mutant allele, suggesting that this preferential inactivation is not directly related to higher *XIST* expression. Consistent with *Xist* having a role in choosing, the skewing observed in heterozygous mice with a knockout of the *Xist* gene on one X chromosome arises from primary nonrandom X chromosome inactivation of the normal X chromosome. Since the mutant X chromosome is preferentially chosen to remain active, *Xist* appears to have a negative influence on choice (128). This is in distinct contrast to Searles translocation mice where choice of X inactivation is largely random and the observed skewing in somatic tissues is the result of cell death in those cells that inactivate the translocated chromosome.

Recently, another component of choosing in the XIC was identified. This component, *Tsix*, is an anti-sense transcript of *Xist* (102). This anti-sense transcript initiates approximately 14kb downstream of *Xist* within a CpG island whose differential methylation has been linked to the different Xce alleles (44), suggesting that *Tsix* may be functionally involved in the Xce. Like the *Xist* RNA, the *Tsix* RNA is localized to the nucleus. However, unlike *Xist*, *Tsix* RNA does not coat the inactive X chromosome and is found associated only with the XIC. *Tsix* is expressed biallelically at low levels prior to X inactivation but during X inactivation it shows a reverse expression pattern as compared

to *Xist*; its expression continues on the active X chromosome but is silenced on the inactive X chromosome. These characteristics are consistent with *Tsix* playing a positive role in choosing, a hypothesis supported by the genetic data. Knockout of *Tsix* expression on one X chromosome results in complete skewing of inactivation to the deleted chromosome by primary nonrandom X chromosome inactivation (104). This suggests that *Tsix* expression is required for an X chromosome to be chosen. This result is reiterated in a 65kb deletion immediately downstream of *Xist* that also results in complete skewing of inactivation to the deleted allele (40). Taken together, these observations strongly implicate *Tsix* as a positive choosing component of X inactivation, but they also indicate that *Tsix* is not a component of silencing since X inactivation occurs on the X chromosome with the deleted *Tsix* allele (104). Instead, it has been suggested that X chromosome choosing, at least in mice, is determined by an as yet undetermined interaction between the positive and negative effects of *Tsix* and *Xist* respectively, which determines the level of stable *Xist* RNA. Both RNA duplex destabilization and transcriptional interference by *Tsix* transcription have been proposed as possible mechanisms by which *Tsix* modulates *Xist* levels (102, 104).

Neither *Xist* nor *Tsix* appear to be involved in the counting mechanism of X inactivation. This is evident since mice heterozygous for the *Xist* knockout still undergo X inactivation and therefore count both X chromosomes even though one does not have a functional *Xist* allele (129, 157). Similarly, knockout of *Tsix* results in skewed inactivation rather than outright failure of X inactivation so both X chromosomes are counted (104). In contrast, ring X-chromosomes and translocation fragments lacking the

XIC are not counted and not inactivated, leading to severe phenotypes since both the normal and ring chromosomes remain active (41, 136, 209).

After X inactivation initiates, it is thought to spread bi-directionally along the length of the X chromosome. It is unclear whether this silencing is continuous or discrete since some genes escape X chromosome inactivation (46). However, recent evidence suggests that genes which escape inactivation may actually inactivate during the initial spreading of X chromosome inactivation and then reactivate (118). Interestingly, in the mouse, the distribution of *Xist* along the inactive X chromosome is discontinuous and appears to be localized primarily to coding DNA (48). However, it is unclear if this reflects the initial distribution of *Xist* during spreading or is simply the maintenance pattern. Spreading of inactivation into autosomes in both X:autosome translocations and by *Xist* transgenes is both incomplete and variable (48, 103, 170-172, 206). This suggests that X chromosomal material somehow favors spreading of inactivation as compared to autosomal material. To explain this phenomenon, Gartler and Riggs have proposed a “way station” model which suggests that the inactivation signal must be periodically “boosted” as it travels down the chromosome (55). These “way stations” are hypothesized to be more prevalent on the X chromosome than on autosomes. Work by White et al. suggests that these “way stations” might be sites of strong *Xist* RNP interaction (206) and Lyon (127) has suggested that they might be long interspersed DNA sequence elements or LINES, which are on all chromosomes but enriched on the X chromosome. Goldman et al. have proposed that these “way stations” may in fact be inactivation signals for chromatin domains on the X chromosome, and that those genes that escape X inactivation do so because their domains lack such a signal (61). Likewise,

domains on autosomes would not consistently harbor such an inactivation signal (53). However since spreading can occur into autosomes, the actual mechanisms of transcriptional silencing by X activation are not unique to the X chromosome.

Once X inactivation is complete, each X chromosome maintains its transcriptional status in all somatic cell progeny. While the mechanisms involved in this maintenance are still unclear, maintenance does not require the *XIST* gene product (31). Several of the differences observed between the active and inactive X-chromosomes suggest possible mechanisms of maintenance, including differential chromatin structure, replication timing, histone acetylation, and DNA methylation (70). Differential chromatin structure was one of the earliest identified differences between the active and inactive X chromosome. In 1961 Barr and Carr made the association between a cytologically distinct dense nuclear heterochromatic body, subsequently known as the Barr body, and the inactive X chromosome (4). Aside from this morphological difference, further evidence has accumulated that this Barr body is different from the active X chromosome in both composition and structure. In addition to the accumulation of *XIST/Xist* on the inactive human X chromosome (25, 29), macroH2A (43, 133) has been shown to be significantly enriched on the inactive X, as have various hypoacetylated histone species (9, 82). In addition, examination of the nuclease sensitivity of various X-linked genes has clearly demonstrated a reduced accessibility of inactive X-linked genes as compared to their active counterparts (117, 158, 213). Since the two X chromosomes in each female cell reside in the same nuclear environment, and are therefore exposed to the same transcription factors, the differential accessibility of the active vs. inactive X chromosomes may play a vital role in their differential transcription.

Late replication timing is a hallmark of the inactive X chromosome, which is the last chromosome to enter replication (176). This differential replication timing is also one of the earliest developmental characteristics of the inactive X chromosome and occurs coincident with the accumulation of *Xist* on the inactive X chromosome and the transcriptional silencing of various X-linked genes by X inactivation (90, 187). Furthermore, late replication of the inactive X chromosome is conserved among all mammals including marsupials and egg laying mammals, suggesting that it may be part of the ancestral mechanism of X inactivation (131). It has been suggested that late replication timing might deprive the late replicating chromatin of cell cycle-specific factors which mark transcriptionally active chromatin (135). Thus late replication timing may not only distinguish the inactive X chromosome but may actually have a functional role in maintaining its inactivity. However, initiation of inactivation by late replication is unlikely because aberrant inactivation by a stable transgenic *Xist* transcript in undifferentiated cells results in inactivation but not a shift to late replication. Nevertheless, the shift from reversible to irreversible X inactivation does correlate quite tightly with the appearance of late replication on the inactive X chromosome, indicating that it may be the first mechanism of maintenance (212). Examination of individual genes on the X chromosome shows a consistent correlation between transcription and replication timing; the genes that escape inactivation replicate synchronously on both chromosomes while the genes subject to X inactivation replicate late on the inactive X chromosome (reviewed by Heard et al. (70)). The late replication timing of the inactive X chromosome is significant because late replication is a general characteristic of inactive chromatin (68, 191). Therefore, the mechanisms responsible for late replication of the

inactive X chromosome may be directly involved in its silencing. Reactivation studies with 5-aza-deoxycytidine have suggested that DNA methylation may be involved in this maintenance process (68, 80).

Histone hypoacetylation is also a general characteristic of the inactive X chromosome as well as a general marker of transcriptional inactivity (9, 82). Recently, Gilbert and Sharp (57) have refined the localization of hypoacetylated histones in the inactive X chromosome to the promoters of inactive X-linked genes and have conversely found that acetylation in the body of the gene is largely independent of transcriptional status. This would suggest that transcriptional repression by hypoacetylation specifically targets the promoter. Unlike late replication timing, histone hypoacetylation occurs significantly after initiation of X inactivation and is therefore unlikely to be involved in the initial silencing event (90). However, the growing evidence that histone deacetylation mediates the inhibitory effects of various transcriptional repressors as well as DNA methylation (21, 95) suggests that the hypoacetylation observed on the inactive X chromosome may play an integral role in maintaining its transcriptional repression.

DNA methylation is thought to be involved in X inactivation for several reasons. While the active and inactive X-chromosomes are overall comparably methylated (11), hypermethylation is observed at the promoter of many X-linked genes on the inactive X chromosome, particularly with respect to the X-linked housekeeping genes (65, 75, 160, 193). That this differential promoter methylation is functional is strongly suggested by the fact that demethylating agents such as 5-aza-cytidine or 5-aza-deoxycytidine can reactivate individual loci on the inactive X-chromosome (50). Consistent with the role of methylation in transcriptional repression, reactivation is correlated with complete

demethylation of the promoter at the reactivated locus (75, 159). Taken together, these observations suggest that this hypermethylation of the promoter of many X-linked genes functionally represses transcription and thereby maintains X inactivation.

It is currently controversial whether methylation is involved in the initiation of X inactivation since some X-linked gene promoters appear to be methylated coincident to X inactivation whereas others do not methylate until well after the initial inactivation event (62). In any case, initiation of X inactivation does not strictly require methylation. Methylation is not observed in either somatic X chromosome inactivation in marsupials or in imprinted inactivation of the X chromosome in mammalian extra-embryonic tissues (70). Furthermore, X inactivation in the female germline also does not appear to require DNA methylation (47, 64, 125, 183).

Since demethylating agents reactivate individual loci rather than the entire X chromosome, maintenance of X chromosome inactivation may occur at a local rather than chromosomal level. This hypothesis is consistent with the observation that the 3 genes clustered in the *G6PD* region are coordinately reactivated by 5aCdr treatment (194, 208). It is further supported by the observation that genes that escape inactivation occur in clusters on the X chromosome (139, 140). If the maintenance of X chromosome inactivation occurs at the level of individual loci or domains, examination of one such “unit of inactivation” could provide insight into the overall mechanism governing X inactivation. I have chosen to examine the X-linked human hypoxanthine phosphoribosyl-transferase gene locus for this purpose.

DNA Methylation in Mammals

In mammals DNA methylation occurs exclusively at the 5 position of cytosine in 5'-CpG-3' dinucleotides. Between 60-90% of 5'-CpG-3' dinucleotides in vertebrate genomes are methylated (144). This methylation is accomplished by transferring a methyl group from S-adenosylmethione to cytosine using DNA methyltransferases. DNA methylation occurs symmetrically on both strands of DNA since the sequence complementary to 5'-CpG-3' is also 5'-CpG-3'. This allows DNA methylation patterns to be maintained and inherited by daughter cells. During replication, each daughter cell receives one methylated strand of DNA, generating 5'-CpG-3' sites that are hemimethylated. These sites are the preferred substrate for maintenance DNA methyltransferases such as Dmmt-1 that rapidly methylate the other strand to regenerate fully methylated sites, thus passing the methylation pattern of the parent cell to the daughter cells (1). Both *de novo* and maintenance DNA methylation are observed *in vivo* and are thought to be carried out by different methyltransferases (112).

In many invertebrate eukaryotes, DNA methylation is absent, indicating that it does not have a universal function in eukaryotic cells (19). However, DNA methylation is retained in vertebrate eukaryotes, suggesting that it has retained or acquired a function in vertebrate genomes. For those lower eukaryotes that have DNA methylation, the methylation is confined to a "compartment" which is composed primarily of repetitive elements and does not contain endogenous genes (20, 169). In contrast, DNA methylation in vertebrates is distributed at low levels across the entire genome. This low level of methylation reflects the relative scarcity of CpG dinucleotides in vertebrate genomes (only ~25% of the expected level based on base composition) rather than the efficiency of

CpG methylation since 70% of CpGs are methylated in mammals (17). Interestingly, extremely GC rich regions known as CpG islands are almost always unmethylated (15) (the exception being the CpG islands associated with the inactive alleles of X-linked housekeeping genes (166)). That DNA methylation is necessary in mammals is demonstrated by the fact that homozygous knockout of *dmnt-1*, which is thought to be the primary maintenance methyltransferase in mammals, is embryonic lethal in mice (112). The presence of residual methylation in this mutant strongly indicates the presence of *de novo* methyltransferases, some of which have been recently identified (149). The cost of DNA methylation in mammals is high; despite the relative scarcity of CpGs in mammalian genomes, more than one third of all mutations leading to human disease are due to CpG to TpG transitions (85). These transition mutations are the product of oxidative deamination of the methylcytosine in CpGs to thymidine and are thought to be the reason for the relative scarcity of the 5'-CpG-3' dinucleotide in methylated genomes (16). With such a high price for DNA methylation, what are its functional benefits?

DNA methylation is thought to have three primary functions in mammals: as a defense against parasitic DNA (17, 216), as a mechanism for chromatin condensation and stabilization (86, 89, 109, 143, 144), and for transcriptional repression of endogenous genes (49, 86, 143, 189). Defense against foreign DNA is thought to be the ancestral function of DNA methylation (17, 216) and may be related to RIP (Repeat Induced Point mutation) in *Neurospora* (177, 178) and MIP (Methylation Induced Premeiotically) in *Ascobolus* (63). Unlike prokaryotes, which couple methylation of their own DNA with restriction endonucleases that attack unmethylated parasitic DNA, in eukaryotes, DNA methylation occurs in the foreign DNA, resulting in its transcriptional repression and

assembly into heterochromatin. Evidence for this ancestral function is seen in lower eukaryotes that retain DNA methylation. In these eukaryotes, DNA methylation is almost exclusively restricted to regions lacking host genes and instead is confined to specific repeat regions that are thought to be of viral origin (17). This silencing of parasitic retroviral and transposable genomes is vital to the survival of mammals since more than 35% of mammalian genomes consist of these elements and almost 90% of DNA methylation occurs in these repetitive sequences (216). That DNA methylation is capable of inactivating parasitic sequences has been clearly demonstrated *in vitro* (69, 96, 199). Significant evidence exists for the importance of this ancestral function of DNA methylation. Treatment of chicken cells with demethylating agents results in the reactivation of quiescent provirus in the genome (66). Similarly, knockout of the *dmnt-1* gene in mice results in reactivation of proviral genomes, contributing to the embryonic lethality observed (203). Conversely, injection of retroviral provirus into mice results in the methylation and transcriptional repression of the provirus (81). Likewise, introduction of transgenes into both humans and mice results in methylation and transcriptional repression of the introduced DNA, a significant problem in gene therapy (73).

From this ancestral function, the role of DNA methylation appears to have expanded to include modulations of normal functions within the cell. One of these new functions appear to be heterochromatization and stabilization of the eukaryotic genome (86, 89, 109, 143, 144). DNA methylation is distributed throughout the mammalian genome but is significantly enriched in heterochromatic regions (109). That methylation may be involved in the formation of heterochromatin has been suggested by various studies. Methyl-cytosine is found primarily in the nuclease resistant fraction of chromatin

as assayed by DNA solubilization by MNase (184) suggesting preferential assembly of methylated DNA into nucleosomal arrays. That this association with heterochromatin is a property of DNA methylation is suggested by experiments done by Keshet et al. (91). When *in vitro* methylated constructs are integrated into the genome, they adopt DNase I insensitive conformations whereas unmethylated constructs consistently adopt DNase I sensitive conformations. Conversely, 5aCdr-induced DNA demethylation is associated with chromatin opening, as assayed by endonuclease sensitivity, well before transcription initiates (119, 174). Furthermore, Davey et al. have recently shown direct evidence that methylation can affect nucleosomal positioning (45), a finding predicted by previous examination of the helical distortion generated by 5'-CpG-3' methylation (196). A direct link between DNA methylation and chromatin structure has been recently identified. Nan et al. (143) and Jones et al. (86) have demonstrated that the methylated DNA binding protein MECP2 recruits histone deacetylase complexes via interactions with Sin3. Since histone deacetylation is thought to increase the affinity of the histone lysine tails for DNA, thereby increasing the binding affinity of the nucleosome for DNA, it is thought to reduce the accessibility to that DNA. However, histone acetylation cannot completely account for the reduced accessibility to methylated sites in DNA. Antequera et al. have shown that Msp I and Tth I, two methylation insensitive endonucleases, are preferentially blocked from cutting at methylated sites but not at non-methylated sites in nuclei. This resistance is not observed at adjacent endonuclease sites lacking 5'-CpG-3' dinucleotides (2).

The "packaging" of DNA into a relatively inaccessible chromatin conformation by methylation is postulated to serve three purposes. First, it is thought to reduce the

effective complexity of the genome, making it easier for transcription factors to find their appropriate targets (12, 15). This is important in large genomes since the density of consensus transcription factor binding sites in bulk chromatin is estimated to be approximately 14 per 100bp (164). It is also thought to act to repress low-level inappropriate initiation at cryptic promoters (18). Finally, it is thought to be involved in stabilizing the genome, preventing erroneous recombination and rearrangement, especially of repetitive elements (5, 60).

The other novel function postulated for DNA methylation is the specific transcriptional repression of endogenous genes. In general, in mammals, an inverse correlation exists between the methylation status of a promoter and its activity. However, whether this methylation is the cause or result of transcriptional repression is still a matter of controversy, especially with respect to the role of methylation in mammalian development (202). The crux of the dispute is whether the waves of DNA demethylation and methylation observed in embryos are responsible for developmental regulation. Walsh et al. have shown that the methylation status of various tissue specific genes is not well correlated with expression in embryonic tissues (202). Furthermore, knockout of *dmnt-1* does not cause aberrant expression of tissue-specific genes even though these genes are significantly hypomethylated. These knockout mice embryos also do not exhibit teratology or incipient developmental abnormality, which should occur if the developmental program is disrupted by reduced DNA methylation (112). Finally, although the development programs of metazoans are well conserved, many do not exhibit any DNA methylation at all (202). This would suggest that transcriptional silencing associated with differentiation is not mediated by DNA methylation. Since the

expression patterns of most genes are set during development and differentiation, DNA methylation does not appear to be responsible for determining the expression pattern of most genes.

Nevertheless, several lines of evidence suggest that DNA methylation, particularly in the promoters of genes, can repress transcription. Transfection studies have demonstrated that *in vitro* methylation of the promoter in various reporter constructs results in transcriptional silencing (32, 33, 92, 185, 215). Likewise, introduction of 5-methylcytosine triphosphate into cells can deactivate many endogenous genes (74, 148). Conversely, demethylating agents such as 5-aza-cytidine and 5-aza-deoxycytidine can reactivate many genes *in vivo*, particularly in transformed cells (reviewed by Gartler and Goldman (54)). These observations indicate that DNA methylation has an inherent capacity to inhibit transcription.

Since DNA methylation does not appear to set the expression patterns of most endogenous genes, but nevertheless has obvious repressive capacity, what is its function? The special case of X chromosome inactivation may provide insight into the role of methylation in repression. In somatic cells, a particularly strong correlation exists between DNA methylation in the promoter of X-linked housekeeping genes and their transcriptional repression on the mammalian X chromosome (75, 120, 150, 160, 192, 194). However, the actual inactivation of these genes does not appear to require methylation. For example, the X-linked *Hprt* gene in mice is inactivated well before it becomes methylated (121). In addition, X inactivation in the female germline does not involve differential methylation (47, 64, 125, 183) nor does imprinted X inactivation in

extra-embryonic tissues (70). Furthermore, marsupial X inactivation which is paternally imprinted does not appear to involve DNA methylation at all (88, 122).

While the actual onset of X chromosome inactivation does not seem to require methylation, the stability of X chromosome inactivation appears to be dependent on methylation. In the female germline, X inactivation is transient since both X chromosomes must be reactivated during oogenesis. Similarly, X inactivation in extraembryonic tissues is unstable and prone to reactivation in culture (137, 138). Likewise, X inactivation in marsupials is quite leaky (42). In contrast, X inactivation in the somatic cells of mammals is extremely stable. It is therefore likely that in X chromosome inactivation, DNA methylation in mammals stabilizes and maintains the inactive transcriptional state rather than establishes it (70). This maintenance function may potentially be generalized to the entire genome and is consistent with the correlation between promoter methylation and transcriptional repression in adult tissues despite the poor correlation in embryonic tissues. Furthermore, while embryonic tissues fail to correlate lack of expression with methylation at the promoter, in fact, the presence of methylation at the promoter was positively correlated with repression (202).

In addition to this maintenance function, methylation does appear to have a direct and integral role in imprinted gene expression. Not only do imprinted genes have clear differential methylation of the paternal vs. maternal alleles (58, 60), but the loss of these methylation imprints during gametogenesis appears to be correlated with bi-allelic expression (181, 186). Furthermore, hypomethylation of imprinted genes arising from *dmnt-1* homozygous null mutations in mice results in inappropriate expression of imprinted genes, particularly *Igf2*, *Igf*, *h19* (111) and *Xist* (6). These observations

strongly suggest that methylation plays a crucial role in the marking of the parent of origin in imprinted genes as well as contributing to the transcriptional silencing of the imprinted allele.

While DNA methylation may alter chromatin structure in general, the correlation between transcriptional repression and DNA methylation is largely limited to methylation in the promoter. In fact, methylation in the body of genes is sometimes associated with transcription rather than repression (70, 181). Within the promoter, significant evidence suggests that methylation of the region immediately adjacent to the transcription initiation site(s) is particularly important for transcriptional repression. In particular, Pfeifer et al. showed that a cluster of five 5'-CpG-3' dinucleotides centered around the transcription initiation site of human *PGK-1* was consistently methylated in all partially demethylated clonal lines which failed to express *PGK-1* in a human/hamster hybrid. Furthermore, this was the only cluster of more than two 5'-CpG-3's which was consistently methylated in all non-reactivated clones (159). Similarly, Levine et al. demonstrated that insertion of a methylated oligomer at sites flanking the SV40 promoter results in significantly greater repression of transcription than insertion at a downstream site (108). Likewise, Tommasi et al. showed that the only fully methylated 5'-CpG-3' site in the heterogeneously methylated inactive mouse *Pgk-1* promoter lies immediately downstream of the transcription initiation site (192). Park and Chapman make similar observations in the inactive mouse *Hprt* allele, where they show that the highest level of methylation of the promoter on the inactive allele in various cell lines coincides with the transcription initiation sites (150). Finally, Hata and Sakaki identify four 5'-CpG-3' sites immediately downstream of the transcription initiation site of LINE elements whose

methylation appear to be both necessary and sufficient for transcriptional inhibition *in vivo* and *in vitro* (69).

Despite the abundant evidence that methylation at the promoter represses transcription, the exact mechanisms of this repression remain elusive. Even the issue of whether transcription is inhibited by methylation at specific critical sites, or by the overall density of methylation at the promoter, is unclear. Evidence in favor of both models exists. In favor of the methylation density model, transcription at the Rous Sarcoma virus (RSV) promoter (72, 78) and the α -collagen promoter (165) appear to be an inverse function of the density of methylation in transfection assays. Furthermore, an inverse correlation is observed between the level of methylation at the normally unmethylated p15(INK4B) CpG island and its expression in primary acute leukemia (35). Also, the HIV LTR is more rapidly silenced in transient transfection assays when it is densely methylated than when sparsely methylated (67). Interestingly, Boyes and Bird have demonstrated that low-density methylation can silence weak promoters but not strong promoters; dense methylation, however, can silence both weak and strong promoters (24). In general, these observations suggest that the mechanism of repression by a “threshold” of methylation density acts via indirect mechanisms, possibly via methylated DNA binding proteins such as MECP1 and MECP2(14, 24).

Contrary to this view, data also exist supporting a role of critical sites of methylation within the promoter of genes. Specifically, the importance of methylation adjacent to the transcription initiation sites of genes suggests that the effects of methylation at different sites or regions of the promoter are non-equivalent. Particularly, both Hata and Sakaki and Levine et al. demonstrate that the exact position of methylation

within the promoter drastically affects its ability to repress transcription (69, 108). Furthermore, the methylation of a single 5'-CpG-3' in the downstream enhancer of the mouse lysozyme gene is sufficient to abolish both its *in vitro* and *in vivo* expression (94). Similarly, the testis-specific rat *H2B* promoter contains a factor binding site which has been shown to be methylation sensitive *in vitro* and whose methylation represses *H2B* transcription *in vivo* (37). Overall, these observations are consistent with methylation acting by direct inhibition of transcription factor binding.

These disparate observations have led to the three distinct models of how methylation mediates transcriptional repression. The first model suggests that the primary function of DNA methylation is to directly inhibit the binding of transcription factors to the promoter. This model is based on the fact that several transcription factors have been found which are sensitive to DNA methylation at their cognate binding sites and will not bind methylated DNA efficiently *in vitro* (reviewed by Tate and Bird (189)). It is also consistent with the finding that methylation at specific transcription factor binding sites in some promoters completely inhibits transcription *in vivo* (94). A caveat to this model is the fact that many transcription factors are insensitive to DNA methylation of their binding sites (189). Furthermore, at high template concentrations, *in vitro* transcription does not appear to be impaired in some methylated promoters yet these same promoters are unable to support transcription when stably integrated into DNA (23). Interestingly, Buschhausen et al. have shown that repression of thymidine kinase expression on a methylated reporter construct in transient transfection assays is delayed and requires the formation of chromatin (32). These findings suggest that direct inhibition of transcription

factor binding by DNA methylation cannot alone account for the observed methylation-mediated repression of transcription.

To account for this discrepancy, an alternative indirect model of transcriptional repression has been proposed. This model suggests that DNA methylation at transcription factor binding sites makes them suitable substrates for binding by methylated DNA binding proteins, such as MeCP1 (24). Displacement of the transcription factors by high affinity binding of methylated DNA binding proteins would reduce the effective occupancy of these binding sites by the transcription factors, thus inhibiting transcription. This hypothesis is supported by the observation that methylation can repress transcription of some promoters at low but not high template concentrations *in vitro*, suggesting that inhibition is mediated by a soluble factor that can be titrated out by excess substrate. Furthermore, this inhibition can be overcome by adding methylated competitor DNA, suggesting that the inhibitor interacts with methylated DNA (23). This binding by methylated DNA binding proteins might also account for the relative insensitivity of methylated CpG sites in chromatin to MspI while adjacent endonuclease sites are unaffected in nuclei (2).

However, mere displacement of transcription factors by methylated DNA binding proteins cannot account for the requirement for chromatin formation observed by Buschhausen et al. (32). Furthermore, DNA methylation outside transcription factor binding sites appears to also affect transcription. This has led to the hypothesis that DNA methylation affects chromatin structure, a suggestion supported by the recent finding that a number of the methylated DNA binding proteins form complexes with histone deacetylases (86, 143, 145, 146). Based on these findings, it is thought that DNA

methylation acts by recruiting histone deacetylase to methylated chromatin, resulting in local histone deacetylation which increases the affinity of the nucleosome for DNA and thus reduces its accessibility in solution. This reduced accessibility hinders transcription factor binding and silences transcription.

Chromatin Structure

Differential chromatin structure and accessibility, particularly at the promoter, have long been recognized as characteristics that distinguish active versus inactive genes. Active genes are in general more accessible to regulatory factors than inactive genes as assayed by nuclease sensitivity. This enhanced general sensitivity of active chromatin to nucleases such as DNase I is thought to reflect a more relaxed chromatin structure in active genes that provides transcription factors greater access to their cognate binding site in DNA. Histone hyperacetylation and chromatin remodeling complexes such as SWI/SNF are thought to play an integral role in creating and maintaining this differential accessibility (87, 100, 211). The promoters of active genes often exhibit marked DNase I hypersensitivity as well, particularly in the vicinity of transcription factor binding sites. This hypersensitivity is postulated to be due to changes in the chromatin architecture of the promoter and may represent nucleosomal displacement (98, 214), stretches of single stranded DNA, torsionally stressed DNA, or other distortions in chromatin structure arising from factor binding (100).

The nucleosomal organization of the promoter is an integral component of chromatin structure and how it modulates transcription. The nucleosome is the basic subunit of chromatin structure and is the immediate target of many of the mechanisms

that modify chromatin structure, including histone hyperacetylation and chromatin remodeling complexes. It consists of a nucleosomal core made up of a histone octamer around which 146 bp of DNA wraps 1.7 times and a spacer region of variable length. The basic function of the nucleosome is thought to be repressive since *in vitro* nucleosomal assembly of DNA templates drastically reduces its capacity to support basal transcription (154, 155). Both direct steric hindrance of transcription complex binding by histone/DNA interactions (59, 79) and the inability of the basal transcription complex to displace nucleosomes appear to play a role in this inhibition since basal transcription is inhibited whether the transcription initiation sites lie within the nucleosome or in the spacer (154).

The translational position of nucleosomes on a DNA template (i.e. the linear position of the nucleosome relative to the DNA sequence (179)) affects the accessibility of various transcription factors as well as the basal transcriptional complex. Whether a transcription factor binding site is incorporated into the nucleosomal core or is exposed in the linker region between nucleosomes can dramatically affect its accessibility *in vitro*. The inhibitory effect of incorporating a transcription factor binding site into a nucleosomal core can vary widely among transcription factors. The glucocorticoid receptor (GR), the progesterone receptor (PR), the thyroid hormone receptor (TR) and Fos/Jun show only slightly reduced affinities while Gal4, c-Myc, heat shock factor, SP1 and TFIID exhibit at least one order of magnitude reduction in binding affinity and NF-1 and TBP show at least 2 orders of magnitude reduction in binding affinity (22, 116). Furthermore, within a nucleosome, the translational position of transcription factor binding sites relative to the dyad axis has been shown to affect the affinities of factors such as the glucocorticoid receptor (115), Sp1 (110) and suGF1(22).

The rotational orientation of the DNA helix as it winds around a nucleosomal core also affects its accessibility to transcription factors (116). For instance, the rotational orientation of the TATA box within a nucleosome strongly affects the binding of TBP. Similarly, rotating a glucocorticoid receptor binding site 180° so that its major groove faces the histone octamer drastically reduces its ability to bind the glucocorticoid receptor in reconstituted nucleosomes (114). Likewise, altering the rotational orientation of the thyroid response element (TRE) relative to the DNA helical axis within a nucleosome significantly reduces both the ability of a thyroid receptor/ retinoic acid receptor heterodimer (TR/RXR) to bind and activate transcription *in vitro* (210). These findings suggest that both the translational position and rotational orientation of transcription factor binding sites can significantly affect their accessibility in the context of nucleosomal arrays.

In addition to their repressive effects on transcription, nucleosomal positioning and orientation are thought to be involved in modulating transcriptional activation. In particular, nucleosome positioning is thought to mediate the cooperative binding of some transcription factors, allowing for rapid and robust induction. For instance, while Gal4 binding affinity is reduced in nucleosomal templates, cooperative binding is observed for multiple Gal4 sites in reconstituted chromatin but not in naked DNA (190, 201). Similar cooperativity between a weak and a strong binding site in the PHO5 promoter in yeast has also been suggested for *pho4* (200). In the same vein, the nucleosomal organization of chromatin is thought to set up a sequential hierarchy of transcription factor binding, with those factors that can bind to their cognate sites in nucleosomes binding first and remodeling the nucleosome so other factors can subsequently bind and activate

transcription (190). For instance, binding of NF1 and OCT is facilitated by GR binding at the MMTV promoter on chromatin templates although these factors bind independently on naked DNA (101). Likewise, Gal4/VP16 has been shown to facilitate TBP binding and transcription complex formation on nucleosomal templates (154). Both cooperative binding and hierarchical facilitated binding are thought to be mediated by recruitment of histone acetyltransferase or ATP-dependent chromatin remodeling complexes(116)

Precisely positioned nucleosomes are also thought to alter the spatial relationship among promoter elements, affecting both their proximity and orientation. Translationally positioned nucleosomes are thought to mediate the juxtaposition of distant promoter elements located within adjacent nucleosomal cores or linkers in the hsp26 promoter (124), the vitellogenin B1 promoter (175), and the pS2 promoter (179), allowing interactions which are not possible on naked DNA. Alternatively, the curvature of the DNA along the nucleosomal surface is thought to allow otherwise unfavorable binding of multiple transcription factors in close proximity for both the MMTV promoter (198) and the serum albumin enhancer (132). Together, these studies strongly suggest that examination of the nucleosomal organization of endogenous promoters is vital to the understanding of their transcriptional regulation.

CHAPTER 2 MATERIALS AND METHODS

Cell Lines

Two cell lines, 8121 and 4.12, described previously (77), were used for methylation analysis and nucleosome positioning analysis of the of the active and inactive human *HPRT* promoter. An additional cell line, X8-6T2 was used in both 5aCdr and TSA reactivation studies. 8121 and X8-6T2 are human/hamster hybrids each containing a single inactive human X chromosome, whereas 4.12 is a human/hamster hybrid containing a single active human X chromosome. 4.12 cells were grown in Dulbecco's modified Eagle's medium (D-MEM) supplemented with 10% fetal bovine serum, 1% penicillin-streptomycin, and 1X HAT (hypoxanthine/ aminopterin/ thymidine; Gibco/BRL) supplement. 8121 and X8-6T2 cells were maintained in D-MEM supplemented with 10% fetal bovine serum, 1% penicillin-streptomycin, and 1X 6-thioguanine (2-amino-6-mercaptapurine; Sigma). All cells were maintained in culture at 37° C in 5% CO₂.

5-aza-deoxycytidine (5aCdr) Treatment and Isolation of Single Cell-Derived Clones

8121 cells were switched to medium lacking 6-thioguanine, grown to approximately 80% confluence in T-75 culture flasks, and then treated for 24-48 h with 20ml of D-MEM containing 10% FBS, 1% penicillin/streptomycin and 0.5 - 2.0 µg/ml 5aCdr. The cells were then washed with phosphate buffered saline (PBS), trypsinized,

counted by hemacytometer and serially diluted. Cells were plated at a density of 10 to 10^3 cells/dish in medium without HAT or 6-thioguanine (non-selective medium), or 10^3 to 10^5 cells/plate in HAT-supplemented medium in 150mm plates. After 2-4 weeks, well-isolated single-cell-derived colonies were cloned with cloning rings and individually expanded in 24 well plates, then in individual T-25 culture flasks. Sixty-two clones isolated from 5aCdr-treated cells grown without selection and 4 clones isolated from 5aCdr-treated cells grown under HAT-selection were expanded into T-75 flasks for further analysis.

5-aza-deoxycytidine Reactivation Studies

Each cell line was grown to 80% confluence in D-MEM with 10% FBS and 25 μ g/ml gentamycin in T-75 flasks and then treated with 1.0 μ g/ml 5aCdr for 24 hours. The cells were allowed to recover for 24 hrs. in medium without 5aCdr, then trypsinized, counted by haemocytometer, plated in duplicate at a density of 20,000 cells/plate in HAT medium as well as 1,000 cells/plate in non-selective medium (to normalize for plating efficiency), and incubated undisturbed for 10 days at 37° C in 5% CO₂. Single cell-derived colonies in each dish were stained with Coomassie Blue for 5 minutes and counted. The 5aCdr-induced reactivation frequency for each cell line was normalized for plating efficiency by calculating: [(average # of colonies in each HAT-selected dish)/{(average # of colonies on each non-selected dish) x 20}]. Since the reactivation frequency of X8-6T2 is so high, additional dilutions of 2,000 cells/plate in HAT medium and non-selective medium was used to determine reactivation frequency.

Trichostatin A (TSA) Treatment of Cells

Each cell line was grown to 50% confluence in D-MEM with 10% FBS and 1% penicillin/streptomycin and then switched to the same medium supplemented with 300ng/ml TSA. Cells were lysed and RNA was isolated (as described below) after 0, 12, 24, and 48 hours of trichostatin A treatment.

Genomic DNA Preparation

Cells grown to monolayers in T-75s were washed once with PBS and then lysed overnight in 5 ml DNA lysis buffer (150 mM NaCl, 50 mM Tris [pH 8.0], 25 mM EDTA, 0.5% SDS, 300 µg/ml proteinase K). The lysate was then extracted by gently rocking once with Tris-equilibrated phenol [pH 7.0] for 2 h, once with phenol:chloroform (50:50) for 2 h and once with chloroform for 30 min. The 5 ml aqueous phase was then treated with 5 µl of 10 mg/ml RNase cocktail (RNase A [500 U/ml], RNase T1 [2000 U/ml]; Ambion) for 1 h at 37 °C and then extracted once with phenol:chloroform for 2 h and once with chloroform for 30 min. The genomic DNA was precipitated with ½ volume 7.5M ammonium acetate, and 2-½ volumes 100% ethanol and then spooled out and transferred to a microcentrifuge tube. The DNA was then washed twice with 1 ml of 75% ethanol, air-dried for 30 minutes, and then resuspended in TE (10 mM Tris [pH 8.0], 1mM EDTA [pH 8.0]) at approximately 1µg/µl (200 µL) and stored at 4 °C. **Note:** For isolation of genomic DNA which is partially cleaved (i.e. DNase I treatment or MNase treatment), instead of spooling, DNA was precipitated at by centrifugation at 7000g for 1 hr in a Sorval S21 or at 4500 rpm in a tabletop centrifuge for 2 hrs at 4° C. The pellet was then resuspended in 200 µl of TE [pH 8.0], transferred to a microcentrifuge tube and re-

precipitated with 100ul of 7.5M-ammonium acetate and 800μl of 100% ethanol. The pellet was then washed twice with 75% ethanol and resuspended in TE [pH 8.0] at 1μg/μl.

RNA Preparation

RNA was prepared using the Trizol reagent (Gibco/BRL) according to the manufacturer's instructions. Briefly, cells were grown to confluency in T-75 flasks and the media was removed (Note: washing the cells with PBS is not recommended). 8 ml of Trizol reagent were added to each flask and the cell lysate was homogenized by pipetting up and down several times. The cell lysate was transferred to a 15 ml conical tube and incubated at room temperature for 5 min. Then 1.6 ml of chloroform was added and the tube was shaken vigorously for 15 s and incubated at room temperature for 3 min. The sample was then centrifuged at 4000 rpm in a tabletop centrifuge for 15 min at 4° C. The colorless upper aqueous layer was transferred to a new 15 ml conical tube and 4 ml of isopropanol was added and mixed by inversion. The sample was incubated for 10 min at room temperature and then centrifuged at 4000 rpm for 30 min at 4 °C in a tabletop centrifuge. The RNA pellet was washed once with 8 ml of 75% ethanol, air dried for 30min – 1 h and resuspended in 100 μl of diethyl pyrocarbonate (DEPC) -treated dH₂O. RNA concentration was determined by spectrophotometry, adjusted to 1 μg/μl in DEPC-treated H₂O, and the RNA was stored at –20 °C. The approximate total RNA yield was 200-300μg. **Note:** This procedure can be scaled down to one-third volume for use with cells grown in T-25s.

Detection of *HPRT* mRNA by Reverse Transcriptase PCR (RT-PCR)

The presence of *HPRT* mRNA was assayed using a protocol modified from Sasaki et al. (174). Briefly, 1 µg of total RNA in 6 µl of DEPC-treated H₂O was denatured for 5 min at 95° C and then placed on ice for 2 min. The reverse transcription (RT) reaction was then performed in a final volume of 20 µl containing 10U of Rnasin (Promega), 7.5 µM random hexamers, 1 mM dNTPs (1mM each of dGTP, dATP, dTTP, dCTP), 10 mM dithiothreitol (DTT), 50 mM Tris (pH 8.3), 75 mM KCl, 3mM MgCl₂, and 200U of MLV reverse transcriptase (Promega). The RT reaction was performed by incubating for 10 min at room temperature and then 1 hr at 37° C. PCR amplification was performed on 10 µl of the RT products in a final volume of 100 µl containing 0.2 mM dNTPs, 1.75 mM MgCl, 60 pmol each of the *HPRT*-specific primers HPRT1 (5'-TCCTCCTGAGCAGTCAGC-3') and HPRT3 (5'-GGCGATGTCAATAGGACTC-3'), 7.5 pmol each of the human *MIC2* gene (*hMIC2*)-specific primers XMIC2 (5'-ACCCAGTGCTGGGGATGACTTT-3') and XMIC2R (CTCTCCATGTCCACCTCCCCT-3') in 1X PCR buffer (20 mM Tris [pH8.4], 50 mM KCl) using 10U of Taq polymerase (Gibco/BRL). The PCR cycling conditions were: 2 min. at 94 °C; 30 cycles of 1 min at 94 °C, 30 s at 59 °C, and 90 s at 70 °C; 4 min at 72 °C; hold at 4 °C. 10 µl of the PCR reaction was loaded onto a 1% agarose gel, run at 100V for 2 h, stained in ethidium bromide, and visualized by UV fluorescence.

Hydrazine Treatment of DNA for Methylation Analysis

Analysis of the methylation status of each CpG dinucleotide within the 5' region of the *HPRT* gene was accomplished using the cytosine-specific Maxam-Gilbert genomic

sequencing reaction (130) followed by gene-specific amplification using ligation-mediated PCR (LMPCR; (76)). 75 µg of genomic DNA was treated with 60% hydrazine in 1.5 M NaCl for 10 min at 20 °C in a 50 µl volume. The reaction was stopped with 200 µl of hydrazine stop solution (0.3 M sodium acetate [pH 7.5], 0.1 mM EDTA [pH 8.0]) and then precipitated with 750 µl of precooled 100% ethanol in a dry ice bath for 20 min. The hydrazine-treated DNA was pelleted at 12,000g for 20 min at room temperature. The pellet was resuspended in 225 µl of dH₂O, re-precipitated with 25 µl 3M sodium acetate [pH 5.2], washed briefly with 75% ethanol and dried under vacuum. The sample was resuspended in 90 µl of H₂O, and transferred to a screw cap tube. Then 10 µl of piperidine was added and piperidine cleavage was performed at 95 °C for 30 min. Then 1 ml of H₂O was added and the sample was allowed to dry overnight under vacuum to remove the piperidine. The resulting chemically cleaved DNA was resuspended at a final concentration of 1 µg/µl in H₂O. Fragments representing cleavages at unmethylated cytosines within the *HPRT* promoter were amplified by LMPCR.

***In Vivo* DNase I Treatment of Cells for DNase I *In Vivo* Footprinting**

Cells are grown to confluency in T-75 culture flasks. They are washed once with PBS, once with 15 ml of Solution A (150mM sucrose, 80mM KCl, 35mM HEPES [pH 7.4], 5mM K₂HPO₄, 5mM MgCl₂, 0.5mM CaCl₂), and once with 15 ml of Solution B (150mM sucrose, 80mM KCl, 35mM HEPES [pH 7.4], 5mM K₂HPO₄, 5mM MgCl₂, 2mM CaCl₂). Then 1 ml of Solution B containing 0.2% NP-40 and 0-100ug of DNase I (Worthington) (resuspended in 10 mM Tris [pH 7.4] at 1mg/ml. **Note:** DNase I is exquisitely sensitive to shearing. Resuspend gently.) was added to the monolayer, gently

distributed by tilting and incubated at 37 °C for 2 min. DNase I digestion was stopped by adding 4 ml of lysis buffer (see above) and the mixture was then incubated overnight at room temperature. DNA was then isolated by the standard extraction and precipitation techniques described above.

***In Vitro* DNase I Treatment of Naked DNA**

50 µg of genomic DNA was digested to completion with EcoRI (3 fold excess of enzyme for 4 h) for each concentration point. The digested DNA was phenol/chloroform extracted, precipitated and then resuspended in 100 µl of dH₂O and 200 µl Solution B. DNase I was added to a final concentration of 0.0125 – 0.05 µg/ml (2 fold serial dilutions) and incubated for 2 min at room temperature. The reaction was stopped by adding 12 µl of 0.5 M EDTA [pH 8.0] and 3 µl of 20% SDS. The DNA was phenol/chloroform extracted, precipitated, and resuspended in TE [pH 8.0].

LMPCR Amplification

LMPCR amplification was performed essentially as described by Hornstra and Yang (75) except that the PCR step was carried out using Taq polymerase (77) instead of Vent polymerase. For methylation analysis of the *HPRT* promoter, 2 µg of hydrazine-treated DNA was amplified using the E and M LMPCR primer sets as described previously (77). The E primer set was used to examine upper strand methylation, while the M primer set, was used to examine the lower strand. These two primer sets cover the region from approximately positions -235 to -10 relative to the translation start site on both strands and include the entire minimal promoter (168).

DNase I *in vivo* footprinting analysis of the upper strand of the *HPRT* promoter was carried out using the C, E, and J primer sets, described previously (77) (75). Analysis of the lower strand was performed with the A, CA, CB and I primer sets. The region examined extends from approximately -350 to +200 relative to the translation start site of *HPRT* on both strands. The sequence and strand examined by each primer and the relative position and region examined by each primer set is shown in Figure 1-1.

LMPCR was performed as follows. 2-3 μg of cleaved DNA was mixed with 0.6pmol of the extension primer in a total volume of 15 μl in 1X Vent buffer (40 mM NaCl, 10 mM Tris [pH 8.9]). The mixture was denatured at 96° C for 10 min, annealed at 45° C for 30 min., and then cooled to 4° C. Primer extension was performed in 40 mM NaCl, 10 mM Tris [pH 8.9], 3 mM MgSO₄, 0.25 mM 7-deaza-dGTP-deoxynucleotide mix (0.25 mM dATP, 0.25 mM dCTP, 0.25 mM dTTP, 0.1875 mM 7-deaza-dGTP, 0.0625 mM dGTP), and 2U of Vent DNA polymerase in a total volume of 30 μl . For primer extension, this mixture was heated to 53 °C for 1 min, 55 °C for 1 min, 57 °C for 1 min, 60 °C for 1 min, 62 °C for 1 min, 66 °C for 1 min, 68 °C for 3 min, and 76 °C for 3 min. The samples were then cooled to 4 °C.

Ligation was performed by adding 15 μl of dilution mix (2.2 μl 1M Tris-Cl [pH 7.5], 7.2 μl 50 mM MgCl₂, 1 μl 1 M DTT, 0.25 μl BSA (10mg/ml), 9.35 μl dH₂O) and 20 μl of ligation mix (5 μl 50 mM MgCl₂, 0.5 μl 1 M DTT, 0.75 μl 100 mM ATP, 0.125 μl BSA (10 mg/ml), 5 μl of 20 μM double stranded linker primer (ds LP), 0.9 μl T4 DNA ligase (5U/ml), 12.725 μl dH₂O). The ligation reaction was incubated overnight at 17° C. The samples were subsequently extracted once with equal volume phenol:chloroform (50:50), once with chloroform and then precipitated with ½ volume 7.5M ammonium

Primer Set	Strand	Designation	Sequence
C	Upper	C1	5'-AGGCGGAGGCGCAGCAA-3'
		C2	5'-GGGAAAGCCGAGAGGTTTCGCCTGA-3'
E	Upper	E1	5'-AGCTGCTCACCACGACG-3'
		E2	5'-CCAGGGGCTGCGGG TCGCCATAA-3'
J	Upper	J1	5'-CGCCATTTCCACCTTCTCTT-3'
		J2	5'-TTCCCACACGCAGTCCTCTTTTCCCA-3'
A	Lower	A1	5'-AATGGAAGCCACAGGTAGTG-3'
		A2	5'-AGGTCTTGGGAATGGGACGTCTGGT
M	Lower	M1	5'-GAATAGGAGACTGAGTTGGG-3'
		M2	5'-GGAGCCTCGGCTTCTTCTGGGAGAA-3'
CA	Lower	CA1	5'-CCTAGTGAGCCTGCAAAGT-3'
		CA2	5'-AAACTGGTAGGCGCCGGCGTAGG-3'
CB	Lower	CB1	5'-GGGCCTGCTTCTCCTCAG-3'
		CB2	5'-TGCTTCTCCTCAGCTTCAGGCGGCT-3'
I	Lower	I1	5'-TTGCTGCGCCTCCGCCTC-3'
		I2	5'-CGGCTTCTCCTCCTGAGCAGTCA-3'

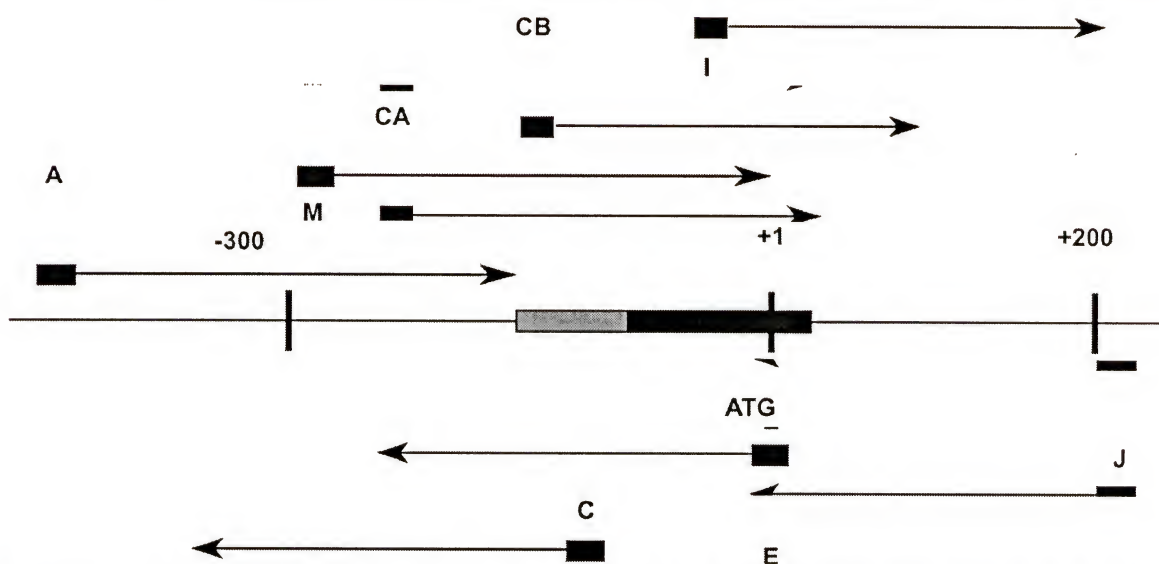


Figure 1-1 Sequence, Strand, and positions of LMPCR primers used in the analysis of the human *HPRT* promoter. The sequence and strand of the LMPCR primers sets used to examine the high resolution methylation pattern and high resolution DNase I cleavage pattern of the human *HPRT* promoter are listed in the table. The first primer of each set is the extension primer and the second is the gene specific PCR primer. The location of the PCR primers relative to the *HPRT* promoter region is schematically shown. The long horizontal line represents the *HPRT* promoter region. The rectangle on the line represents the first exon with the region of multiple transcription initiation sites shown as gray. The small rectangles above and below the line indicate the location of the PCR primer of the specified primer set. The arrows extending from the rectangles indicate the direction and region covered by each primer set. All numbers are relative to the translation initiation site.

acetate in 2 ½ volume 100% ethanol for 1 h and pelleted by centrifugation at maximum speed in a microcentrifuge for 30 min. The pellets were washed once in 75% ethanol, dried in a SpeedVac and resuspended in 20 µl of H₂O.

PCR amplification of ligated fragments was performed in 40 mM NaCl, 10 mM Tris-Cl (pH 8.9), 1.75 mM MgCl, 0.25 mM 7-deaza-dGTP-deoxynucleotide mix, 20 pmol PCR primer, 20 pmol linker primer LP2, and 3U of Taq DNA polymerase in a total volume of 100 µl. The cycling conditions for PCR amplification are as follows: 95° C for 3 min followed by 21 cycles of (95° C for 1 min, 64° C for 1 min, 76° C for 1 min +5 sec per cycle), 76° C for 15 min, hold at 4° C. To ensure the complete extension of PCR products, 5 ml of a booster mix (1X Vent buffer, 1.75 mM MgCl, 5 mM dNTP, 1U Taq DNA polymerase) was added during the 76° C for 15 min step. The PCR products were extracted once with equal volume phenol:chloroform (50:50), once with equal volume chloroform and the precipitated with ½ volume 7.5M ammonium acetate and 2 ½ volume 100% ethanol for 1 h. The PCR products were pelleted at 13,200 rpm in a microcentrifuge for 30 min, washed once with 500 µl of 75% ethanol, dried in a speedvac and resuspended in 20 µl of H₂O.

5 µl of each PCR reaction was dried to completion, resuspended in 2 µl of formamide loading dye and loaded onto a 5% denaturing 30 cm long ranger sequencing gel which was run at 75 V for approximately 1 ½ hr. The gel was cooled for 10 min, transferred to ashless Whatman 1MM and electro-transferred for 30 min at 4° C onto Hybond N+ nylon membrane. The blot was then dried for 1h at 80° C under vacuum to cross-link the DNA to the membrane. The blot was then pre-hybridized for 15 min with 15-20 ml of hybridization solution (38) (0.25 M Na₂HPO₄ [pH 7.2] with o-phosphoric

acid, 7% SDS, 1% BSA (fraction V), 1mM EDTA [pH 8.0]) at 65° C. The blot was then hybridized in 4 ml of hybridization solution with a region specific single-stranded probe (see below for synthesis) for 8-16 h at 65° C. After hybridization, the blot was rinsed vigorously 3 times with 50-100 ml of wash solution (38) (20mM Na₂HPO₄ [pH 7.2 with o-phosphoric acid], 1% SDS, 1mM EDTA) and then washed with wash solution three times for 15 min each at 65° C. The blot was then wrapped in Saran wrap and, depending on signal strength as determined by Geiger counter, exposed to Kodak AR film for 2-16h with screens at -80 °C. The film was developed in a Kodak X-omat developer and the signal intensity between samples was balanced by altering the amount of sample loaded. For analysis purposes, the balanced samples were re-run on a 60cm sequencing gel.

To LMPCR amplify DNase I-treated samples, a modification known as extension product capture (195) was employed. To use this modification, a 5' biotinylated extension primer was used during the extension step. After ligation, the ligated products were mixed with an equal volume (75 µl) of 5 mg/ml streptavidin paramagnetic beads (Promega) (prewashed 3 times and then resuspended at 5 mg/ml in binding buffer (10mM Tris-Cl [pH 7.7], 1mM EDTA, 2M NaCl)) and incubated at room temperature for 15 min. (Note: recent tests have shown that 75 µl of 1mg/ml streptavidin beads are sufficient.) The beads were separated from the solution using magnetic stands and washed once with 75 µl of binding buffer. The unbiotinylated strand was eluted from the beads by incubation in 40 µl of 0.15N NaOH for 10-20 min at 37° C. The supernatant containing the eluted DNA was transferred to a new microcentrifuge tube and neutralized with 40 µl of 0.15N HCl and 8 µl of 1M Tris [pH 7.7]. 10 µg of tRNA was added to act as a carrier and the DNA was then precipitated for 1 hour with 9 µl of 3M sodium acetate [pH 5.2]

and 250 μ l of 100% Ethanol. The DNA was pelleted at 13,200 rpm in a microcentrifuge for 30 min, washed once with 500 μ l of 75% ethanol and resuspended in 20 μ l of H₂O. PCR amplification was carried out as describe above but the number of cycles was increased to 25 cycles.

Single-Stranded Probe Synthesis for LMPCR Analysis

Single-stranded hybridization probes for LMPCR analysis were synthesized essentially as described by Hornstra et al. (76). Probes were synthesized using M13 single-stranded DNA templates containing a 1.8 kb EcoR I to BamH I fragment which contains the entire human *HPRT* promoter. Both the sense and anti-sense single-stranded templates were previously prepared by Ian Hornstra using standard M13 isolation techniques (173). For the upper strand primers, the sense template was used and for the lower strand primers, anti-sense template was used. To synthesize the single-stranded probe, 3-5 μ l of a 1 μ M solution of the gene-specific LMPCR primer (Primer 2 of the primer set) was mixed with 3 μ l of a 0.1 μ M solution of the appropriate single stranded template and 2.5 μ l of 10X React 2 (2 M NaCl, 500mM Tris [pH 8.0]; Gibco/BRL). The mixture was denatured at 95° C for 5 min and annealed at 50° C for 15-30 min. The mixture was then placed on ice and 1 μ l of 100 mM DTT, 2 μ l of 100mM MgCl, and 2 μ l of a 3 mM dNTP mix containing 3 mM each of dATP, dGTP, and dTTP were added. Then 10 μ l of Redivue [α -³²P] dCTP (3000 Ci/mmol, 10 μ Ci/ μ l ; Amersham/Pharmacia) and 2U of Klenow were added at room temperature, mixed and incubated at 37° C for 1h. Next, 35 μ l of formamide loading dye was added and the probe was denatured for 10 min at 95° C and quenched on ice. The probe was size-fractionated on a 6%, 1.5mm thick,

preparative denaturing polyacrylamide gel (6% acrylamide, 40:1 acrylamide: bisacrylamide) in 1X TBE (100 mM Tris, 100 mM boric acid, 4 mM EDTA) for 15-20 min at 20W constant power. The gel was then exposed for 3 min to Type 57 Polaroid film to determine the location of the single-stranded probe in the gel. The probe was cut out of the gel, crushed in a 10 ml conical tube using a glass rod and resuspended in 4 ml of hybridization solution at 65°C. This solution was used to probe the LMPCR blots.

***In Vivo* DNase I Treatment of Cells for DNase I General Sensitivity and Hypersensitivity Analysis.**

Cells were grown to confluency in a T-150s (approximately 3×10^7 cells per T-150) and then washed with PBS, and trypsinized. The cells were then pelleted by centrifugation at 500 G in a tabletop centrifuge and washed once with 25 ml of PBS, once with 25 ml of Solution A (150 mM sucrose, 80 mM KCl, 35 mM HEPES [pH 7.4], 5 mM K_2HPO_4 , 5 mM $MgCl_2$, 0.5 mM $CaCl_2$) and resuspended in 1ml of Solution B (150 mM sucrose, 80 mM KCl, 35 mM HEPES [pH 7.4], 5 mM K_2HPO_4 , 5 mM $MgCl_2$, 2 mM $CaCl_2$) per T-150. Then 500 μ l of Solution B containing 0.4% NP-40 and 0 - 100 μ g of DNase I (1mg/ml; Worthington) at 10 μ g increments was added to the 500 μ l of cell suspension in a 15 ml conical tube, mixed by pipetting and incubated for 2 min at 37° C. The digestion was stopped with 4 ml of lysis buffer (50 mM Tris [pH8.0], 150 mM NaCl, 25 mM EDTA [pH8.0], 0.5% SDS, 300 μ g/ml Proteinase K) and incubated overnight at room temperature. DNA was subsequently isolated as described above and resuspended at 1mg/ml in TE [pH 8.0].

MNase Treatment of Cells *In Vivo*

Cells were grown to confluency in T-150 culture flasks and 1 T-150 (approximately 3×10^7 cells) was used per MNase concentration point. Cells were trypsinized, combined in a 50 mL conical tube, and gently pelleted at $\sim 500g$ in a tabletop centrifuge. They were then washed gently once in 25 ml of Solution A (150 mM sucrose, 80 mM KCl, 35 mM HEPES [pH 7.4], 5 mM K_2HPO_4 , 5 mM $MgCl_2$, 0.5 mM $CaCl_2$) and once in 25 ml of Solution B (150 mM sucrose, 80 mM KCl, 35 mM HEPES [pH 7.4], 5 mM K_2HPO_4 , 5 mM $MgCl_2$, 2 mM $CaCl_2$) and then resuspended at 500 μ l per T-150 flask in Solution B. For each treatment, 500 μ l of cells were combined with 500 μ l of Solution B +0.4% NP-40 (Sigma) and the appropriate amount of MNase (resuspended at 20U/ μ l (Sigma)) at 10U (range 0-100U) or 20U increments (range 0-200U; for more complete digestion and visualization of lower molecular weight bands), mixed gently and incubated at room temperature for 2 minutes. Digestion was stopped by the addition of 4 ml of DNA lysis buffer (50 mM Tris [pH8.0], 150 mM NaCl, 25 mM EDTA [pH8.0], 0.5% SDS, 300 μ g/ml Proteinase K) and the mixture was incubated overnight at room temperature. MNase-treated DNA was isolated as described above.

MNase treatment of Genomic DNA *In Vitro*

10 μ g of genomic DNA was digested with Bcl I per MNase concentration point. The digested DNA was phenol/chloroform extracted, precipitated and resuspended in 100 μ l of Ex50 Buffer (10 mM HEPES [pH 7.6], 60 mM KCl, 1.5 mM $MgCl_2$, 0.5 mM EGTA [pH 8.0], 10% glycerol, 10 mM glycerol phosphate) + 5 mM $CaCl_2$. Two-fold serial dilutions from 0-2U of MNase (diluted from 20U/ μ l with Ex50 Buffer) were added and

the reaction is allowed to incubate for 2 minutes at room temperature. The reaction was stopped with 50 μ l of stop solution (2.5% sarkosyl, 100 mM EDTA [pH 8.0]). The treated DNA was then phenol/chloroform extracted, precipitated and resuspended in TE [pH 8.0] at 1 μ g/ μ l.

Southern Blot Analysis of the *HPRT* Promoter by Indirect End-labeling

Genomic DNA was completely digested with Bcl I, size-fractionated on a 1.4% agarose gel at 60V for 12hrs in 1X TAE, ethidium bromide stained and transferred to Hybond N+ by capillary transfer. Indirect end-labeling was achieved using a 400bp probe just upstream of a Bcl I restriction site in intron I of *HPRT* (see Figure 4-1). This probe was PCR-amplified from a plasmid containing a BamHI to Pst I restriction fragment from intron 1 of the *HPRT* gene. This fragment contains a previously described single copy region known as Probe A (117) in which the reference Bcl I site is located. PCR amplification of the 400 bp probe was carried out using the following primer set: MnaseBcl400 (GTTTGGGGTGCGATGGTGAGG) and MnaseBcl downstream (CAGAACGGTTGAGGAGGGAGGCCA). The PCR product was gel purified using the Qiagen Gel Extraction kit as per manufacturer instructions and radiolabeled by random priming using the Gibco/BRL Random Primer Labeling kit (see below). The blot was prehybridized for at least 15 min with 20 ml of hybridization solution (0.25 M Na₂HPO₄ [pH 7.2] with o-phosphoric acid, 7% SDS, 1% BSA (fraction V), 1 mM EDTA [pH 8.0])) and then hybridization was performed at 65° C overnight in 4 ml of hybridization solution. The blot was washed at 65° C in wash solution (20 mM Na₂HPO₄ [pH 7.2 with

o-phosphoric acid], 1% SDS, 1 mM EDTA) and exposed to Kodak MR film 4-5 days with BioMax MS intensifying screens at -80°C .

Probe Synthesis by Random Priming

Probe synthesis from double-stranded DNA templates by random priming was performed as follows using the Gibco/BRL Random Primer Labeling Kit. Twenty-five nanograms of DNA template was brought up to a total volume of 23 μl with H_2O , denatured at 95°C for 5 min, and then placed immediately on ice. Then 15 μl of Random Primer Mix (Gibco/BRL), 2 μl each of 0.5mM dATP, dTTP, and dGTP, 5 μl of Redivue [$\alpha\text{-}^{32}\text{P}$] dCTP (3000 Ci/mmol, 10 $\mu\text{Ci}/\mu\text{l}$; Amersham/Pharmacia) and 1 μl of Klenow (1U/ μl) were added on ice and mixed. The reaction was incubated for 1-2 hr at 37°C . (Note: Longer incubations give higher specific activities but incubation over 4 h seems to increase background). The probe was then loaded onto a Sephadex G-50 column and spun at 3000 rpm in a tabletop centrifuge to remove unincorporated nucleotides. The resulting solution was denatured for 5 min at 95°C and then placed immediately on ice. This probe was then added to 4 ml of hybridization solution at the appropriate temperature and added to the blot.

DNA Methylation of Plasmid Templates *In Vitro*

DNA methylation at CpG dinucleotides *in vitro* was performed using Hpa II, HhaI, and SssI Methylases (New England Biolabs). Hpa II methylates the cytosine residue of the CpG dinucleotide in the recognition sequence 5'-CCGG-3' whereas HhaI methylates the cytosine of the CpG dinucleotide in the recognition sequence 5'-GCGC-

3'. SssI methylates all CpG dinucleotides within a target sequence. The methylation reaction was performed as follows: 5 μ l of the appropriate 10X NEB buffer, 2.5 μ l of 3.2 mM S-adenosylmethionine (SAM; diluted from a 32 mM stock), 5 μ l of plasmid DNA (1 μ g/ μ l), 30 μ l of H₂O, and 5 μ l of the appropriate methylase(s) were mixed and incubated for 1 hr at 37° C. Hpa II and Hha I both use the same 10X Hpa II methylase Buffer (500mM Tris-HCl [pH 7.5], 100 mM EDTA, 50 mM 2-mercaptoethanol) whereas SssI methylase uses 10X NEBuffer 2 (500 mM NaCl, 100 mM Tris-HCl, 100 mM MgCl₂, 100 mM DTT, pH 7.9 at 25°C). The stock enzyme concentrations for each enzyme are as follows: 2U/ μ l for SssI, 4U/ μ l for HpaII and 25U/ μ l for HhaI. When both HpaII and HhaI were used, 2.5 μ l of each was added. The methylated DNA was then phenol/chloroform extracted, precipitated and resuspended at 100ng/ μ l. It was subsequently tested for complete methylation by digestion with Hpa II and Hha I.

Reconstitution of Nucleosomes onto the *HPRT* Promoter *In Vitro*

The DNA template used for *in vitro* reconstitution of chromatin was the pBS HPRT 1.8Kb plasmid, which is a pBluescript-derived plasmid containing the 1.8 Kb EcoRI to BamHI fragment that includes the entire *HPRT* promoter. This protocol was acquired from Dr. Jorg Bungert and modified from the original protocol by Peter Becker (7). Briefly, 10X MacNAP buffer was freshly made up as follows: 46 μ l of H₂O was combined with 3 μ l of 1M MgCl₂, 10 μ l of 100 mM DTT, 30 μ l of 1M creatine phosphate, 10 μ l of 300 mM ATP, and 1 μ l of creatine phosphokinase (1mg/ml in 100 mM Imidazole). 7 μ l of 10X MacNAP was mixed on ice with 6 μ l of template DNA (100 ng/ μ l), 37 μ l of Ex50 Buffer (10 mM HEPES [pH 7.6], 60 mM KCl, 1.5 mM MgCl₂, 0.5

mM EGTA [pH 8.0], 10% glycerol, 10 mM glycerol phosphate) and 20 μ l of *Drosophila* extract for a total volume of 70 μ l and then incubated at 26° C for 6 h. The reconstituted chromatin was then digested with either MNase or DNase I as described below.

Assessment of Translational Phasing of Nucleosomes on *In Vitro* Reconstituted Chromatin by MNase Digestion and Southern Analysis

The reconstituted chromatin (total volume= 70 μ l; see above) was mixed with 100 μ l of a pre-assembled MNase mix (94 μ l Ex50 buffer, 5 μ l 100 mM CaCl₂, 1 μ l MNase [50U/ μ l; Sigma]) and incubated at room temperature. At 0, 1, 2, and 5 minutes 40 μ l of this digestion mix was removed and mixed with 20 μ l of stop solution (2.5% sarkosyl, 100 mM EDTA [pH 8.0]) to stop the reaction. To remove RNA and proteins, 1 μ l of RNase cocktail (Ambion), 8 μ l of 2% SDS and 5 μ l of Proteinase K (resuspended at 10mg/ml; Gibco/BRL) were added to each time point and the mixtures were incubated at 37° C overnight. The digested DNA from each time point was then purified by equal volume extractions with phenol, phenol:chloroform and chloroform and precipitated with 1/10 volume NaCl and 2 ½ volumes 100% ethanol with 1 μ l of glycogen (10 mg/ml; Boehringer Mannheim) as a carrier. The DNA from each time point (approximately 150ng) was then resuspended in 10 μ l of TE [pH 8.0]. To assess nucleosomal assembly this DNA was size fractionated on a 1.6% agarose gel and visualized by ethidium bromide staining and UV fluorescence. Translational phasing of nucleosomes was assessed by southern analysis using indirect end-labeling as described below.

The purified DNA from each MNase digestion time point was digested to completion with a 4-fold excess of BamHI for 4 hr at 37° C. The digested DNA was size-

fractionated on a 1.6% agarose gel at 100V for 4 hrs. The DNA was then transferred to Hybond N+ by capillary transfer and the blot was baked at 80° C for 1 hr.

The blot was prehybridized with 20 ml of hybridization solution and then hybridized with an oligonucleotide radioactively phosphorylated with ^{32}P , which was synthesized as follows. Briefly 5 pmol of the oligonucleotide BamHINuc1Probe, which corresponds to the sequence immediately downstream of the downstream BamHI site in the *HPRT* promoter, was mixed with 5 μl of 5X Forward Reaction Buffer (Gibco/BRL) and brought up to 22.5 μl . Then 2.5 μl of [γ - ^{32}P] ATP (10 $\mu\text{C}/\mu\text{l}$, 3000 Ci/mmol) and 1 μl of T4 Polynucleotide Kinase (Gibco/BRL) was added, mixed and incubated for 10 min at 37° C. The reaction was stopped by heat inactivation for 10 min at 65° C and the volume brought up to 100 μl with H_2O . The labeled oligonucleotide was separated from unincorporated [γ - ^{32}P] ATP by passing the sample through a Sephadex G-50 column. The labeled oligonucleotide was then added to 4 ml of hybridization solution at 40°C and this solution was added to the prehybridized blot. Hybridization was performed overnight at 40° C and the blot was then washed with wash solution at 40°C and wrapped in Saran Wrap. The blot was visualized by exposure to Kodak AR film at room temperature for 1h.

CHAPTER 3
EVIDENCE THAT SILENCING OF THE *HPRT* PROMOTER BY DNA
METHYLATION IS MEDIATED BY CRITICAL CPG SITES

Introduction

In mammals, DNA methylation at CpG dinucleotides in the 5' region of genes is frequently associated with transcriptional silencing (49), particularly in housekeeping genes on the inactive X chromosome. Numerous studies suggest that this association between promoter hypermethylation and transcriptional repression has a functional basis. For instance, individual loci on the inactive human X chromosome in human/hamster hybrid cell lines may be reactivated using demethylating agents such as 5-aza-cytidine (50, 142). Likewise, *in vitro* methylation of various promoter constructs results in inhibition of transcription in transient expression assays (32, 33, 92, 185, 215). However, despite significant evidence that DNA methylation represses transcription, specific mechanisms of this repression are only now becoming apparent.

Recent reports suggest that DNA methylation mediates transcriptional repression indirectly, via binding of the methylated DNA-binding protein MeCP2, which in turn recruits histone deacetylases that modify the local chromatin structure (86, 143). However, additional mechanisms may also act to repress transcription by methylation, such as direct inhibition of transcription factor (TF) binding to its cognate site in DNA. Indeed, methylation of the binding sites of several TF's has been shown to alter the affinity of the factor for its binding site (reviewed by Tate et al. (189)).

Whether transcriptional repression relies on methylation at specific critical CpGs or on the overall level of promoter methylation remains unclear. Several studies indicate that methylation of CpG dinucleotides in the vicinity of the transcriptional initiation site(s) of genes is important for gene silencing (69, 108, 150, 159, 192). Therefore, perturbation of the methylation pattern in this region may identify specific CpG sites whose methylation is required to maintain silencing, and provide insight into mechanism(s) by which methylation mediates transcriptional repression.

The X-linked human hypoxanthine phosphoribosyl transferase (*HPRT*) gene exhibits strong differential methylation in the promoter region on the active and inactive X chromosomes. High-resolution methylation analysis by ligation-mediated PCR (LMPCR)-assisted genomic sequencing indicates that the promoter on the active X chromosome is unmethylated, while the promoter on the inactive X chromosome is methylated at most, but not all, CpG dinucleotides (75). DNA-demethylating agents such as 5-aza-deoxycytidine (5aCdr) can alter the methylation pattern of the inactive *HPRT* allele and can reactivate the gene on the inactive X chromosome in rodent/human hybrid cell lines (50, 142, 174). Cis-acting regulatory elements in the *HPRT* promoter region have been identified by dimethyl sulfate (DMS) *in vivo* footprinting (77).

By examining the altered methylation patterns of the *HPRT* promoter in single-cell-derived clones from 5aCdr-treated cells, we have identified 3 specific CpG dinucleotides in the promoter region whose methylation is highly correlated with maintaining transcriptional repression of the *HPRT* gene on the inactive X chromosome. Consistent with the requirement for methylation of specific critical CpG sites, we find no correlation between the level of pre-existing demethylation and the reactivation

frequency of the gene when clonal lines that have undergone partial demethylation of the promoter are re-treated with 5aCdr. We also find that the inactive *HPRT* allele is insensitive to trichostatin A (TSA) reactivation and also show that this resistance to TSA reactivation cannot be overcome by partial demethylation of the promoter region. Furthermore, we present evidence for *de novo* methylation of the *HPRT* promoter upon 5aCdr treatment and discuss its potential relevance to transcriptional silencing by DNA methylation.

Results

Identification of Critical CpG Dinucleotides

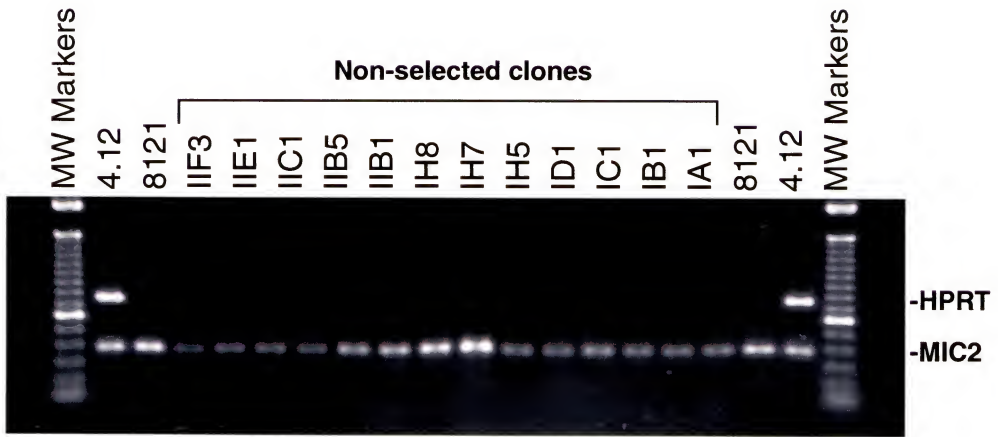
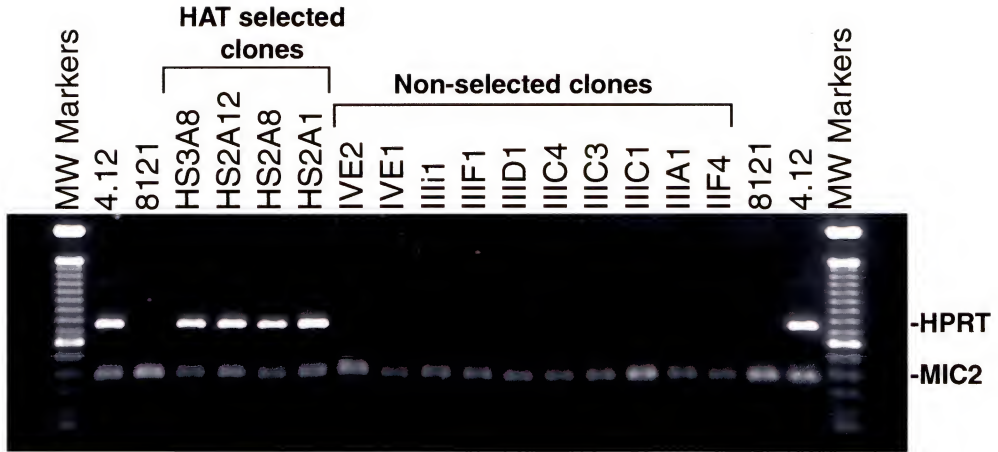
To identify specific CpG sites within the promoter region whose methylation may be critical for maintaining transcriptional repression of the *HPRT* gene on the inactive X chromosome, we treated 8121 cells (containing an inactive human X chromosome) with the demethylating agent 5aCdr and isolated both HAT-selected (HAT selects for the *HPRT*⁺ phenotype) and non-selected single-cell-derived clones. If critical CpG sites exist within the *HPRT* promoter region, these sites should remain methylated after exposure to 5aCdr in all clones that fail to reactivate the *HPRT* gene (and, conversely, undergo demethylation in all clones that do reactivate). Each of 4 HAT-selected and 62 non-selected clones was screened for expression of *HPRT* mRNA by RT-PCR. The RT-PCR assay was performed on total RNA as a multiplex reaction using both *HPRT*-specific primers and human *MIC2* (*MIC2*)-specific primers. Because *MIC2* is an X-linked gene which escapes X inactivation, *MIC2* expression serves as an internal positive control for the RT-PCR reaction. As expected, RT-PCR analysis revealed that all 4 HAT-resistant clones had reactivated the *HPRT* gene (Figure 3-1A). In addition, one of the 62 non-

selected clones examined also had reactivated the *HPRT* gene following 5aCdr treatment. To determine the sensitivity of the RT-PCR assay, total RNA from 4.12 cells (which contain an active human X chromosome and expresses the *HPRT* gene) was serially diluted with total RNA from 8121 cells and the resulting mixtures were subjected to RT-PCR. The results (Figure 3-1B) indicate that the RT-PCR assay can readily detect as little as 0.2% of "wildtype" (i.e., 4.12 cells) *HPRT* mRNA levels. All 5 clones that reactivated the *HPRT* gene after 5aCdr treatment exhibited full wildtype *HPRT* mRNA levels, and all 61 clones that failed to reactivate the *HPRT* gene after 5aCdr treatment showed no detectable *HPRT* mRNA; no low or intermediate *HPRT* mRNA levels were observed for any of the clones examined in our RT-PCR assays.

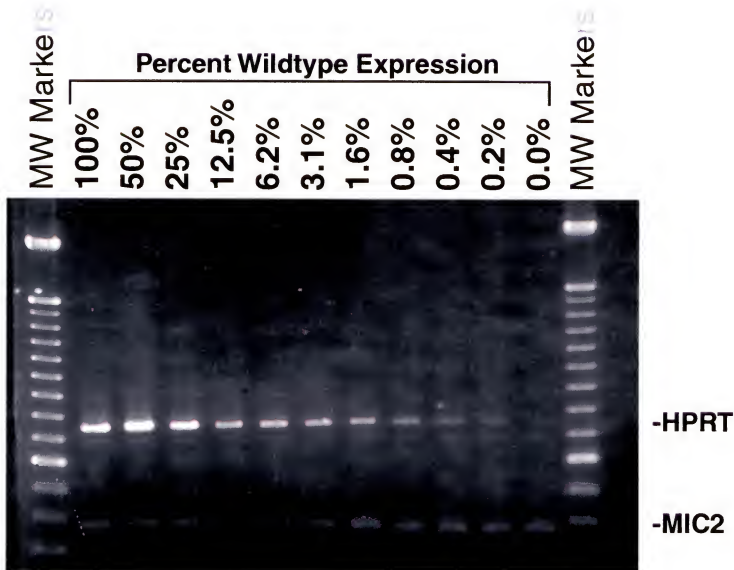
All clones assayed for *HPRT* reactivation by RT-PCR were also subjected to high-resolution DNA methylation analysis by LMPCR genomic sequencing (Figures 2 and 3). The specific region of the *HPRT* promoter examined extends from approximately 140bp upstream to 90bp downstream of the two major transcription initiation sites identified by Kim et al. (93) and encompasses the entire minimal promoter (151) and all but one of the transcription factor binding sites previously identified by DMS *in vivo* footprinting (77). This region was chosen for analysis because previous studies suggest the region surrounding transcription initiation sites is crucial for transcriptional repression by DNA methylation (69, 108, 150, 159, 192). In the parental 8121 cell line, this region contains 20 symmetrically methylated CpG sites (where paired CpG's on the upper and lower strand count as a single site) and 12 unmethylated sites (75). Purified genomic DNA from each clone was subjected to the Maxam-Gilbert cytosine-specific sequencing reaction followed by ligation-mediated PCR (LMPCR). The cytosine-specific reaction

Figure 3-1. RT-PCR analysis of *HPRT* mRNA expression. **A.** Representative RT-PCR analysis of HAT-selected and non-selected single-cell-derived clonal lines from 5aCdr-treated 8121 cells. The lane designations indicate the name of each clone examined. *8121* is the parental human/hamster hybrid cell line containing an inactive human X chromosome. *4.12* is a human/hamster hybrid that contains an active human X chromosome. *HPRT* indicates the position of the expected *HPRT*-specific RT-PCR product. *MIC2* indicates the expected location of the *MIC2*-specific RT-PCR product. **B.** Sensitivity of the RT-PCR assay to detect *HPRT* mRNA. Total RNA from 4.12 cells (wildtype) was serially diluted with total RNA from 8121 cells and the RNA mixture subjected to RT-PCR analysis. Percentages from 0% – 100% indicate the portion of the total RNA that is derived from 4.12 cells. *HPRT* and *MIC2* represent the expected location of the respective RT-PCR products.

A



B



uses hydrazine to modify cytosine nucleotides in DNA, but this modification is significantly inhibited by methylation at the 5 position of cytosine. The differential reactivity of hydrazine with cytosine vs. 5-methyl-cytosine allows for examination of the methylation status of every cytosine (including CpG dinucleotides) within a region of interest (75, 76, 120). In this high-resolution assay, demethylation at a specific cytosine results in the appearance of a new band (relative to a methylated sample) in the autoradiogram of the cytosine-specific sequencing ladder (Figure 3-2). A site was scored as “demethylated” in 5aCdr-treated clones if a new cytosine-specific band was detected that was previously undetectable (i.e., methylated) at the same position in the cytosine-specific ladder from the 8121 parental cells. All sites designated as “methylated” showed no detectable band on the cytosine-specific sequencing ladder above background levels; therefore, a site in the 5aCdr-treated clones was considered “demethylated” if the associated band was detectable above background (Figure 3-3).

All clones which reactivated the *HPRT* gene after 5aCdr treatment demethylated all CpG's in the region around the major transcription initiation sites of the *HPRT* gene (data not shown), a pattern identical to that of the active *HPRT* allele on the active X chromosome and consistent with previous 5aCdr reactivation studies of the *HPRT* gene (75). In addition, two HAT-selected 8121-derived clones that had spontaneously reactivated the human *HPRT* gene in the absence of 5aCdr treatment also exhibited complete demethylation of all CpG's in the same region of the promoter (data not shown). These data suggest that the complete demethylation of this region of the *HPRT* promoter in transcriptionally reactivated clones is not simply an artifact of 5aCdr or HAT treatment, and is a requirement for transcriptional activation of the gene.

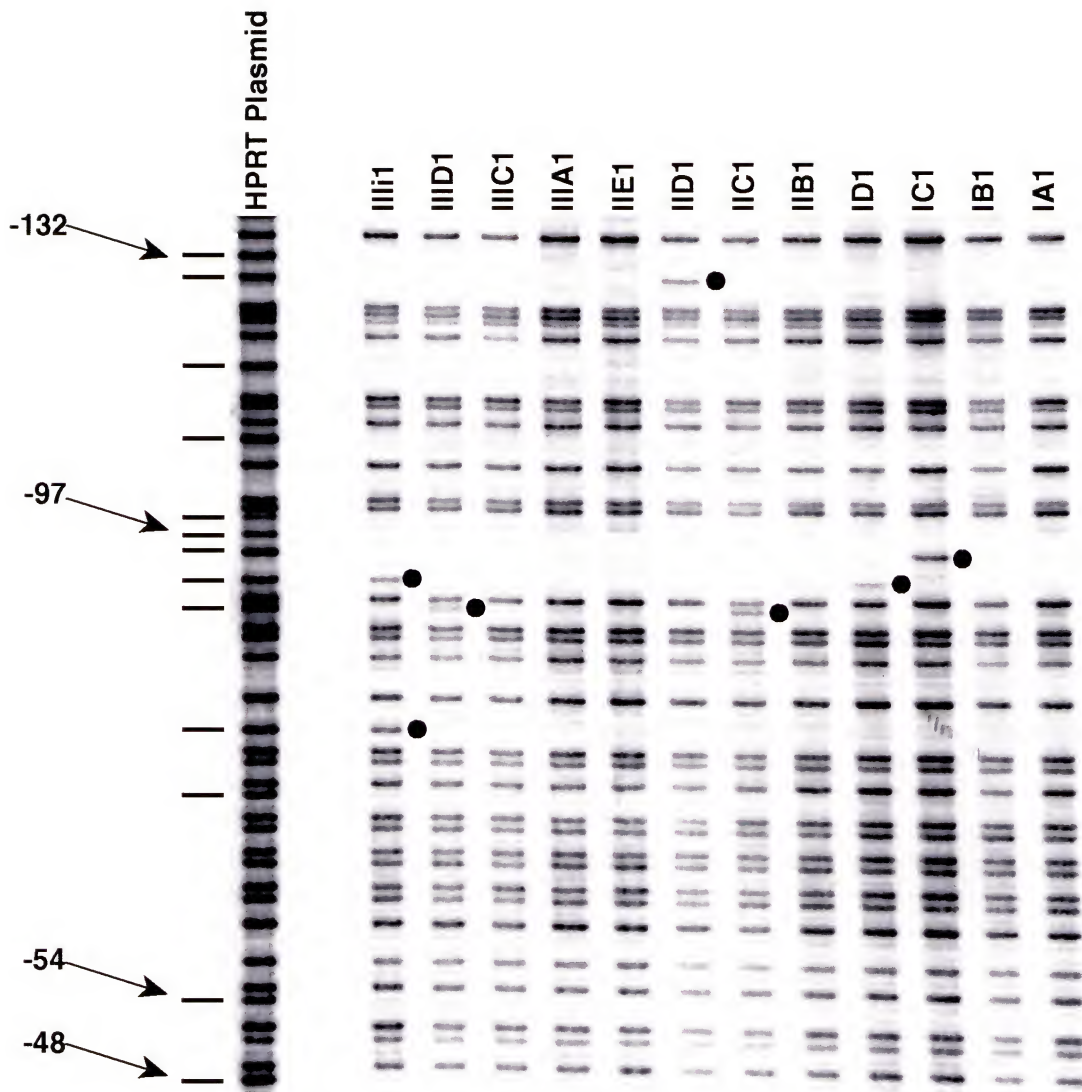


Figure 3-2. Representative autoradiogram of genomic sequencing analysis of the upper strand of the *HPRT* gene 5' region. The designation over each lane indicates the name of the clone examined. *HPRT plasmid* is a control sample showing the cytosine-specific sequencing ladder derived from plasmid DNA containing an unmethylated subclone of this region of the *HPRT* gene and reveals the position of every cytosine in the region. The horizontal bars on the left side of the figure indicate the positions of each CpG dinucleotide in the region. Demethylation events in each cell line appear as new bands in the cytosine-specific ladder at the position of the demethylation event. The solid circles indicate the position of demethylation events that have occurred in each clone. All position numbers are relative to the translation initiation site.

Consistent with these results, clones that failed to reactivate the *HPRT* gene following 5aCdr treatment had promoters that remained relatively hypermethylated compared to the unmethylated active *HPRT* allele (Figure 3-2). Among unreactivated clones, the extent and pattern of 5aCdr-induced demethylation at the *HPRT* promoter were quite variable, with as few as 0 and as many as 11 demethylated CpG sites out of a possible 20 methylated sites in the parental 8121 cells, with an overall frequency of 7.8% demethylation/site. Nevertheless, even the clone with 11 demethylated sites failed to express any detectable *HPRT* mRNA as determined by RT-PCR, suggesting that the repressive effect of methylation on transcription is not simply cumulative nor directly proportional to the number of methylated CpG sites.

Since any methylation site(s) essential for transcriptional repression should remain methylated in all unreactivated clones, the methylation patterns of each of the 61 unreactivated clones (see Appendix A) were compared (and summarized in Figure 3-3). This analysis identified 3 CpG's at positions -48, -54 and -97 (relative to the translation initiation site), which remain methylated on both strands in all 61 unreactivated 5aCdr-treated clones. The site at position -97 is located immediately upstream of a major transcription initiation site, and the sites at positions -48 and -54 are located approximately 35-45 bp downstream of the two major transcription start sites (in the portion of the gene encoding the 5' untranslated region). The perfect correlation between methylation at these 3 "critical" CpG sites and transcriptional repression of the *HPRT* gene in 61 independent clones suggests that methylation at these sites is necessary for maintaining repression of *HPRT* on the inactive X chromosome. In contrast, all other CpG sites examined in this region exhibited demethylation in at least one unreactivated

Figure 3-3. Summary of methylation analysis of the *HPRT* gene 5' region in unreactivated clones. The rows of squares immediately above and below the nucleotide sequence indicate the methylation pattern of the parental 8121 cell line. Open squares indicate unmethylated CpG dinucleotides, solid squares indicate methylated CpG dinucleotides and half-filled squares indicate sites methylated in some cells but not others. ? indicates sites for which the methylation status could not be determined due to technical limitations of the genomic sequencing methodology. Only those unreactivated clones whose methylation state differed from the parental pattern at a given CpG site are scored as open or solid circles. Each open circle represents one unreactivated clone that exhibited demethylation at the indicated CpG site. Each solid circle represents one unreactivated clone that exhibited *de novo* methylation at the indicated CpG site. Numbers in parentheses indicate the number of clones that demonstrated *de novo* methylation at a given CpG site. In these cases of *de novo* methylation, the number of circles is scaled to half the number of methylation events at each site. *ND* indicates that the methylation status of the CpG site was not determined because it could not be resolved with the primer set used for that strand. The large vertical ovals indicate the location of the 3 critical methylation sites that remain methylated in all 61 unreactivated clones. Bolded italicized *G*'s within the sequence indicate the location of DMS *in vivo* footprints in the region (75). Large open rectangles indicate the location of GC boxes. The arrowheads indicate the location of the two major transcription initiation sites determined by Kim et al. (91), while the dashed line between the upper and lower strands of the nucleotide sequence indicates the region of multiple transcription initiation sites described by Patel et al. (149). All position numbers shown are relative to the translation start site (149).

clone, indicating that methylation at each of these sites is not essential for maintaining transcriptional repression.

Statistical Analysis of the Demethylation Pattern in Unreactivated Clones

The 5aCdr-induced demethylation pattern observed in the 61 unreactivated clones was subjected to statistical analysis to determine the likelihood that the three critical CpG sites escaped 5aCdr-induced demethylation simply by chance. This analysis was performed by Dr. Mark C.K. Yang, Professor of Statistics at the University of Florida. To simplify the analysis, statistical analysis was performed using data only from the upper strand (which was informative at more sites than the lower strand). The null hypothesis H_0 is that the frequency of demethylation in the $m=20$ methylation sites examined in each clone is in fact uniform and the pattern observed is based on sampling error. We reject the null hypothesis if the number of sites that never demethylate, X , is too large. Let there be $r = 61$ clones and at the k^{th} clone, n_k of the sites have not been demethylated at least once. Then the p-value to reject the null hypothesis is calculated by the probability

$$[1] \quad \text{p-value} = \Pr\{X \geq x_0\},$$

where x_0 is the observed number of sites which never demethylated. Probability [1] can be computed recursively by letting

$$p(k, i) = \text{Probability that there are still } i \text{ methylated sites never demethylated after } k \text{ clones have been observed.}$$

Then, under H_0 ,

$$p(k,i) = \sum_{j=0}^m p(k-1,j) \binom{j}{i} \binom{m-j}{n_k-i} / \binom{m}{n_k}, k=2, \dots, r.$$

With the initial condition

$$p(1,i) = \begin{cases} 1 & \text{if } i=n_k \\ 0 & \text{otherwise} \end{cases}$$

The p-value [1] is

$$\text{p-value} = \sum_{i=x_0}^m p(r,i) \quad \text{for } m=20, r=61, n_k=19,20,17, \dots, 18 \text{ for } k=1,2,3, \dots, 61.$$

Based on this calculation, the p-value to reject the null hypothesis H_0 is 0.00003.

Therefore, the distribution of 5aCdr-induced demethylation events among the 20 methylated CpG sites examined is not uniform or random. This indicates that failure to demethylate the three critical methylation sites at -48, -54, and -97 in unreactivated clones is statistically significant and not due merely to chance. This analysis supports the notion that methylation of these CpG sites is required to maintain transcriptional repression of the *HPRT* gene.

Whether or not these 3 sites will ever demethylate in a 5aCdr-treated unreactivated clone is unclear. To distinguish between sites that never demethylate and those that have only a very small chance of demethylating would require an impractical volume of additional data. However, if we make the simplifying assumption that each of the three potential critical sites (at positions -48, -54, and -97) have the same demethylation probability p_1 , we can roughly estimate the maximal demethylation

frequency of these three sites relative to the other sites in the region. The average probability of demethylation at the 17 sites that did demethylate can be calculated as

$$p_0 = \frac{\text{total \# of demethylations}}{\text{total \# of sites examined}} = \frac{95}{17 \times 61} = 0.0916$$

Since the total # of demethylations in the 3 critical sites is 0, we cannot estimate a demethylation probability. However if we take a 95% upper bound for the probability of all three sites remaining methylated, this probability is $p_3 = -\ln(0.05)/95 = 0.0315$. The upper bound probability for each site then is

$$p_1 = 1 - (1 - 0.0315)^{1/3} = 0.0106$$

Therefore, we have a 95% confidence that the demethylation probability (p_1) of each of these three critical sites is no more than 1/9 the average demethylation probability (p_0) of each of the other 17 methylated sites. The significant difference in the maximal demethylation probability of the 3 critical sites relative to the other sites in the region is consistent with a functional role for methylation at these sites in unreactivated clones.

De Novo Methylation of the Human HPRT 5' Region

An unexpected finding in these studies is the 5aCdr-induced *de novo* methylation of the *HPRT* promoter just upstream and extending into a cluster of 5 GC boxes (spanning positions -217 to -163; see Figure 3) which are normally unmethylated on both the active and inactive X chromosomes (75). Every unreactivated 5aCdr-treated clone exhibited some level of *de novo* methylation in this region, with nearly 50% of the clones showing *de novo* methylation at positions -232, -220, -218, and -212, and

occasional *de novo* methylation occurring at positions –216 and –191. This *de novo* methylation occurs too frequently to simply arise from a small subpopulation of aberrantly methylated cells in the parental 8121 cell line. Because 5aCdr is a demethylating agent, *de novo* methylation is most likely a secondary rather than primary effect of 5aCdr treatment. However, since none of the clones that reactivated the *HPRT* gene (either spontaneously or as a result of 5aCdr treatment) show *de novo* methylation at any of these sites, the absence of methylation at these sites may be necessary for transcriptional reactivation. On the other hand, methylation at these sites is not a requirement for transcriptional repression, since the parental 8121 cells (where the *HPRT* gene is inactive) are not methylated at these sites (75). Recently, Broday et al. (27) also reported evidence for *de novo* methylation of silenced transgenes in cells treated with 5-azacytidine.

Reactivation Frequencies of Partially Demethylated Clones

To examine what role the overall level of promoter methylation may play in the transcriptional silencing of the *HPRT* gene, we further analyzed 12 clones which had not reactivated the *HPRT* gene after 5aCdr treatment but exhibited partial demethylation of the promoter to varying degrees. Each clone was subjected to a second round of 5aCdr treatment and the reactivation frequency of the *HPRT* gene in each clone was determined by selection in HAT medium (after normalizing for the plating efficiency of each clone in the absence of HAT). If transcriptional repression of the *HPRT* gene is dependent upon a threshold level of overall promoter methylation, clones with higher levels of pre-existing demethylation should exhibit a higher 5aCdr-induced reactivation frequency. However, if

methylation of specific critical sites is more important for maintaining repression, the reactivation frequency should be largely unaffected by the increasing levels of pre-existing demethylation at non-critical sites. The results of this experiment are shown in Table 3-I.

We found no correlation between pre-existing levels of stable demethylation in the promoter region and the 5aCdr-induced reactivation frequency of the *HPRT* gene. Most demethylated clones showed reactivation frequencies similar to that of the parental 8121 cells (no demethylated clone showed more than a 2-fold increase in reactivation frequency above 8121 cells), and the clone with the highest degree of pre-existing demethylation, (IIIA4), exhibited a normalized reactivation frequency slightly lower than 8121 cells. In fact, clones that showed the highest reactivation frequencies were one carrying no demethylated sites (NS2A11) and one carrying only a single demethylated site (IH7), while the clone with the lowest reactivation frequency had 8 demethylated sites (IIH1). Furthermore, the overall reactivation frequency of all partially demethylated clones re-treated with 5aCdr was 1.3% (calculated by: $(\text{Sum of all HAT-resistant colonies}) / (20 \times \text{Sum of all viable colonies})$), a level essentially identical to that of the 8121 parental cells.

This lack of correlation between overall levels of pre-existing demethylation and 5aCdr-induced reactivation frequencies is consistent with the existence of specific critical CpG sites whose methylation is required to maintain repression of the *HPRT* gene on the inactive X chromosome. Since all of the critical sites are methylated in all of the unreactivated clones, if reactivation requires demethylation of the critical sites, partial demethylation of non-critical sites would not be expected to affect subsequent 5aCdr-

Table 3-1. Human *HPRT* gene reactivation frequencies of clones after a second round of 5aCdr treatment.

Clone Designation	Number of Demethylated Sites	Plating Efficiency		Reactivation Frequency		Normalized Reactivation Frequency
		# of viable colonies / plate	% viable	# of HAT resistant colonies / plate	% reactivated	
NS1A4	0	278, 290	0.30	62, 56	0.28	1.0
ID1	0	320, 342	0.42	89, 79	0.33	1.3
IIIA2	0	394, 390	0.58	111, 119	0.39	1.5
IIIC1	0	520, 520	0.91	190, 174	0.52	1.7
NS2A11	0	370, 382	0.98	200, 190	0.38	2.6
IH7	1	264, 225	0.58	113, 119	0.24	2.4
IIIC2	3	621, 584	0.62	119, 130	0.60	1.0
IIC1	3	419, 383	0.54	118, 96	0.40	1.3
IVE1	4	339, 321	0.47	82, 105	0.33	1.4
IIIi1	5	600, 552	0.63	125, 128	0.58	1.1
IIHI	8	378, 405	0.05	8, 11	0.39	0.1
IIIA4	11	800, 820	0.75	138, 160	0.81	0.9
8121	N/A	475, 492	0.61	108, 134	0.48	1.2
X8-6T2*	N/A	1142*, 1095*	20.0	501*, 485*	0.45	44.0

Clonal lines were derived from 8121, a human/hamster hybrid cell line containing an inactive human X chromosome, after treatment with 5aCdr. The initial number of demethylated sites in the *HPRT* 5' region for each clone was determined by genomic sequencing. Each clonal line was treated with 1.0mg/ml of 5aCdr for 24 hours. Plating efficiency was determined by plating 1000 cells in each of two duplicate 150mm plates in nonselective medium and counting colonies after 10 days. Reactivation frequency was determined by plating 20,000 cells/150mm plate in duplicate under selection in HAT supplemented medium and counting HAT resistant colonies after 10 days. Normalized reactivation frequency is normalized for plating efficiency and calculated as described in Experimental Procedures. (*) Because it has a much higher reactivation frequency, both plating efficiency and reactivation frequency for X8-6T2 were determined by plating 2500 cells in duplicate in non-selective medium and HAT medium respectively.

induced reactivation. On the other hand, these results are not consistent with models that invoke threshold levels of overall promoter methylation for maintaining repression of transcription. Since partially demethylated clones should be closer to the threshold level of demethylation required for reactivation of the gene, these clones should undergo reactivation at consistently higher frequencies after re-treatment with 5aCdr. Because data in Table 3-I show this is not the case, and that partial demethylation of non-critical sites has little effect on subsequent reactivation frequencies, methylation at non-critical sites seems to play a secondary role in maintaining transcriptional repression.

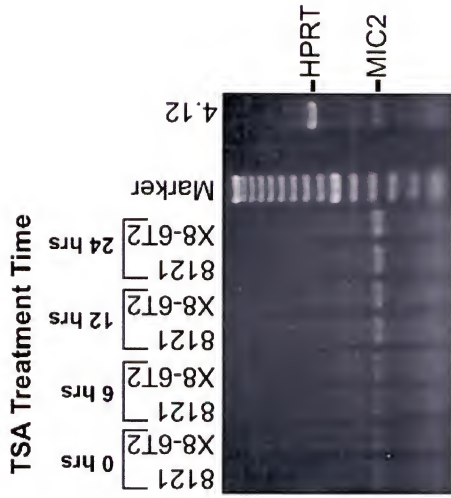
Effects of Trichostatin A Treatment on *HPRT* Transcription

Recent reports have suggested that MECP2 may mediate transcriptional repression at methylated promoters by recruiting histone deacetylases (86, 143). Therefore, it is possible that the 3 critical methylated sites in the *HPRT* promoter region may function on the inactive X chromosome by binding MeCP2 and recruiting histone deacetylases that, in turn, maintain the repressive chromatin structure of the promoter. However, *in vivo* footprinting studies of both the *HPRT* gene (77) and the human *PGK-1* gene (*PGK-1*) on the active and inactive X chromosomes (158, 160) have not detected any evidence for stable binding of MeCP2 at methylated CpG dinucleotides on the inactive X chromosome (i.e., no *in vivo* footprints have been detected over methylated CpG's). Despite this caveat, MECP2 may still play a role in repression of the *HPRT* locus since the absence of a footprint could indicate that either MECP2 binding is transient or that MECP2 simply does not footprint well.

Since trichostatin A (TSA) has been shown to alleviate MECP2-mediated repression (86, 143), two independent human/hamster hybrid cell lines, 8121 and X8-6T2, each containing an inactive human X chromosome, were treated for 0-24 h with TSA to assess the role of histone deacetylase-mediated repression of the *HPRT* promoter. If *HPRT* gene repression by DNA methylation functions primarily via histone deacetylases, TSA treatment should reactivate the *HPRT* gene on the inactive X chromosome. Furthermore, because X8-6T2 reactivates at a significantly higher frequency than 8121, both spontaneously and upon 5aCdr treatment (see Table 3-I), it may be more responsive to TSA-induced reactivation. Results of this study are shown in Figure 3-4A. While TSA treatment did appear to enhance the expression level of the control *MIC2* gene (an X-linked gene which escapes inactivation), as has been previously observed in other gene systems (83, 141), it failed to re-activate the *HPRT* gene on the inactive X chromosome in both cell lines as determined by RT-PCR (Figure 3-4A). The greater susceptibility of X8-6T2 cells to 5aCdr-mediated reactivation apparently does not confer a greater susceptibility to TSA-induced reactivation. These results are similar to that reported by Riggs et al. (167). Since these same cell lines can be reactivated by 5aCdr treatment, repression of the *HPRT* gene by DNA methylation is probably not mediated primarily by the mechanism identified by Nan et al and Jones et al. (86, 143).

Recently, Cameron et al. (34) have shown that high density methylation at the promoter may prevent TSA from reactivating genes even when histone deacetylases are involved in their transcriptional repression. Partial demethylation of the promoter can overcome this resistance to TSA-mediated reactivation, revealing a role for histone deacetylases in maintaining repression. To determine if the high density methylation of

A



B

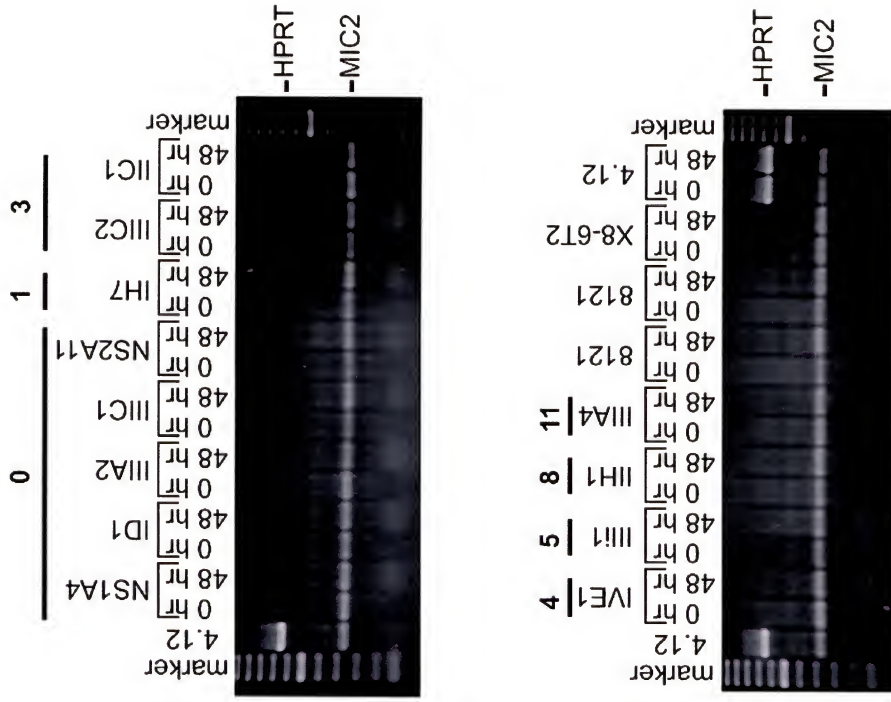


Figure 3-4. Trichostatin A treatment of cell lines containing an inactive *HPRT* allele. A. Time course of trichostatin A treatment of 8121 and X8-6T2 cells. RT-PCR analysis of HPRT gene reactivation in 8121 and X8-6T2 cells, two human/hamster hybrid cell lines containing an inactive human X chromosome, during a 24hr TSA (300nM) treatment time course. HPRT indicates the expected position of the HPRT RT-PCR product. MIC2 indicates the expected position of the RT-PCR product for human MIC2, a gene that escapes X inactivation and serves as an internal RT-PCR control. 4.12 is a human/hamster hybrid cell line containing an active human X chromosome and serves as an external positive RT-PCR control. B. Analysis of HPRT gene reactivation after 48 hrs of TSA treatment in cell lines, clonally derived from 8121 cells, that failed to reactivate the HPRT gene after 5aCdr treatment. The bolded numbers above the clone designations indicate the number of sites in the HPRT 5' region which are demethylated in each clone. Other designations are as above.

the *HPRT* promoter is preventing reactivation of the *HPRT* gene by TSA, each of the 12 partially and stably demethylated clonal lines shown in Table 3-I above were treated with TSA for 0-48 hours and assayed for *HPRT* expression by RT-PCR. Each of these single cell derived clones from 8121 cells carried 0 to 11 CpG sites that were stably demethylated after 5aCdr treatment, yet maintained stable repression of the *HPRT* gene. As shown in Figure 3-4B, regardless of the level of pre-existing promoter demethylation (i.e., number of pre-existing demethylated CpG's), TSA treatment failed to reactivate the *HPRT* gene in any of the partially demethylated clones. This was true even for clone IIIA4 which is stably demethylated at 11 of 20 CpGs in the promoter. These results indicate that inhibition of histone deacetylation is not sufficient to overcome the repressive effects of DNA methylation, even in the context of reduced levels of promoter methylation. Because all of the demethylated sites in each of these TSA-treated clones are non-critical sites, these results are also consistent with a mechanism of DNA methylation-dependent repression involving specific critical sites of methylation.

Discussion

We have examined the high-resolution methylation pattern of the endogenous *HPRT* promoter region in 61 clonally-derived lines that have undergone 5aCdr-induced demethylation but failed to reactivate the *HPRT* gene. Statistical analysis reveals a highly significant ($p=0.00003$) correlation between maintenance of transcriptional repression and methylation at 3 specific CpG sites. In contrast, the other CpG's in the promoter region (outside these 3 "critical" sites) appear to be able to undergo demethylation without affecting repression of the gene, even when as great as 55% of the CpG sites in

the promoter are demethylated (see clone IIIA4 in Table 3-I). Furthermore, prior demethylation of the promoter region at non-critical CpG sites does not increase the frequency of *HPRT* gene reactivation after re-treatment of cells with a second round of 5aCdr. These data argue that 3 critical sites in the promoter region contribute disproportionately to the repression of the *HPRT* gene on the inactive X chromosome, and that methylation of critical sites rather than the overall level of promoter methylation (or a certain threshold level of promoter methylation) is involved in maintaining transcriptional silencing.

None of the 3 critical sites of methylation fall within any of the transcription factor binding sites previously identified by DMS *in vivo* footprinting (77), although the critical site at -97 lies just upstream of a DMS footprinted region (see Figure 3). The other two critical sites at positions -54 and -48 are located at least 21 bp from the nearest DMS *in vivo* footprinted region and DNase I *in vivo* footprinting studies fail to detect footprints at or near these two sites on either the active or inactive X chromosome (C. Chen, T.P. Yang; in preparation). Therefore, it is unlikely that a major mode of action for the 3 critical CpG sites involves interference with transcription factor binding upon methylation of these sites as proposed by Tate et al. (189). Furthermore, Rincon Limas et al. (168) have shown that the region containing the 3 critical CpG sites is not required for maximal expression of the *HPRT* gene in transient expression assays. Thus, this region may be required more for repression of the gene on the inactive X chromosome than for activation or expression.

This suggests, at least in part, an indirect mechanism of methylation-mediated repression of the *HPRT* gene. Recent reports have indicated that repression by

methylation involves MECP2 recruitment of histone deacetylases (86, 143), a mechanism that was shown to be TSA sensitive. However, we find the *HPRT* gene on the inactive X chromosome is resistant to reactivation by TSA, even when the promoter is partially (and stably) demethylated by 5aCdr treatment. This would suggest that methylation-mediated repression of the *HPRT* gene on the inactive X chromosome could act by either of two possible mechanisms. One possibility is that silencing of the *HPRT* gene does not involve a histone deacetylase complex; however, antibodies against acetylated histone H4 clearly show that the inactive X chromosome is hypoacetylated (82). Alternatively, repression of the *HPRT* gene by methylation could involve one or more histone deacetylases that are TSA-resistant, similar to those reported in yeast (36). It is also possible that the dynamic turnover of deacetylated histones on the inactive X chromosome is so slow, or histone acetylation occurs at such a low level on the inactive X, that inhibiting histone deacetylases does not lead to significant hyperacetylation of the *HPRT* gene.

While transcriptional repression of the *HPRT* gene may require methylation at specific critical sites, reactivation appears to require complete demethylation of the promoter. The association between complete promoter demethylation and transcriptional reactivation is not specific to 5aCdr-induced reactivation because it also occurs in spontaneous reactivants. Complete promoter demethylation is also seen in the X-linked human phosphoglycerate kinase gene (*hPGK-1*) upon 5aCdr-mediated reactivation (159). Together with the fact that the promoters of other X-linked housekeeping genes on the active X chromosome are also generally unmethylated (120, 160, 192, 194), these observations argue that the absence of methylation in the promoter *in vivo* is essential for transcription of the *HPRT* gene and other X-linked housekeeping genes.

Since demethylation of all 20 CpG sites in the promoter region in a single cell appears to be required for reactivation of the *HPRT* gene, the average overall 5aCdr-induced demethylation frequency of 7.8% at each CpG is too low by itself to account for the observed reactivation frequency of the 8121 parental cells (see Table 3-I). Therefore, in order to achieve full promoter demethylation and the *HPRT* reactivation frequency we observed for 8121 cells, active demethylation of the promoter region must occur following a crucial initial 5aCdr-induced demethylation event. Such demethylase activities have been reported recently (13, 205). We propose that the crucial event that triggers active demethylation of the promoter (and subsequent gene reactivation) is the stable demethylation of one of the 3 critical sites. Thus, the reason we never detected one of the critical sites in an unmethylated state in unreactivated clones is because demethylation of a single critical site resulted in active global promoter demethylation and gene reactivation.

Alternatively, the actual 5aCdr-induced demethylation frequency may be significantly higher than what is observed in the stable cell lines due to active remethylation of the promoter after 5aCdr is removed. The high frequency of *de novo* methylation observed at certain CpG sites in the *HPRT* promoter of unreactivated clones suggests that active remethylation of the promoter does occur in these cells. This remethylation activity could account for the discrepancy between the overall stable demethylation frequency we observe and the reactivation frequency of the 8121 cell line. Since the critical methylation sites are always methylated in cell lines that fail to reactivate the *HPRT* gene, these critical sites may either be relatively resistant to demethylation or have a propensity to remethylate. This tendency to maintain the

methyated status of the critical sites might act to prevent full promoter demethylation and reactivation of the *HPRT* gene.

Overall, these studies suggest that transcriptional repression by methylation is a complex process involving non-equivalent methylation sites that appear to repress transcription by indirect mechanisms. The complete demethylation apparently necessary for reactivation and the evidence for *de novo* methylation further suggest that methylation itself is dynamic, a product of intrinsic active methylation and demethylation processes.

CHAPTER 4
EXAMINATION OF THE TRANSLATIONAL AND ROTATIONAL POSITIONING
OF NUCLEOSOMES ON THE ACTIVE AND INACTIVE *HPRT* PROMOTER

Introduction

Differential chromatin structure is one of the hallmarks distinguishing active and inactive genes. For the X-linked human hypoxanthine phosphoribosyltransferase gene (*HPRT*), this difference in chromatin structure is particularly evident in the promoter where both general DNase I sensitivity and hypersensitivity is enhanced in the active versus inactive alleles. To better understand the interrelationship between nucleosomal organization, chromatin accessibility, DNA methylation and transcription at the *HPRT* promoter, we have examined both the translational positioning of nucleosomes and the rotational orientation of these nucleosomes on the active and inactive *HPRT* promoters *in vivo*. Translational positioning of nucleosomes was determined by micrococcal nuclease (MNase) digestion *in vivo* and the rotational orientation of nucleosomes was determined by high-resolution *in vivo* DNase I cleavage analysis.

The *in vivo* micrococcal nuclease digestion pattern of chromatin from the active allele reveals an ordered array of translationally phased nucleosomes in the promoter region except over a 350 bp region which is either non-nucleosomal or contains structurally altered nucleosomes based on hypersensitivity to both micrococcal nuclease and DNase I. This 350 bp region includes the entire minimal promoter and all of the transcription initiation sites of the *HPRT* gene. It also encompasses all of the *in vivo*

transcription factor binding sites identified by either dimethyl sulfate (77) or DNase I *in vivo* footprinting.

In contrast, analysis of the inactive *HPRT* promoter reveals neither translational phasing of nucleosomes nor hypersensitivity to either DNase I or micrococcal nuclease. Despite this absence of translationally phased nucleosomes on the inactive promoter, high-resolution *in vivo* DNase I cleavage analysis indicates rotational phasing of nucleosomes over a region of at least 210 bp including the entire minimal promoter on the inactive allele. This rotational phasing of nucleosomes is not observed on the active allele. These results suggest that rotationally phased nucleosomes repress *HPRT* transcription and that disruption of this rotational phasing and establishment of a translationally phased nucleosomal array are involved in transcriptional activation.

Results

To better understand the role that chromatin structure plays in the differential transcriptional regulation of the X-linked human *HPRT* gene, we have examined both the translational positioning and rotational orientation of the nucleosomes at the endogenous *HPRT* promoter on the active and inactive X chromosomes in permeabilized cells. Identifying the differences in the nucleosomal organization of the active vs. inactive *HPRT* promoters will improve our understanding of the underlying basis for differential chromatin accessibility. Furthermore, understanding the spatial relationship of functional elements of the promoter relative to its nucleosomal structure may provide insight into the mechanisms of transcriptional activation and repression at the endogenous *HPRT* locus.

Translational Positioning of Nucleosomes on the *HPRT* Promoter *In Vivo*.

To examine the translational position of nucleosomes at the human *HPRT* promoter *in vivo*, cells containing either the active *HPRT* allele on the active human X chromosome or the inactive *HPRT* allele on the inactive X chromosome were permeabilized using the detergent, NP-40, and then treated with micrococcal nuclease (MNase). MNase preferentially cleaves DNA within the linker region between nucleosomal cores and, in conjunction with indirect end-labeling, can thus identify the presence and positions of translationally phased nucleosomes within a region of chromatin. The positions of the *in vivo* MNase cleavages within the chromatin of the *HPRT* promoter were mapped relative to a downstream Bcl I site in the first intron of the *HPRT* gene using a 400bp hybridization probe located just upstream of the Bcl I site (Figure 4-1). To determine the positions of known DNase I hypersensitive sites relative to these *in vivo* MNase cleavages, NP-40 permeabilized cells containing the active *HPRT* allele were treated with DNase I and the DNase I hypersensitive sites in chromatin of the *HPRT* promoter were mapped relative to the same Bcl I site.

Figure 4-2 shows the Southern blot analysis of the DNase I and MNase cleavage patterns on the active and inactive *HPRT* promoters in permeabilized cells (*In vivo*) or in naked DNA (*In vitro*). *In vivo*, the active *HPRT* promoter exhibited a pattern of strong MNase cleavages with a periodicity of approximately 200 bp as represented by cleavages at -260, -460, -660, -840, -1040, -1220 and -1420 relative to the translation initiation site (Figure 4-2B *In vivo* samples). This cleavage ladder is indicative of 6 distinct translationally phased nucleosomes positioned immediately upstream of the potential

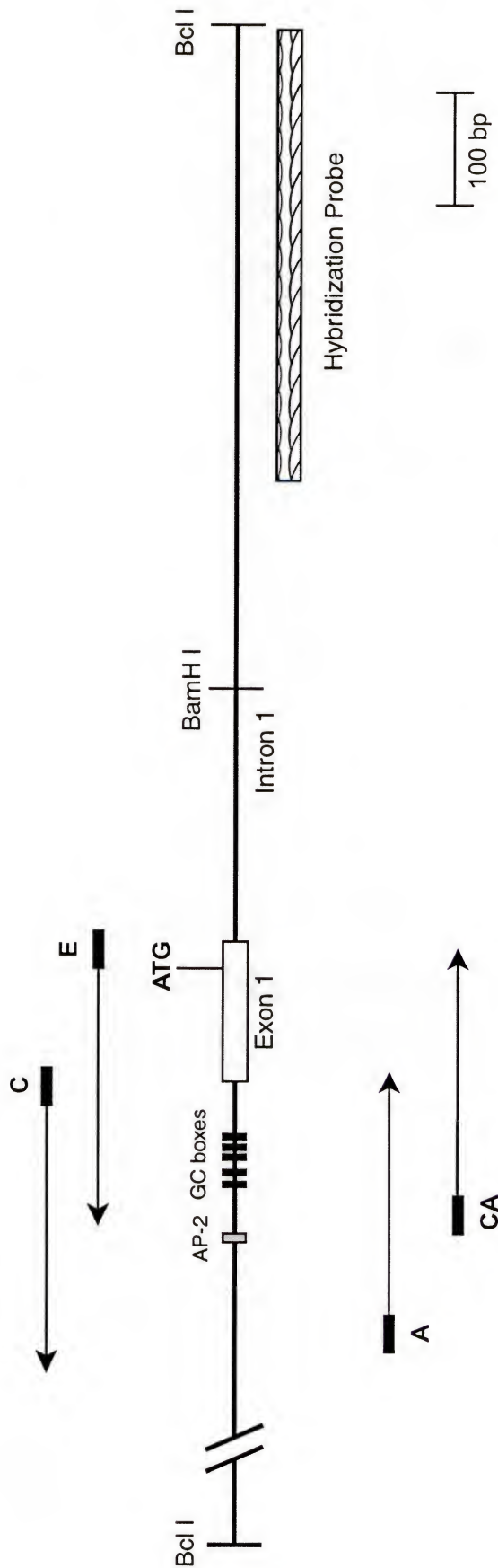
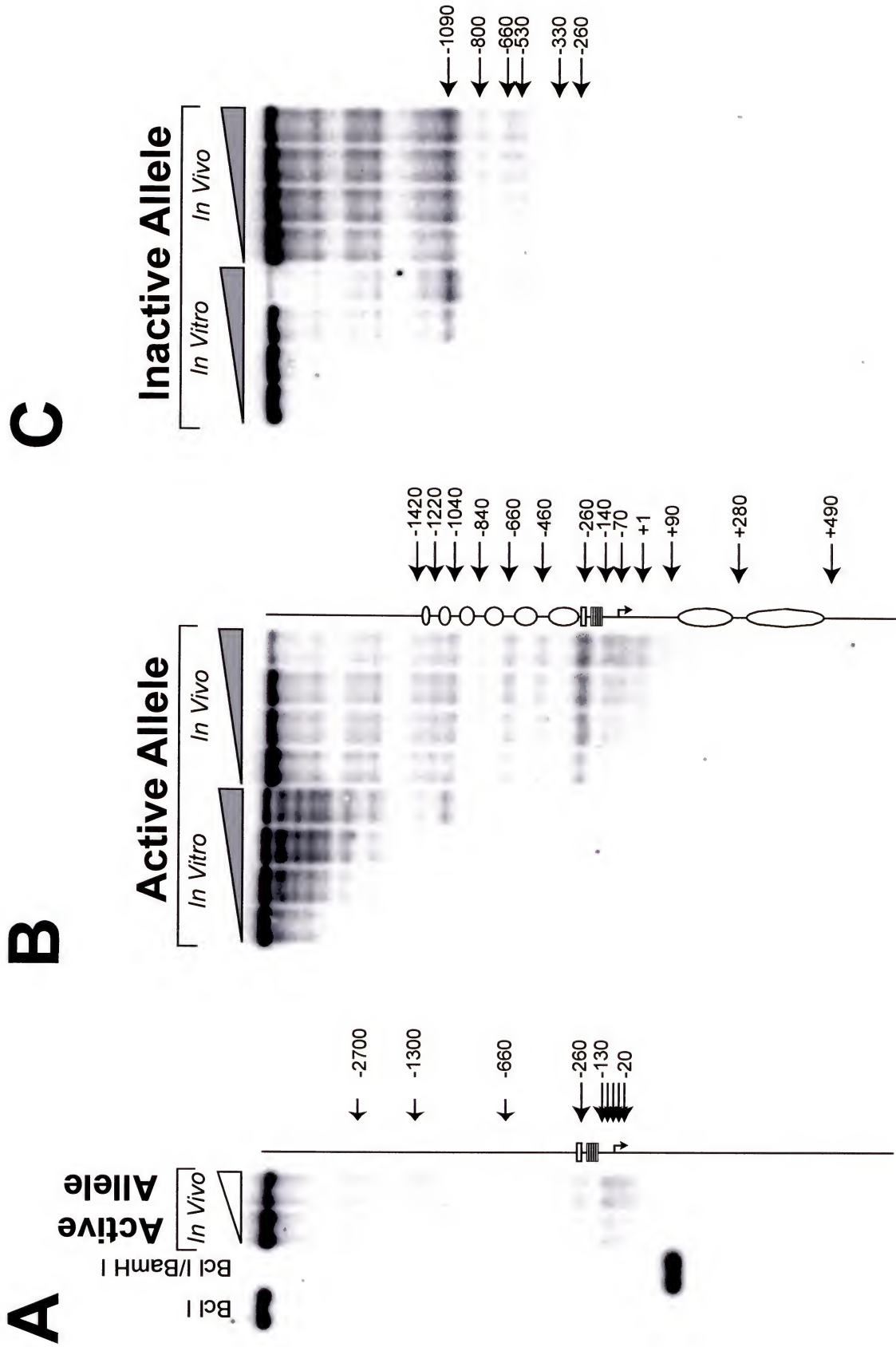


Figure 4-1: Locations of probes and primers used for mapping nucleosomal position and rotational orientation within a Bcl I fragment containing the *HPRT* promoter. The thick line bounded by vertical hatches labeled Bcl I represents the Bcl I fragment containing the *HPRT* promoter. On this line, the small gray box represents the potential AP-2 site and 5 small black boxes represent the cluster of GC boxes in the *HPRT* promoter. The large white box represents the first exon of the *HPRT* gene including the region of multiple transcription initiation sites in the promoter and ATG indicates the translation initiation site. BamH I indicates the position of a reference BamH I site 100 bp downstream of the translation initiation site. The large cross-hatched box below the line indicates the position of the hybridization probe used to map DNase I and MNase hypersensitive sites in the *HPRT* promoter by indirect end-labeling. The black rectangles above and below the line indicate the positions of the LMPCR primer sets used to map the high-resolution DNase I cleavage pattern of the *HPRT* minimal promoter and the arrows extending from these boxes indicate the strand and region examined by each primer set.

AP-2 site on the active *HPRT* promoter (see Figure 4-1 and 4-2B). A second ladder consisting of 3 weak MNase cleavage sites at +90, +280, and +490 defined an additional two translationally phased nucleosomes in the first intron of the *HPRT* gene (Figure 4-2B *In vivo* samples). While these downstream sites were relatively weak, they were consistently reproducible in multiple independent MNase assays and were clearly present in longer exposures (data not shown). An additional weak cleavage site was observed within the first downstream nucleosome at position +170 upon longer exposures and may represent a preferential cleavage site for MNase in naked DNA. The gap between the upstream and downstream nucleosomal arrays is approximately 350 bp and includes the all of the known transcription factor binding sites of the *HPRT* promoter as well as the multiple transcription initiation sites. This 350 bp region appears to be hypersensitive to MNase cleavage as represented by the cleavages at -170, -70, and +1 and the greatly enhanced cleavage at -260 (Figure 2B). The pattern of periodic cleavages observed in the chromatin of the active allele is not observed on MNase treated naked DNA (Figure 4-2B *In vitro* samples), even at MNase concentrations sufficient to completely degrade the parental 4.3 Kb Bcl I band (data not shown), indicating that these periodic cleavages are a product of nucleosomal organization rather than the DNA sequence

Unlike the active allele, the MNase cleavage pattern of the inactive *HPRT* promoter in permeabilized cells did not exhibit a 200 bp periodicity (Figure 4-2C *In vivo* samples). In fact, the *in vivo* MNase cleavage pattern of the inactive *HPRT* promoter was essentially identical to that of MNase-treated naked DNA (*In vitro* samples in Figure 4-2C). The similarity of the MNase cleavage pattern between the chromatin of the inactive allele in permeabilized cells as compared to naked DNA was verified at higher MNase

Figure 4-2: Mapping of DNase I hypersensitivity and nucleosomal positioning on the promoters of the active and inactive *HPRT* alleles in permeabilized cells by indirect end-labeling. All lanes in figure 2 represent a single autoradiograph from a single agarose gel but are divided here for clarity. All fragments are visualized by indirect-labeling with a probe just upstream of a reference Bcl I site 838 bp downstream of the translation initiation site of the *HPRT* gene. *Active Allele* indicates DNA from cells containing an active *HPRT* gene on the active human X chromosome. *Inactive Allele* indicates DNA from cells containing an inactive *HPRT* gene on the inactive human X chromosome. *In vivo* indicates DNA from permeabilized cells which were treated *in vivo* with increasing concentrations of DNase I or MNase. *In vitro* indicates naked genomic DNA treated *in vitro* with increasing concentrations of MNase. All numbers are relative the translation initiation sites of the *HPRT* gene. **A)** Mapping of DNase I hypersensitive sites within the active *HPRT* promoter. The band in the lane labeled Bcl I indicates position of the full length Bcl I fragment containing the *HPRT* promoter. The band in the lane labeled Bcl I/BamH I indicates the relative position of a BamH I site 100 bp downstream of the translation initiation site. The lanes labeled Active Allele show the relative positions of DNase I hypersensitive sites on the active *HPRT* allele. The diagram to the right indicates the positions of the DNase I hypersensitive sites relative to transcription factor binding sites (small boxes) and the major transcription initiation sites of the *HPRT* promoter. **B)** Mapping of translationally phased nucleosomes on the active *HPRT* promoter by MNase digestion. All designations are as above. The diagram to the right of the autoradiograph indicates the apparent translational positions of phased nucleosomes (ovals) on the active allele of the *HPRT* promoter as determined by the *in vivo* MNase cleavage pattern. **C)** Absence of translationally phased nucleosomes on the inactive *HPRT* promoter by MNase digestion.



concentrations that allowed more complete examination of lower molecular weight bands (data not shown). This similarity between the *in vivo* and naked DNA MNase cleavage patterns in the inactive allele (albeit at much higher MNase concentrations *in vivo*), indicates that MNase cleavage at the inactive allele is largely determined by the underlying DNA sequence rather than the nucleosomal structure, suggesting that nucleosomes are randomly positioned on the inactive *HPRT* promoter *in vivo* and therefore cannot bias MNase cleavage.

Since DNase I hypersensitivity is characteristic of the active *HPRT* promoter *in vivo*, we mapped the location of the DNase I hypersensitive sites in the active promoter relative to the phased nucleosomes in the promoter to examine the basis of this hypersensitivity. Two major and 3 minor DNase I hypersensitive regions were observed in the chromatin of the active *HPRT* promoter (Figure 4-2A, lanes labeled *Active Allele*). All three minor hypersensitive sites, centered at approximately -670, -1300 and -2700, co-mapped to complete or partial Alu repeat elements, possibly indicating transcription factor binding at these repeats. However, both of the major DNase I hypersensitive sites, centered at -260 and -70, map to the 350 bp region which did not exhibit translational nucleosomal phasing on the active promoter. The major DNase I hypersensitive site centered at about -260 mapped between the potential AP-2 site and the cluster of CG boxes in the active *HPRT* promoter. The other DNase I hypersensitive site, which was much broader and encompassed the region from about -20 to -130, mapped immediately downstream of the CG boxes in a region which encompasses the major transcription initiation sites (4-Figure 2A). On the active *HPRT* allele, these two major DNase I hypersensitive regions also exhibit significant MNase hypersensitivity as seen by the

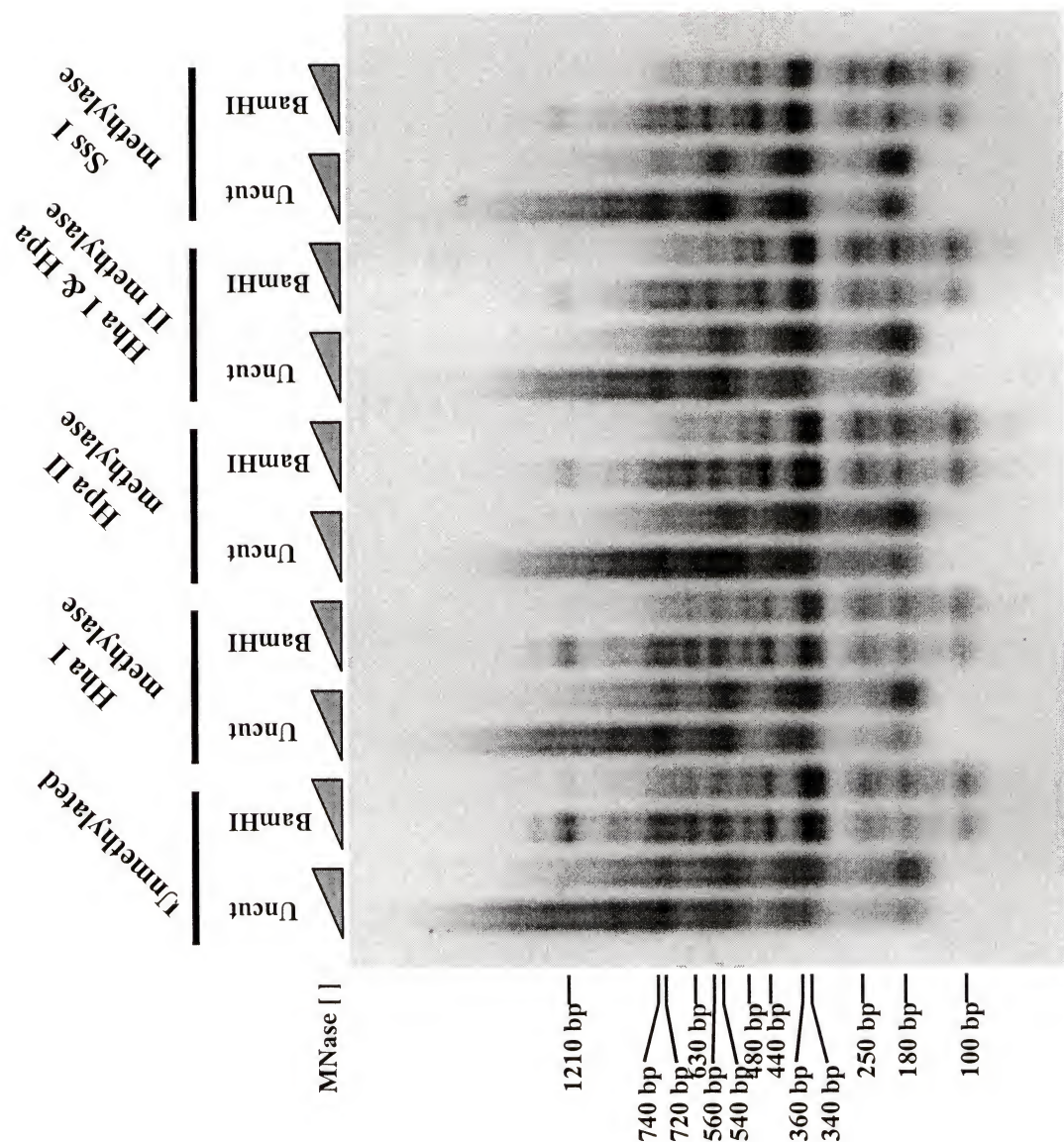
MNase cleavages at -260, -140, -70, and +1 (Figure 2B, *In vivo* samples) but were not hypersensitive to either DNase I ((117)) or MNase on the inactive allele (Figure 4-2C, *In vivo* Samples). These MNase hypersensitive bands were also not present in MNase-treated naked DNA from cells containing either the active or inactive *HPRT* genes even at much higher MNase concentrations than shown in Figure 4-2 (data not shown), indicating that this MNase hypersensitivity in the active allele is a product of the chromatin structure of the active allele rather than the underlying DNA sequence. The DNase and MNase hypersensitivity of this 350 bp region on the *active HPRT* promoter is likely to indicate that this region is devoid of nucleosomes or has modified nucleosomes which are more accessible to trans-acting factors.

Overall, the data in Figure 4-2 suggest that the promoter of the transcriptionally active *HPRT* allele is assembled into an ordered array of translationally phased nucleosomes interrupted by a nuclease hypersensitive 350 bp interval that contains most of the known functional elements of the *HPRT* promoter including the AP-2 site, the cluster of GC boxes and the region of multiple transcription initiation sites. The DNase I and MNase hypersensitivity of this 350 bp region suggest that nucleosomes are either completely excluded from this region or modified to become nuclease hypersensitive, and therefore more accessible to trans-acting factors. In contrast, no translational phasing is evident on the inactive *HPRT* promoter and hypersensitivity to DNase I and MNase within this 350 bp region is also absent.

Effects of DNA Methylation on the Translational Phasing of Nucleosomes on the *HPRT* Promoter *In Vitro*

Since the active and inactive *HPRT* promoters exhibit differential DNA methylation, we examined the possibility that this differential methylation is responsible for the differences in the translational positioning of nucleosomes between the active and inactive *HPRT* promoters. This analysis was carried out by reconstituting nucleosomes *in vitro* onto unmethylated versus methylated supercoiled plasmid constructs containing the human *HPRT* promoter. The reconstituted chromatin was then digested with MNase and the positions of MNase cleavages within the methylated and unmethylated *HPRT* promoter constructs were examined relative to a BamHI site within the first intron. The results of this analysis can be seen in Figure 4-3. When the reconstituted chromatin is cleaved only with MNase (Figure 4-3, lanes labeled *Uncut* for each template), an approximately 180 bp ladder is observed. This pattern indicates that nucleosomes are being assembled in ordered arrays onto all templates regardless of their methylation status. However, when the templates are subsequently digested with BamHI, this 180 bp ladder disappears in all templates, regardless of their methylation status (Figure 4-3, lanes labeled BamHI for each template). This result suggests that the ordered arrays of nucleosomes that assemble *in vitro* onto the *HPRT* promoter templates are not predominantly in a single translational phase. This is in direct contrast to the strong translational positioning observed on the active *HPRT* promoter in permeabilized cells. Furthermore, the cleavage pattern generated upon BamHI cleavage is identical regardless of the methylation status of the template (Figure 4-3, lanes labeled BamHI for each template), suggesting that DNA methylation does not affect the translational positioning of nucleosomes on the *HPRT* promoter *in vitro*.

Figure 4-3: Effects of DNA methylation on the translational positioning of nucleosomes on the human *HPRT* promoter *in vitro*. Nucleosomes were assembled *in vitro* onto methylated and unmethylated DNA templates containing the human *HPRT* promoter. *HpaII* methylase, *HhaI* methylase, and *SssI* methylase indicate the DNA methyltransferases used to methylate each template. *Uncut* indicates reconstituted chromatin that was digested with MNase but not BamHI. *BamHI* indicates reconstituted chromatin that was digested with MNase, purified and then digested with BamHI. All samples were probed with BamHINuc1Probe, an 18-mer oligonucleotide immediately upstream of the BamHI site in the first intron of the *HPRT* gene. The triangles indicate increasing MNase concentrations used to cleave the reconstituted chromatin. The numbers to the left of the figure indicate the approximate sizes of each band.

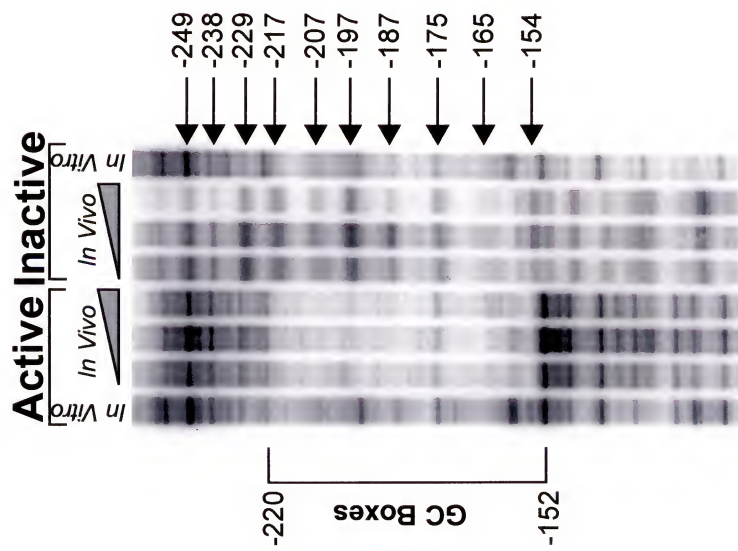
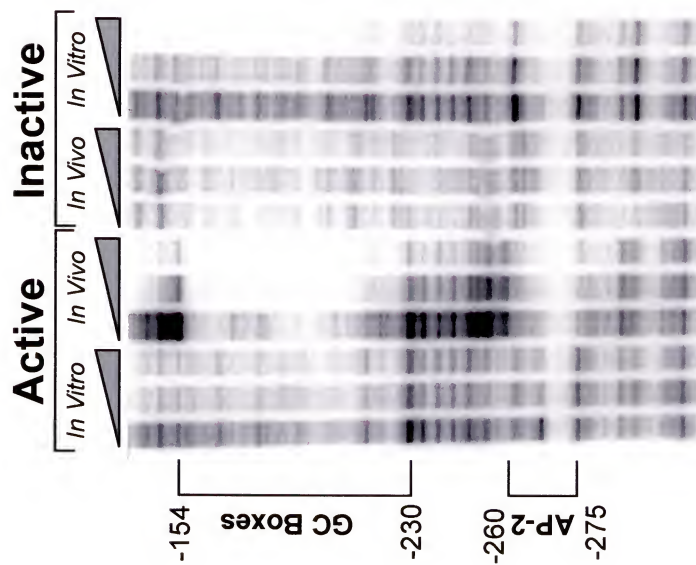
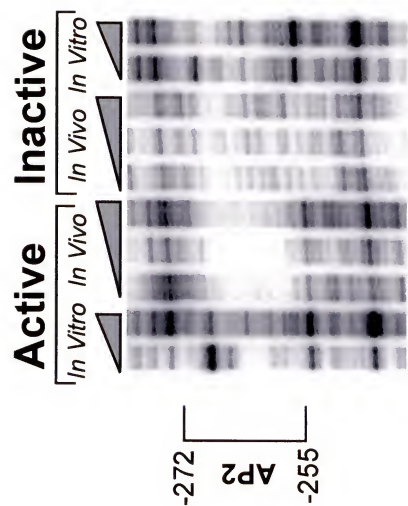


DNase I *In Vivo* Footprinting of the Human *HPRT* Promoter

The translational organization of nucleosomes in the chromatin of the active *HPRT* promoter relative to the major transcription initiation sites, the potential AP-2 binding site and the cluster of GC boxes strongly suggests that the 350 bp nuclease hypersensitive region is the functional promoter *in vivo*. To more closely examine this region, we performed DNase I *in vivo* footprinting analysis, concentrating on the minimal promoter within this region. DNase I *in vivo* footprinting is based on the steric hindrance of DNase I cleavage by factors bound to DNA *in vivo*, resulting in “footprints” consisting of regions which appear to be relatively protected from DNase I cleavage as compared to naked DNA. DNase I *in vivo* footprints are also characterized by enhanced DNase I cleavage at the borders of the footprint, although the reason for this hypersensitivity is not known. DNase I *in vivo* footprinting analysis was performed by treating permeabilized cells with increasing concentrations of DNase I, purifying the genomic DNA, and examining the DNase I cleavage pattern of the region of interest by ligation-mediated PCR (LMPCR). The strand and region covered by each of the LMPCR primer sets used in this analysis are shown in Figure 4-1.

This analysis of the minimal promoter identified two major DNase I *in vivo* footprints on the active *HPRT* allele, which corresponded to the potential binding site for AP-2 and the cluster of GC boxes (Figure 4-4). The footprint over the GC boxes extended from -152 to -220 on the upper strand (Figure 4-4A) and -154 to -230 on the lower strand (Figure 4-4B). The footprint over the potential AP-2 binding site spanned -255 to -272 on the upper strand (Figure 4-4C) and -260 to -275 on the lower strand (Figure 4-4B). This study complements previous dimethyl sulfate (DMS) *in vivo* footprinting

Figure 4-4: DNase I *in vivo* footprinting analysis of the human *HPRT* promoter. *Active* indicates samples from cells containing an active *HPRT* gene on the active human X chromosome. *Inactive* indicates samples from cells containing an inactive *HPRT* gene on the inactive human X chromosome. *In vitro* indicates naked DNA treated *in vitro* with DNase I. *In vivo* indicates DNA from permeabilized cells treated *in vivo* with DNase I. The bracket labeled *GC Boxes* indicates the position of a DNase I *in vivo* footprint over the 5 GC boxes in the human *HPRT* promoter. *AP-2* indicates the position of a DNase I *in vivo* footprint over a putative consensus AP-2 site in the human *HPRT* promoter. All numbers are relative to the translation initiation site of the *HPRT* gene. **A)** DNase I *In vivo* footprinting analysis of the upper strand of the *HPRT* promoter using the E primer set. This analysis identifies footprints over a cluster of 5 GC boxes in the active *HPRT* promoter. The arrows indicate an apparent 10 bp ladder consistent with a rotationally phased nucleosome on the inactive *HPRT* promoter. **B)** DNase I *in vivo* footprinting analysis of the lower strand of the *HPRT* promoter using the A primer set. This analysis identifies footprints over both a cluster of 5 GC boxes and a putative AP-2 site in the active *HPRT* promoter. **C)** DNase I *in vivo* footprinting analysis of the upper strand using the C primer set. This analysis identifies a DNase I *in vivo* footprint over a putative AP-2 site on the active *HPRT* promoter and a weaker footprint over the 5 GC boxes (see figure 4-6).

A**B****C**

studies (77), which identified footprints over the potential AP-2 binding site and the cluster of GC boxes, by further defining the extent of protein/DNA contact at these sites. However, the DMS *in vivo* footprinting study also identified a footprint over the two major transcription initiation sites of the active promoter. This footprint was not observed by DNase I *in vivo* footprinting in 4.12, the human/hamster hybrid containing the active X chromosome that was used in both studies. Interestingly, a DNase I *in vivo* footprint was present at the major transcription initiation sites in human male fibrosarcoma cell line, HT1080, suggesting that the hamster factors which bind at this site may be detectable by DMS but not DNase I *in vivo* footprinting (data not shown).

In contrast, *in vivo* footprinting analysis did not reveal any DNase I footprints on the inactive *HPRT* promoter. These results agree with previous DMS *in vivo* footprinting studies that indicate that no transcription factors are bound on the inactive allele. The absence of DNase I *in vivo* footprints on the inactive *HPRT* allele is also consistent with the absence of the nuclease hypersensitive sites on the inactive *HPRT* promoter. These data suggest a functional relationship between the hypersensitivity of the *HPRT* promoter and the binding of transcription factors to the promoter *in vivo*.

Rotational Orientation of Nucleosomes at the *HPRT* Promoter

The high-resolution DNase I cleavage pattern generated by DNase I *in vivo* footprinting can also identify the presence of rotationally phased nucleosomes in chromatin. DNase I interacts with the minor groove of DNA and can cleave DNA wrapped around the histone octamer but the accessibility of the minor groove to DNase I varies as a function of the helical path of the DNA as winds around the histone octamer.

Where the minor groove is faced directly away from the histone octamer and therefore maximally exposed to the solution, DNase I is thought preferentially cleave the DNA. When a nucleosome is rotationally phased within the population of cells, this differential accessibility of the DNA wrapped around the histone octamer results in a pattern of preferential DNase I cleavages at approximately 10 bp intervals corresponding to the helical pitch of DNA that can be visualized as a 10 bp pair ladder in a sequencing gel (147).

Such a 10 bp ladder was in fact observed on the inactive allele of the *HPRT* promoter *in vivo* (Figures 4-4A, 4-5 & 4-6). Interestingly, while there was some overlap, the 10 bp ladder was strongly evident on only one strand at a time. This 10 bp ladder on the inactive promoter was most strongly seen on the lower strand of the *HPRT* promoter from positions -75 to -167 (Figure 4-5A, Inactive *in vivo* samples) but extended both upstream and downstream from positions -154 to -259 (Figure 4-4A & 4-6B, Inactive *in vivo* samples) and positions -38 to -107 (Figure 4-5B, Inactive *in vivo* samples), respectively, on the upper strand. A summary of the preferential DNase I cleavages making up the 10 bp ladders on the upper and lower strands is shown in Figure 4-7. The slight shift observed in the 10 bp ladders between the upper and lower strands reflects the fact that maximal exposure of the minor groove does not occur at the same nucleotide position for the two strands simultaneously. This 2-4 bp staggering of the ladders on the upper and lower strands has been previously described (113). Together, the *in vivo* pattern of 10 bp ladders on the upper and lower strands suggest that nucleosomes are rotationally phased over a region of at least 210 bps on the inactive *HPRT* promoter, starting from approximately 110 bp downstream of the GC boxes and extending to just

Figure 4-5: High resolution DNase I cleavage analysis of the *HPRT* minimal promoter using the CA and E primer sets. All designations are the same as for figure 3. The * indicates the positions of the two major transcription initiation sites of the *HPRT* promoter determined by Kim et al (91). The arrows indicate the 10 bp ladders suggestive of rotational phasing of nucleosomes on the inactive *HPRT* allele. **A)** *In vivo* DNase I cleavage analysis of the lower strand of the *HPRT* minimal promoter using the CA primer set. **B)** *In vivo* DNase I cleavage analysis of the upper strand of the *HPRT* minimal promoter using the E primer set.

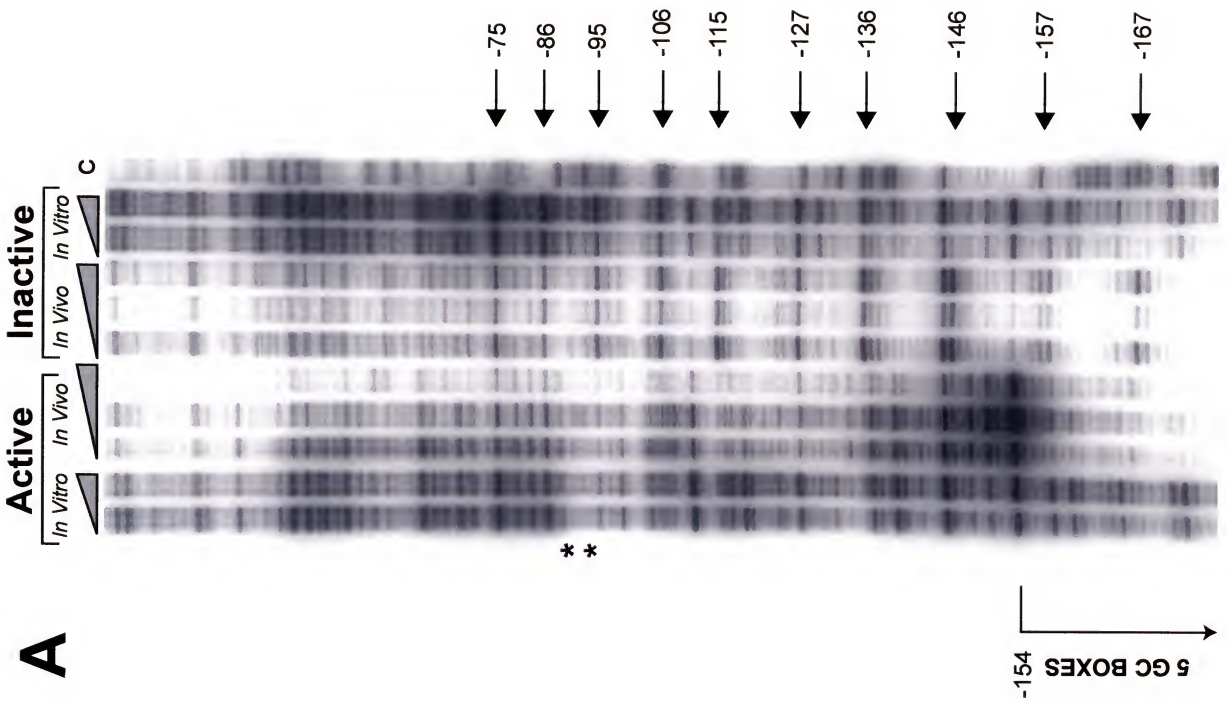
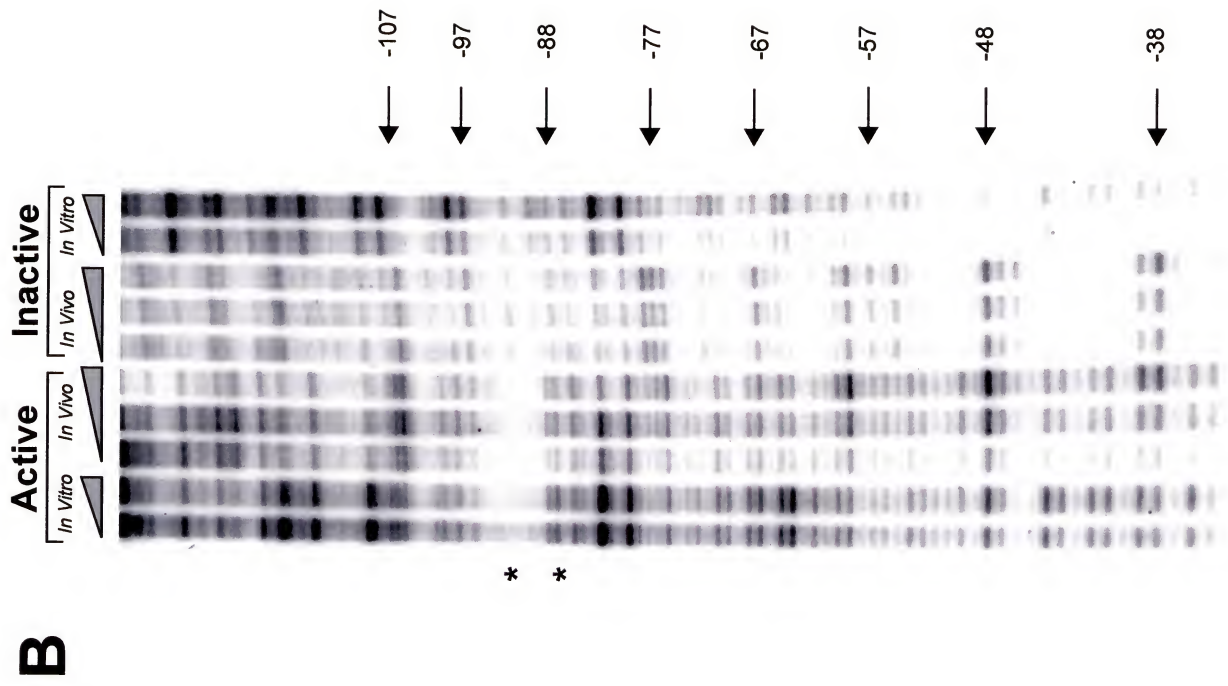


Figure 4-6: High resolution DNase I cleavage analysis immediately upstream of the *HPRT* minimal promoter using primer sets A and C. All designations are the same as for figures 4-4 & 4-5. The dashed arrows indicate the 10 bp cleavage ladder suggestive of a rotationally phased nucleosome on the active *HPRT* allele. **A)** *In vivo* DNase I cleavage analysis of the lower strand immediately upstream of the *HPRT* minimal promoter using primer set A. **B)** *In vivo* DNase I cleavage analysis of the upper strand immediately upstream of the *HPRT* minimal promoter using primer set C.

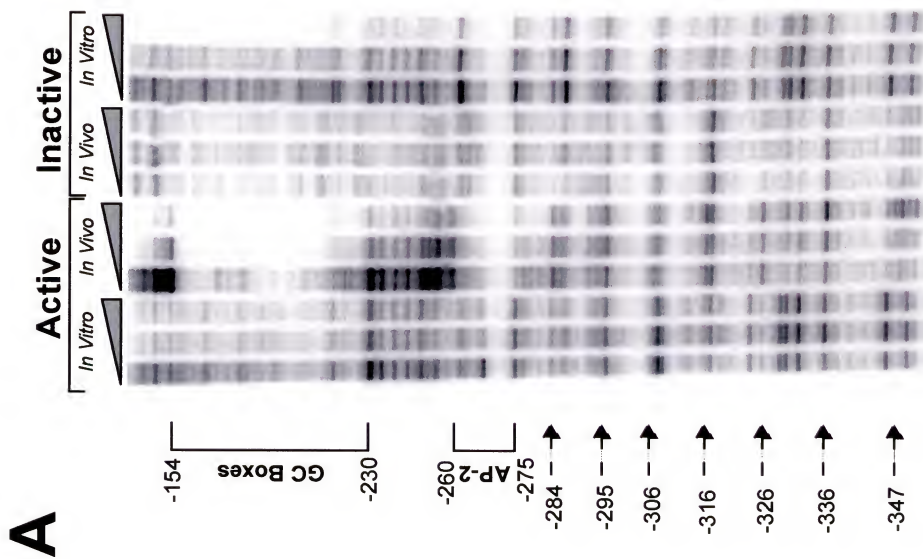
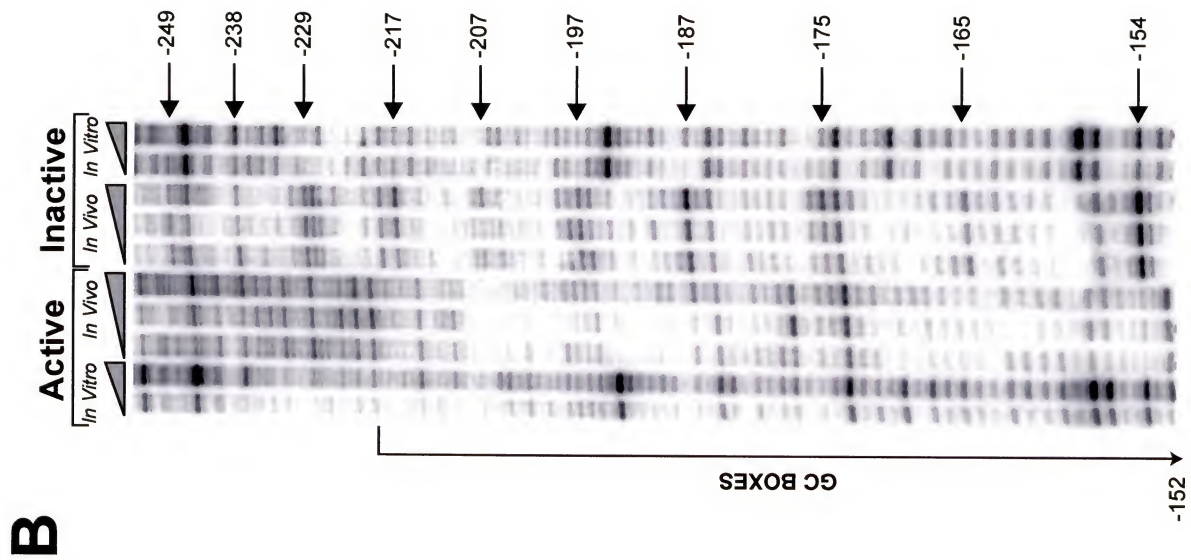


Figure 4-7: Summary of the *in vivo* DNase I cleavage data supporting rotational phasing of nucleosomes on the active and inactive *HPRT* minimal promoters. The gray partial ovals indicate the approximate positions of the translationally positioned nucleosomes on the active *HPRT* promoter as determined by MNase cleavage. The open boxes indicate the positions of transcription factor binding sites. The bent arrows indicate the positions of the two major transcription initiation sites identified by Kim et al. (91). The black triangles above the sequence indicate the positions of the cleavages on the upper strand making up the 10 bp ladder suggestive of rotationally phased nucleosomes in the inactive minimal promoter. The gray triangles below the sequence indicate the positions of the cleavages on the lower strand making up the 10bp ladder suggestive of rotationally phased nucleosomes in the inactive minimal promoter. The white triangles indicate the cleavages on the lower strand making up the 10bp ladder which suggest that the translationally phased nucleosome immediately upstream of the minimal promoter is also rotationally phased. The small vertical ovals indicate the positions of 3 CpG dinucleotides whose methylation is strongly correlated with transcriptional repression of the *HPRT* gene on the inactive allele (Chen et al, in preparation).

-279

TGAATAGGAGACTGAGTTGGAGGAAAGGGGCTTCGCTGGGGAGCCCTCGGCTTCTTCT
 ACTTATCCCTCTGACTCAACCCTCCCTTCCCCGAAAGGACCCCTCGGAGCCGAAGAAG

-219

GGGAGAAATTTCCCA TGGCTACCTAGTAGCCTGCAAACTGGTAGGCGCCGGCGTAGGCG
 CCTCTTTTAAGGGT FCCGATGGATCACTCGGACGTTTGACCATCCGCGGCCGCATCCCGC

-159

CGCGGGCGGGCCGGGGGCGCTGCCGEGGCGGTGGCGGGCGGCAGAGGGCGGGGCC
 GCGCCCGCCCGGCC CCGGC CCGGACGCTCCGCA CCGC CCGGCCCGTCT CCGGCC CCGG

-99

TGCTTCTCCTCAGCTTCAGGGGGCTGCGACGAGCCCTCAGGCGAACTCTCGGCTTCC
 ACGAAGAGGAGTCGAAAGTCCGCCGACGCTGCTCGGGAGTCCGCTTGGAGAGCCGAAAGGG

-39

GCGGGCGCGCTTTGCTGGCCCTCCGCCCTCCTCTGCTCCGCCACGGCTTCCCTC
 CCGCCCGGGCGGAGAACGACGCGGAGCGGGAGGAGGAGACGAGCGGTGTCGAAGGAG

22

CTCCTGAGCAGTCAGCCCGCGGCCGGCTCCGTTATGGCGACCCGCCAGCCCTGGCG
 GAGGACTCGTCACTCGGGCGCGGCCCGGCGGCAATACCGCTGGGCGTCCGGACC

82

TCGTGtgtagcagctcggccctcggccctcggccctcggccctcggccctcggccctcggcc
 AGCACcactcgtcgagccggaaggccggccggccggccggccggccggccggccggccggcc

+1

downstream of the AP-2 site (Figure 4-7). This region of rotationally phased nucleosomes on the inactive promoter encompasses the minimal promoter of *HPRT* (168) and all of the major transcription initiation sites (93, 151) suggesting a potential role for rotational phasing of nucleosomes in the transcriptional repression of the inactive *HPRT* promoter.

In contrast, while the high-resolution *in vivo* DNase I cleavage pattern of the chromatin of active *HPRT* minimal promoter revealed the *in vivo* footprints described above, it did not, for the most part, exhibit a 10 bp periodicity of cleavages indicative of rotationally phased nucleosomes. In fact, other than the *in vivo* footprints, the DNase I cleavage pattern of the active *HPRT* promoter *in vivo* largely resembled that of naked DNA (Figures 4-4, 4-5 & 4-6, regions outside *in vivo* footprints), suggesting that this region is devoid of nucleosomes. The exception to this similarity to naked DNA was a region just outside the 350 bp nuclease hypersensitive region and immediately upstream of the potential AP-2 binding site where a translationally phased nucleosome is thought to map by MNase digestion (Figure 4-2B). Here, a moderately strong 10bp ladder was observed on the active allele (Figure 4-6A Active *in vivo* samples) from -284 to -387. While this laddering pattern is suggestive that this upstream nucleosome is both translationally and rotationally phased, the presence of a similar but not identical DNase I cleavage pattern in the naked DNA (Figure 4-6A Active *in vitro* samples) makes interpretation difficult. With the exception of this region, no other part of the active *HPRT* minimal promoter examined reveals a 10 bp ladder, suggesting that the minimal promoter does not contain rotationally phased nucleosomes.

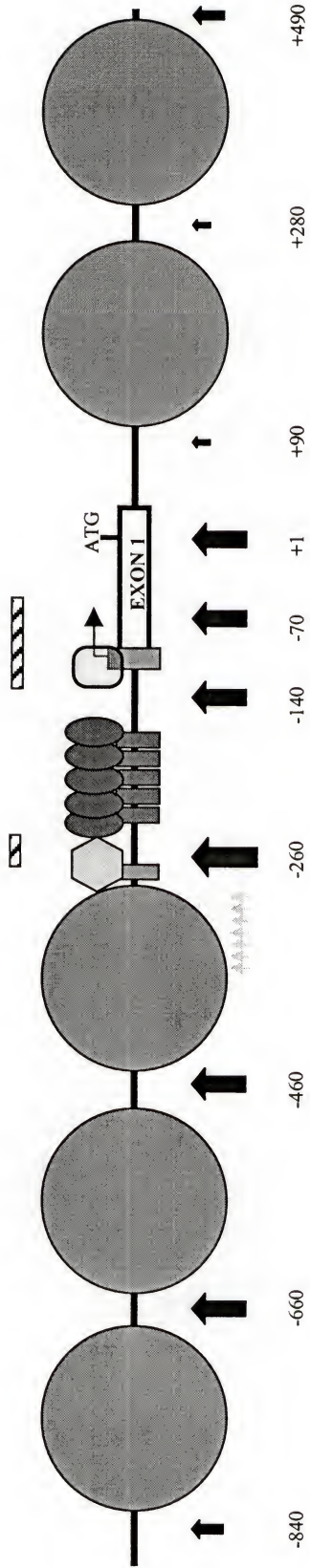
Discussion

These data indicate that the nucleosomal organization of the *HPRT* promoter differs dramatically between the active and inactive X chromosomes. A schematic summary of these differences is shown in Figure 4-8. The active promoter is assembled into an ordered array of six upstream and two downstream translationally phased nucleosomes which flank a 350 bp nuclease hypersensitive region that includes the minimal promoter and the region of multiple transcription initiation sites in the *HPRT* gene. In agreement with previous DMS *in vivo* footprinting studies (77), DNase I *in vivo* footprinting analysis shows that the AP-2 site and the cluster of GC boxes that reside in this region are occupied on the active promoter. Both its hypersensitivity to DNase I and MNase, and the resemblance of its high-resolution DNase I cleavage pattern to naked DNA suggest that this 350 bp region on the active allele is devoid of nucleosomes. Consistent with this interpretation, high-resolution *in vivo* DNase I cleavage analysis of the active *HPRT* promoter also does not identify any rotationally phased nucleosomes in this nuclease hypersensitive region.

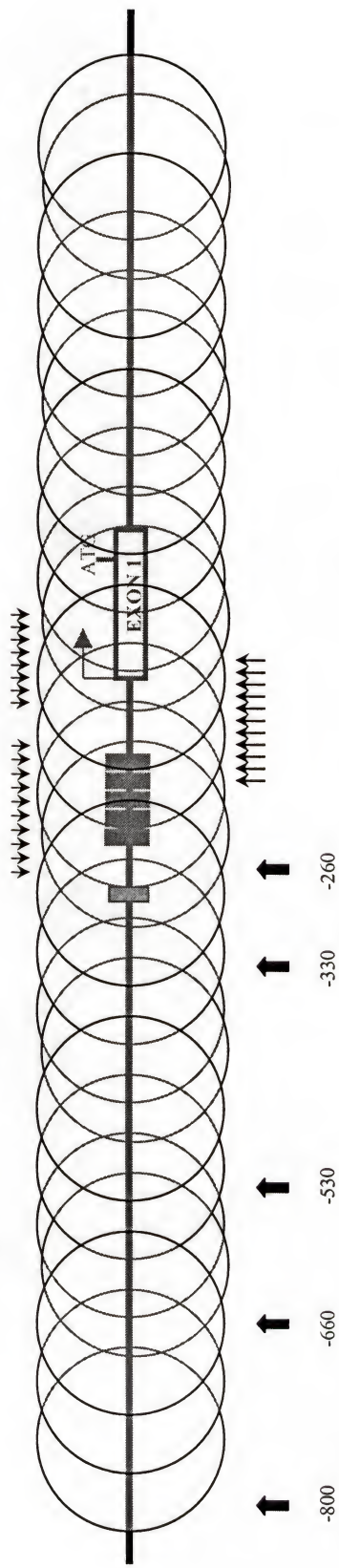
In contrast, no translational phasing of nucleosomes is observed on the inactive allele by *in vivo* MNase analysis (Figure 4-2C). Furthermore, the similarity between the MNase I cleavage patterns of the inactive allele and naked DNA suggest that translational positioning at the inactive promoter may be random (Figure 4-2C). Unlike the active allele, the inactive allele exhibits no DNase I hypersensitivity and the equivalent MNase hypersensitive sites at -260, -140, -70, and +1 are similarly absent or greatly reduced (Figure 4-2C). Consistent with this finding, the AP-2 site and the cluster of GC boxes on the inactive promoter appear to be unoccupied by sequence-specific DNA binding

Figure 4-8: Summary of the nucleosome organization of the active and inactive *HPRT* promoters. The dark circles on the active allele indicate the positions of translationally phased nucleosomes. The overlapping circles on the inactive allele represent nucleosomes with random translational positioning on the inactive promoter. The hexagon and ovals indicate transcription factors identified by DNase I and DMS *in vivo* footprinting (75) and the rectangles represent their binding sites. The bent arrow indicates the position of the two major transcription initiation sites on the *HPRT* promoter. The white box indicates the first exon of the *HPRT* gene and the ATG indicates the position of the translation initiation site. The broad arrows indicate the approximate positions and intensities of the major MNase cleavage sites in the *HPRT* promoter. The small triangular and barbed arrows indicate the positions of the high-resolution *in vivo* DNase I cleavage ladders suggestive of rotationally phased nucleosomes on the active and inactive *HPRT* promoters respectively. The slightly longer length of the arrows on the lower strand in the inactive allele indicates that this ladder was unusually prominent. The cross-hatched bars indicate the approximate locations of the DNase I hypersensitive sites on the active *HPRT* promoter *in vivo*. All numbers are relative to the translation initiation site. *The pattern of cleavages observed on the inactive allele is identical to that of MNase treated naked DNA.*

ACTIVE ALLELE



INACTIVE ALLELE



proteins as determined by both DNase I *in vivo* footprinting and previous DMS *in vivo* footprinting analysis (77). However, *in vivo* DNase I cleavage analysis does identify strong rotational phasing of nucleosomes over the inactive promoter. The region exhibiting this rotational phasing of nucleosomes on the inactive allele extends at least 210 bp, from immediately downstream of the potential AP-2 binding site through the cluster of GC boxes and the region of multiple transcription initiations site to about 40 bp upstream of the translation start site of the *HPRT* promoter. The location of this rotational phasing of nucleosomes argues that it may be involved in the transcriptional inhibition of the *inactive HPRT* allele.

Significance and Mechanisms of Translational Nucleosomal Phasing on the Active *HPRT* Promoter

The translational organization of nucleosomes on the active *HPRT* promoter preferentially exposes a 350 bp nuclease hypersensitive region that appears to be the functional promoter *in vivo*. Conceivably, this nucleosomal organization may act to limit the exposure of the DNA to trans-acting factors, thereby directing transcription factor binding to regions where nucleosomes are modified or absent (56). This is important because the average density of consensus transcription factor binding sites in DNA is estimated at approximately 14 per 100 bp (164), so the potential for inappropriate transcription factor binding is high. The inclusion of the multiple transcription initiation sites of the *HPRT* gene within this 350 bp exposed region is also important since transcriptional initiation but not elongation is inhibited by nucleosomal assembly (123). Therefore, the precise translational phasing of nucleosomes at active promoters may act to expose specific regulatory regions such as promoter and enhancer elements while

sequestering the majority of the DNA sequence to prevent inappropriate transcription factor binding. This hypothesis is consistent with other studies, which indicate that the promoters and enhancers of active genes are assembled into ordered nucleosomal arrays (132, 152) (8, 179, 197). In all of these cases, the nucleosomes over transcription factor binding sites and the transcription initiation sites of the promoter appear to be modified or absent as suggested by hypersensitivity to DNase I, or enhanced sensitivity to restriction enzymes. The human *PGK-1* promoter appears to be an exception to this trend since the inactive promoter is thought to contain translationally phased nucleosomes that are displaced upon activation (158). However, it is noteworthy that the criteria for translation phasing in this study was based on the presence of distinct 10 bp ladders which are primarily markers for rotational rather than translational phasing.

The mechanisms responsible for establishing the translational phasing of nucleosomes are not well understood but both the underlying sequence and boundary proteins have been implicated (116). Nucleosomal phasing sequences have been identified by *in vitro* reconstitution of phased nucleosomal arrays on the murine mammary tumor virus (*MMTV*), *vitellogenin*, *hsp26*, *beta globin*, and *pS2* promoters (161, 162) (175) (124) (10) (179). When these nucleosomal phasing sequences are present, translational phasing of nucleosomes appears to be the default state of the chromatin since these promoters all exhibit translational phasing of nucleosomes on both the active and inactive alleles (124, 175, 197) (10) (179). In contrast, the *HPRT* promoter does not appear to harbor a nucleosomal phasing sequence since *in vitro* reconstitution of nucleosomes on the promoter does not reveal a predominant translational nucleosomal register (Figure 4-4). Furthermore, unlike promoters containing a nucleosome phasing

sequence, the chromatin of the inactive *HPRT* promoter *in vivo* is not organized into phased nucleosomes (Figure 4-2C).

For promoters lacking a nucleosomal phasing sequence, the translational phasing of nucleosomes observed on the active promoter/enhancer is probably a product of the binding of boundary proteins. The ability of proteins to translationally position nucleosomes is well established *in vitro* (99) and has been demonstrated for a number of transcription factors including Grf2 (52), Gal4/VP16(155), Sp1(156, 207), NF-kappa B(156, 207), R3 (153), and HNF3 (182). Furthermore, *in vivo*, the glucocorticoid receptor has been linked to the redistribution of unphased nucleosomes into a phased nucleosomal array on the *MMTV* promoter in *Xenopus* oocytes (8) and HNF3 has been implicated in the translational positioning of nucleosomes in the mouse serum albumin enhancer (132, 182). For the active *HPRT* promoter, binding of a boundary protein, possibly AP-2, at the potential AP-2 binding site may be involved in translational phasing since a very strong MNase cleavage site at -260 lies immediately adjacent to the AP-2 binding site (Figure 4-2B) suggesting a strongly phased nucleosome immediately upstream of AP-2 binding site. However, in light of recent findings in the mouse lysozyme promoter in myeloid cells (97), it cannot formally ruled out that the boundary proteins involved in nucleosomal phasing at the active *HPRT* promoter are bound transiently prior to transcriptional activation and are subsequently replaced by end stage trans-activating factors.

Interestingly, the mechanism of translational phasing appears to be dependent on the type of promoter involved. While the correlation is not perfect, inducible promoters tend to have nucleosome phasing sequences (124, 161, 162, 175, 179) and are therefore

organized into ordered nucleosomal arrays regardless of their transcriptional status. In contrast, constitutive promoters, such as the active *HPRT* promoter, tend to derive their nucleosomal organization from boundary proteins (132, 152) and therefore lack translational nucleosomal phasing on the inactive allele. This difference between inducible and constitutive promoters may reflect the requirement of inducible promoters to be poised for induction. This possibility is supported by the observation that the precise translational positioning of nucleosomes *in vitro* appears to significantly affect the inducibility of both the *vitellogenin* (175) and *hsp26* (124) promoters. Conceivably, this functional constraint in inducible promoters may have resulted in an evolutionary divergence of inducible vs constitutive promoters.

Significance of Rotational Phasing of Nucleosomes on the Inactive *HPRT* Promoter

The absence of translationally phased nucleosomes on the inactive *HPRT* promoter does not indicate the absence of nucleosomes altogether. Instead, the 10 bp ladders observed by high-resolution DNase I cleavage analysis of the inactive promoter *in vivo* (Figures 4-4, 4-5, and 4-6, Summary in Figure 4-7) indicate clear rotational phasing of nucleosomes at the inactive promoter. The positions of these ladders over the cluster of GC boxes and the region of multiple transcription initiation sites are highly suggestive that the rotational phasing of nucleosomes on the inactive *HPRT* promoter is involved in its transcriptional repression. The absence of rotationally phased nucleosomes in this same region on the active *HPRT* promoter is also consistent with this interpretation. While there are few *in vivo* studies on the rotational orientation of nucleosomes within promoters, evidence from the human *PGK-1* (158), *phaseolin* (113),

and *pS2* promoters (179) also indicate that rotational phasing of nucleosomes over the promoter represses transcription and that disruption of this rotational phasing is a prerequisite for activation.

The mechanisms by which rotationally phased nucleosomes repress transcription are less clear. However, *in vitro* data for TBP (79), GR (114), and TR/RXR (210) suggest that at least some transcription factors are sensitive to the rotational orientation of their binding sites on the surface of the histone octamer. Therefore, the specific rotational orientation of rotationally phased nucleosomes on the inactive *HPRT* promoter may inhibit transcription factor binding in the region. This possibility is particularly relevant for the factors such as Sp1, which can bind to the cluster of 5 GC boxes, and for the transcription initiation complex since the sites bound by these proteins/complexes are incorporated in the 210 bp region which appears to be rotationally phased on the inactive allele. Alternatively, the rotational phasing of nucleosomes in this region may be indicative of the preferential placement of nucleosomes over this phased region. The mere presence of the 10 bp ladder suggests that a nucleosome is placed in a single rotational orientation within this region in a high percent of the cells in the population. It is therefore noteworthy that the strongest 10 bp ladder corresponds with the region of multiple transcription initiation sites, suggesting that rotationally phased nucleosomes preferentially assemble over these sites in the population of cells. If this is the case, the observed rotational phasing may be a manifestation of this preferential placement of nucleosomes and the repression observed could be largely due to the presence of nucleosomes over the region. However, these two potential mechanisms are not mutually exclusive and may be acting in concert to varying degrees.

Since the inactive *HPRT* promoter is devoid of transcription factor binding, at least as assayed by either DNase I or DMS *in vivo* footprinting (77), the rotational orientation of nucleosomes on the inactive promoter is probably determined by the underlying DNA sequence. The importance of the underlying sequence in determining the rotational orientation of nucleosomes is emphasized by the fact that the rotational phasing of nucleosomes on the *phaseolin* (113) and *pS2* (179) promoters *in vivo* can be recapitulated *in vitro* by nucleosomal assembly onto naked DNA templates using purified histones. The potential for the underlying sequence to dictate rotational positioning at the inactive *HPRT* promoter is increased by the high GC content of the promoter which increases its inherent curvature, a characteristic of nucleosomal positioning sequences (196).

For X-linked housekeeping genes such as the *HPRT* gene, the DNA sequence dependence of the rotational orientation of nucleosomes within the promoter is further complicated by DNA methylation. Davey et al. (45) have demonstrated that CpG methylation can affect the preferred translational setting of a nucleosome *in vitro*. While translational orientation does not appear to be affected by methylation at the *HPRT* promoter *in vitro* (Figure 4-3), it is still uncertain if rotational phasing is mediated by DNA methylation. Exocyclic groups such as the methyl group added by DNA methylation have been shown to affect the binding affinity of DNA to a nucleosomal core, the intrinsic curvature of DNA, and its flexibility (196), all characteristics which are known to affect nucleosomal positioning. Essentially, the addition of a methyl group is expected to sterically hinder bending at the CG base pair which has a wider minor groove (116) than an AT base pair. This would result in a tendency of the minor groove at the

methylated CpG dinucleotide to face away from the nucleosome surface (196).

Examination of the high resolution DNase I cleavage pattern of the inactive allele bears out this expectation since an unusually high percentage of the cleavages making up the 10 bp ladders on both strands occur at or near CpG dinucleotides (Figure 4-7).

For inducible and tissue-specific promoters, the transition between the active and inactive states is thought to be mediated by the presence or absence of transcription factors which can bind to and remodel nucleosomes (101, 154) (190). However, this is not a satisfactory explanation for X-linked housekeeping genes, such as the *HPRT* gene, which have both a transcriptionally active and a transcriptionally inactive allele in each cell. Instead, early in embryogenesis, one of the two *HPRT* alleles in each cell is chosen to remain active whereas the transcription of the other is silenced by X inactivation (62). This probably allows the chromatin structure of the inactive promoter to revert to its default state of rotationally phased nucleosomes, further locking the inactive promoter in a repressed state. The transcriptional status of the active allele is somehow marked, possibly by alternations in chromatin structure, and this information is retained during mitosis, allowing the transcriptional status of each allele to be passed to daughter cells (134). Since this differential expression of the two alleles of X-linked genes is very stable, the artificial reactivation of the inactive allele by demethylating agents such as 5aCdr almost certainly involves disruption of the chromatin structure of the promoter (119, 174).

Overall, these data suggest that the chromatin structure of the promoter directly promotes or inhibits transcription at the *HPRT* locus. On the active allele, the translational phasing of nucleosomes preferentially exposes the functional promoter,

allowing efficient transcription whereas on the inactive allele, rotationally phased nucleosomes sterically hinder transcription factor binding and initiation complex formation. While not in the scope of this study, the role of DNA methylation and transcription factor binding in determining and maintaining this differential chromatin structure should be explored.

CHAPTER 5
SUMMARY OF MAJOR CONCLUSIONS AND FUTURE EXPERIMENTS

Summary of the Methylation Analysis of the *HPRT* Promoter

Our analysis of DNA methylation at the *HPRT* promoter suggests that transcriptional repression is mediated by methylation at specific critical CpG sites. Examination of the high-resolution methylation patterns of the *HPRT* promoter in clonal cell lines that have partially demethylated the promoter but failed to reactivate the *HPRT* gene *in vivo* identified 3 CpG dinucleotides whose methylation was perfectly correlated with transcriptional repression of the inactive *HPRT* gene (Figure 3-3). Statistical analysis of these methylation patterns indicated that it is extremely unlikely for these 3 CpG dinucleotides to remain methylated in all 61 non-reactivated clones by chance alone ($p=0.00003$), suggesting that methylation of these 3 “critical” CpG sites is functionally required for transcriptional repression of the *HPRT* gene. Reactivation studies of partially demethylated clonal lines did not show a correlation between the initial level of methylation at the *HPRT* promoter in a given clone and its reactivation frequency upon re-treatment with 5aCdr (Table 3-I), suggesting that the critical sites play a disproportionate role in maintaining transcriptional repression of the inactive *HPRT* allele.

While the importance of these critical sites in maintaining transcriptional repression is evident, the mechanism of this repression is not. Still, we have examined the likelihood of two possible mechanisms of methylation-mediated repression. Both DMS

(77) and DNase I *in vivo* footprinting studies (Figure 4-4) suggest that the primary role of methylation at the critical sites is unlikely to be direct inhibition of transcription factor binding since only one critical site lies in the vicinity of an *in vivo* footprint. Likewise, TSA reactivation studies suggest that repression of the inactive *HPRT* allele is not primarily mediated by histone deacetylases, or at least not TSA-sensitive histone deacetylases (Figure 3-4), since TSA is unable to reactivate the *HPRT* gene on the inactive X chromosome, even when the promoter is partially demethylated.

The presence of *de novo* methylation at the *HPRT* promoter in partially demethylated clones and the discrepancy between the reactivation frequency of the *HPRT* gene and the observed demethylation rate of individual CpG sites suggest two potential scenarios for 5aCdr induced reactivation of the *HPRT* gene. First, since the observed demethylation rate of individual CpG sites alone is too low to account for the observed reactivation frequency, a global demethylation event, secondary to 5aCdr-mediated demethylation, may be responsible for the complete demethylation of the *HPRT* promoter observed in clones that have reactivated the *HPRT* gene. Alternatively, significant remethylation of the promoter may occur after the initial 5aCdr-induced demethylation event, thereby masking the actual demethylation rate of individual CpGs. In either case, these observations suggest that methylation at the *HPRT* promoter is significantly more dynamic than previously thought.

Future Studies on DNA Methylation at the *HPRT* Gene

Since we have identified specific CpG sites whose methylation appears to be critical for transcriptional repression of the *HPRT* promoter, the next obvious step is to

determine the mechanism by which these critical sites and/or methylation at the *HPRT* promoter in general represses transcription. To further investigate whether methylation at the *HPRT* promoter represses transcription by direct inhibition of transcription factor binding, either *in vitro* transcription assays or transient transfection assays could be performed using reporter constructs containing the methylated or unmethylated *HPRT* promoter. If methylation at the *HPRT* promoter mediates transcriptional repression by direct inhibition of transcription factor binding, *in vitro* transcription/ transient transfection of the methylated construct should show reduced transcription or none at all. Alternatively, if methylation does not work by direct interference with transcription factor binding, the *in vitro* transcription of the methylated template should be unaffected.

This question might also be addressed by the use of electrophoretic mobility shift assays or EMSA. Focusing on regions that are *in vivo* footprinted on the active *HPRT* allele or on the positions of the critical sites, EMSA assays using methylated and unmethylated templates could examine whether methylation affects factor binding *in vitro*. While this approach is more tedious and subject to more artifacts than *in vitro* transcription or transient transfection assays, it allows a more precise determination of which transcription factor bind sites are affected by DNA methylation. A difference in the EMSA profile of a methylated vs unmethylated template would suggest that a factor binding to one is unable to bind to the other.

To assess the role that chromatin might play in methylation-mediated transcriptional repression, *in vitro* transcription or transient transfection experiments might also be performed using constructs pre-assembled into chromatin *in vitro*. These experiments would test the intrinsic tendencies of the methylated versus unmethylated

promoter to be assembled into a repressive chromatin conformation. Ideally, the *in vitro* transcription experiments should be performed in mammalian nuclear extracts that are known to have active chromatin remodeling complexes and histones acetyltransferases. Likewise, transient transfection should be done in cells that exhibit methylation *in vivo* (i.e. not insect cells) and are therefore able to reproduce methylation-mediated repression. These experiments could also potentially be performed with promoters in which the critical sites have been mutated. While mutation of the critical sites is unlikely to affect transcription of naked DNA templates, since Rincon Limas et al. (168) have shown that the region containing critical sites is not necessary for maximal *HPRT* expression in transient transfection assays, it may affect chromatin assembly on methylated and unmethylated templates and thereby indirectly affect transcription.

Nevertheless, it is likely that none of these experiments can accurately reflect the *in vivo* environment in which methylation acts to repress the *HPRT* allele on the inactive X chromosome. A possible strategy to address this problem is to identify equivalent critical sites in the mouse *HPRT* promoter or to make a transgenic mouse harboring the human *HPRT* gene on the mouse X chromosome. This would then allow mutagenesis of the critical sites *in vivo* by homologous recombination and passage of the mutations through the process of X inactivation in ES cells. If methylation at the critical sites does indeed mediate much of the maintainance of transcriptional repression at the *HPRT* promoter, the transgenic or mutant mouse should exhibit a tendency to reactivate the mutant allele. However, these are extremely difficult experiments and not warranted without further demonstration of the significance of these critical sites by other means.

Summary of Nucleosome Phasing at the *HPRT* Promoter *In Vivo*

Examination of the nucleosomal structure of the active *HPRT* promoter on the active X chromosome reveals an ordered array of 6 upstream and 2 downstream translationally phased nucleosomes that flank a 350 bp region that appears to be essentially devoid of nucleosomes. This 350 bp region contains what appears to be the functional promoter of the *HPRT* gene, including the potential AP-2 binding site, the cluster of GC boxes, a potential initiator element identified by DMS *in vivo* footprinting, and the entire region of multiple transcription initiation sites in the *HPRT* promoter. All *in vivo* footprints detected by either DNase I or DMS *in vivo* footprinting fall within this 350 bp region. Likewise, the DNase I hypersensitivity of the active *HPRT* promoter also maps into this 350 region as does significant MNase hypersensitivity. Overall, these observations suggest that the nucleosomal organization of the active *HPRT* promoter preferentially exposes the functional promoter while sequestering adjacent regions in ordered nucleosomal arrays.

In contrast, the inactive *HPRT* promoter on the inactive X chromosome exhibits no apparent translational phasing of nucleosomes at all. Furthermore, DNase I and MNase hypersensitivity are markedly absent within the 350 bp region, suggesting that these are functional characteristics of the active allele. Instead, the inactive *HPRT* promoter but not the active promoter, exhibits clear rotational phasing of nucleosomes at and extending immediately upstream and downstream of the region of multiple transcription initiation sites. This nucleosomal organization on the inactive allele suggests that the inactive allele is transcriptionally repressed by the assembly of rotationally phased nucleosomes over its minimal promoter, particularly the region of multiple

transcription initiation sites and the cluster of GC boxes. The absence of this rotational phasing on the active allele suggests that this rotational phasing must be disrupted for transcriptional activation.

Future Studies to Examine the Role of Nucleosomal Organization in the Transcriptional Regulation of the *HPRT* Gene

While we have demonstrated clear differential nucleosomal organization at the active and inactive *HPRT* promoters, we have not determined either the mechanisms responsible for this differential organization or the impact of this organization on transcription. While preliminary experiments suggest that no translational nucleosomal phasing sequence is present at the *HPRT* promoter, it is important to test this possibility rigorously. To do this *in vitro* assembly of nucleosomes on the *HPRT* promoter is necessary, preferably using purified histones. The use of purified histones reduces the possibility that a non-histone protein in this assay might mediate the assembly of chromatin on the *HPRT* promoter. Ideally, the Bcl I fragment containing the human *HPRT* promoter should be used as the template for this assessment to allow analysis of the nucleosomal phasing from the same reference Bcl I site. The presence of an ordered array of nucleosomes in this *in vitro* reconstituted chromatin would suggest that a translational nucleosomal phasing sequence does exist in the *HPRT* promoter, whereas the absence of phased nucleosomes would suggest that phasing is a product of the transcriptional activation process, possibly mediated by boundary proteins.

To examine the possibility that boundary proteins are responsible for the nucleosomal organization of the active *HPRT* promoter, it is necessary to first specifically identify the proteins bound to the active *HPRT* promoter *in vivo*. For the

potential AP-2 site and the cluster of GC boxes, potential candidate proteins are known and can be screened by DMS footprinting *in vitro* or EMSA. Demonstration of a DMS footprint *in vitro* that is identical to the *in vivo* footprint using a purified transcription factor is highly suggestive that the transcription factor also binds the site *in vivo*. EMSA can demonstrate an *in vitro* capacity to bind the site in question *in vitro* but is a less ideal test. In cases where no candidate proteins are known the yeast one-hybrid system can be used. While this method generates a lot of false positives, it is the fastest way to identify potential candidate transcription factors which can be subsequently screened by EMSA and DMS footprinting.

Once the factors binding the active *HPRT* promoter *in vivo* have been identified, pre-assembly of these factors onto naked DNA followed by chromatin assembly *in vitro* can assess the ability of these factors to set up the ordered array of translationally phased nucleosomes observed on the active allele. It can also determine the ability of pre-bound factors to maintain the nucleosome free region observed on the active *HPRT* promoter *in vivo*. Assembly of chromatin followed by the addition of these transcription factors can assess their ability to displace nucleosomes *in vivo*. However, considering that the active and inactive *HPRT* alleles both reside in the same cell in females, it is unlikely that these factors can displace nucleosomes, unless displacement of nucleosomes is affected by the differential methylation of the DNA. These chromatinized templates can also be subjected to *in vitro* transcription assays to determine their ability to support transcription.

To determine if the underlying sequence determines the rotational orientation of nucleosomes on the inactive *HPRT* promoter, nucleosomes can be reconstituted on the

HPRT promoter *in vitro* followed by DNase I digestion and high resolution DNase I cleavage analysis. To examine the role of methylation in either determining rotational orientation or stabilizing it, similar experiments can be performed using methylated templates. The ability of the methylated vs unmethylated chromatin template to support transcription can be assessed by *in vitro* transcription assays.

APPENDIX A
METHYLATION PATTERNS OF EACH OF THE 61 CLONES THAT FAILED TO
REACTIVATE THE HPRT GENE AFTER 5ACDR TREATMENT

The raw data of the methylation patterns of each of the 61 single-cell-derived clones that failed to reactivate the *HPRT* gene after 5aCdr treatment is listed in the subsequent pages. The positions of each CpG dinucleotide examined are listed across the top of the chart while the clone designations are listed on the left margin. 0 indicates a methylated site and 1 indicates a unmethylated site. If a band was detected at the correct position at an intensity above background, it was scored as a 1 (unmethylated site).

APPENDIX B
ADDITIONAL PROTOCOLS

Assessment of Rotational Phasing on *In Vitro* Reconstituted Chromatin by High-Resolution DNase I Cleavage Analysis

In Vitro reconstituted chromatin was digested with DNase I as follows. Briefly, 27 μ l of the reconstituted chromatin (see above) was mixed with 73 μ l of Ex50 +MgCl₂ +CaCl₂ (10 mM HEPES [pH 7.6], 60 mM KCl, 11.5 mM MgCl₂, 0.5 mM EGTA [pH 8.0], 10% glycerol, 10 mM glycerol phosphate, 5 mM CaCl₂) and 0, 0.2, 0.4, 0.6, 0.8, or 1.0 μ g of DNase I and incubated at room temperature for 2 min. The digestion was stopped with 40 μ l of stop solution (2.5% sarkosyl, 100 mM EDTA), phenol:chloroform extracted and precipitated with 1 μ l of glycogen (10mg/ml; Boehringer Mannheim) as carrier. The pellet was washed once with 500 μ l of 75% ethanol and dried under vacuum. (Note: This procedure is not fully optimized. I think higher concentrations may be needed). The DNA was then resuspended at 1 ng/ μ l in TE [pH 8.0].

DNase I digestion of the naked DNA template was performed as follows: 200 ng of plasmid DNA was resuspended in 100 μ l of Ex50+MgCl₂+CaCl₂ (see above) and 0, 0.006, 0.0125, 0.025, 0.05, or 0.1 μ g of DNase I (Worthington) was added and mixed gently. The digestion was performed at room temperature for 2 min. and then stopped with 40 μ l of stop solution. The DNA was purified by phenol:chloroform extraction and precipitated with 1 μ l of glycogen (10mg/ml; Boehringer Mannheim). The pellet was

washed once with 500 μ l of 75% ethanol and then dried under vacuum. The DNA was then resuspended at 1ng/ μ l in TE [pH 8.0].

Both the in vitro reconstituted chromatin samples and the naked DNA samples were then subjected to LMPCR using the extension product capture modification (195). Since these were plasmid samples LMPCR was performed on 1ng of DNA instead of the usual 2-5 μ g.

Small scale Preparation of BAC DNA

Small-scale isolation of BAC DNA was performed using a Qiagen miniprep kit essentially as suggested by the manufacturer. Briefly, the bacterial line containing the BAC of interest was grown up in 5 ml of Luria Broth (LB) + 12.5 g/ml of chloramphenicol at 37 C in a roller drum overnight. The bacterial cells pelleted at 13,200 rpm in a microcentrifuge for 10 s. The cells from all 5 ml were collected and resuspended in a total volume of 250 l in Buffer P1 (Qiagen) by pipetting. Then 250 l of Buffer P2 (Qiagen) was added and mixed by gently inversion 4-6 times. Then 350 l of Buffer N3 (Qiagen) was added and mixed by inversion 4-6 times. The mixture was then spun at 13,200 rpm for 10 min in a microcentrifuge. The supernatant was then applied to a Qiaprep spin column and spun for 30-60 at 13,200 rpm. The column was washed with 500 l of Buffer PB (Qiagen) by applying the Buffer PB to the column and spinning at 13,200 rpm for 30-60 s. The column was then washes with 750 l of Buffer PE (Qiagen) also for 30-60 s. Buffer in the collection tube was discarded and the column spun an additional 60 s to remove residual buffer. The DNA was eluted from the column into a clean microcentrifuge tube by applying 50l of TE [pH 8.0] to the center of the

column, waiting for 2 min and then spinning at 13,200 rpm for 60 s. This DNA was significantly contaminated with *E. coli* genomic DNA but still usable for PCR amplification. Approximate yield was about 1-2 g of DNA.

Large Scale Preparation of BAC DNA

Large-scale preparation of BAC DNA was performed using the Qiagen Large Construct Kit essentially as suggested by the manufacturer. Briefly, a 5 ml starter culture of the bacterial line containing the BAC of interests was grown up overnight in LB + 12.5 g/ml of chloramphenicol at 37 C in a roller drum. This starter culture was added to 500 ml of LB + 12.5 g/ml of chloramphenicol and incubated in an orbital shaker at 37 C overnight. The bacteria were pelleted in a Beckman JA-10 rotor at 6000g and the supernatant was discarded. The bacterial pellet was resuspended in 20 ml of Buffer P1 (Qiagen) by pipetting and vortexing. The bacteria was then lysed using 20 ml of Buffer P2 (Qiagen) and mixed by gently inversion 4-6 times (do not incubate in P2 longer than 2 min). Then 20 ml of Buffer P3 (Qiagen) was added, mixed by inversion and the mixture was incubated on ice for 10 min. The mixture was divided into two 50 ml centrifuge tubes and spun in a Sorvall SS-34 rotor at 16.5K rpm for 30 min at 4 C. The supernatant was filtered through pre-wetted Whatman filter paper and then 18 ml of isopropanol was added to each half of the sample at room temperature and mixed. The DNA was then precipitated at 11K rpm in a Sorval SS-34 rotor for 30 min at 4 C. The pellets were washed with 5 ml of 75% ethanol and centrifuged at 11K rpm in a Sorval SS-34 for 15 min at 4 C. The 75% ethanol was decanted the tubes inverted and the pellets allowed to air dry for 5 min. Residual liquid on the side of the tubes was removed

with a micropipetor. The pellets were resuspended in 4.75 ml of Buffer EX (Qiagen) by swirling and combined. Then 200 μ l of ATP-Dependent Exonuclease (Qiagen; provide lyophilized in single-use vials and resuspended in 225 μ l of Exonuclease Solvent just before use) and 300 μ l of 100 mM ATP (pre-prepared as follows: 2.75 g of disodium ATP, 40 ml H₂O. adjust pH to 7.5 with 10M NaOH and bring volume up to 50 ml. Freeze as single use aliquots of 300 μ l.) were added, mixed by swirling, and incubated at 37 C for 1h. During exonuclease digestion, a Qiagen-tip 500 column was equilibrated by applying 10 ml of Buffer QBT (Qiagen) to the column and allowing it to empty by gravity flow. After an hour of digestion, 10 ml of Buffer QS (Qiagen) was added to the DNA sample and the mixture was loaded onto the column and allowed to enter the column by gravity flow. The column was then washed twice with 30 ml of Buffer QC (Qiagen) by gravity flow. The DNA was eluted with 15 ml of Buffer QF prewarmed to 65 C by gravity flow. The DNA was then precipitated with 10.5 ml of isopropanol and centrifuged immediately at 11K in a Sorval SS-34 at 4 C for 30 min. The pellet was then washed once with 5 ml of 75% ethanol and centrifuged at 11K in a Sorval SS-34 at 4C for 15 min. The wash solution was decanted and the pellet was air dried for 15 min. Residual liquid was removed with a micropipetor. The DNA was then resuspended in TE [pH 8.0]. This protocol yields high quality BAC DNA suitable for sequencing and cloning. The yield is about 50-100 g per 500 ml of media.

REFERENCES

1. **Adams, R. L.** 1995. Eukaryotic DNA methyltransferases--structure and function. *Bioessays* **17**:139-45.
2. **Antequera, F., D. Macleod, and A. P. Bird.** 1989. Specific protection of methylated CpGs in mammalian nuclei. *Cell* **58**:509-17.
3. **Avner, P., M. Prissette, D. Arnaud, B. Courtier, C. Cecchi, and E. Heard.** 1998. Molecular correlates of the murine Xce locus. *Genet Res* **72**:217-24.
4. **Barr, M. L., and D. H. Carr.** 1961. Correlations between sex chromatin and sex chromosomes. *Acta Cytol.* **6**:34-45.
5. **Baylin, S. B., J. G. Herman, J. R. Graff, P. M. Vertino, and J. P. Issa.** 1998. Alterations in DNA methylation: a fundamental aspect of neoplasia. *Adv Cancer Res* **72**:141-96.
6. **Beard, C., E. Li, and R. Jaenisch.** 1995. Loss of methylation activates Xist in somatic but not in embryonic cells. *Genes Dev* **9**:2325-34.
7. **Becker, P. B., T. Tsukiyama, and C. Wu.** 1994. Chromatin assembly extracts from *Drosophila* embryos. *Methods Cell Biol* **44**:207-23.
8. **Belikov, S., B. Gelius, G. Almouzni, and O. Wrangé.** 2000. Hormone activation induces nucleosome positioning in vivo. *Embo J* **19**:1023-33.
9. **Belyaev, N., A. M. Keohane, and B. M. Turner.** 1996. Differential underacetylation of histones H2A, H3 and H4 on the inactive X chromosome in human female cells. *Hum Genet* **97**:573-8.
10. **Benezra, R., C. R. Cantor, and R. Axel.** 1986. Nucleosomes are phased along the mouse beta-major globin gene in erythroid and nonerythroid cells. *Cell* **44**:697-704.
11. **Bernardino, J., E. Lamoliatte, M. Lombard, A. Niveleau, B. Malfoy, B. Dutrillaux, and C. A. Bourgeois.** 1996. DNA methylation of the X chromosomes of the human female: an in situ semi-quantitative analysis. *Chromosoma* **104**:528-35.

12. **Bestor, T. H.** 1990. DNA methylation: evolution of a bacterial immune function into a regulator of gene expression and genome structure in higher eukaryotes. *Philos Trans R Soc Lond B Biol Sci* **326**:179-87.
13. **Bhattacharya, S. K., S. Ramchandani, N. Cervoni, and M. Szyf.** 1999. A mammalian protein with specific demethylase activity for mCpG DNA. *Nature* **397**:579-583.
14. **Bird, A.** 1992. The essentials of DNA methylation. *Cell* **70**:5-8.
15. **Bird, A. P.** 1986. CpG-rich islands and the function of DNA methylation. *Nature* **321**:209-13.
16. **Bird, A. P.** 1980. DNA methylation and the frequency of CpG in animal DNA. *Nucleic Acids Res* **8**:1499-504.
17. **Bird, A. P.** 1993. Functions for DNA methylation in vertebrates. *Cold Spring Harb Symp Quant Biol* **58**:281-5.
18. **Bird, A. P.** 1995. Gene number, noise reduction and biological complexity. *Trends Genet* **11**:94-100.
19. **Bird, A. P., and M. H. Taggart.** 1980. Variable patterns of total DNA and rDNA methylation in animals. *Nucleic Acids Res* **8**:1485-97.
20. **Bird, A. P., M. H. Taggart, and B. A. Smith.** 1979. Methylated and unmethylated DNA compartments in the sea urchin genome. *Cell* **17**:889-901.
21. **Bird, A. P., and A. P. Wolffe.** 1999. Methylation-induced repression--belts, braces, and chromatin. *Cell* **99**:451-4.
22. **Blomquist, P., S. Belikov, and O. Wrangé.** 1999. Increased nuclear factor 1 binding to its nucleosomal site mediated by sequence-dependent DNA structure. *Nucleic Acids Res* **27**:517-25.
23. **Boyes, J., and A. Bird.** 1991. DNA methylation inhibits transcription indirectly via a methyl-CpG binding protein. *Cell* **64**:1123-34.
24. **Boyes, J., and A. Bird.** 1992. Repression of genes by DNA methylation depends on CpG density and promoter strength: evidence for involvement of a methyl-CpG binding protein. *Embo J* **11**:327-33.
25. **Brockdorff, N., A. Ashworth, G. F. Kay, P. Cooper, S. Smith, V. M. McCabe, D. P. Norris, G. D. Penny, D. Patel, and S. Rastan.** 1991. Conservation of position and exclusive expression of mouse Xist from the inactive X chromosome. *Nature* **351**:329-31.

26. **Brockdorff, N., A. Ashworth, G. F. Kay, V. M. McCabe, D. P. Norris, P. J. Cooper, S. Swift, and S. Rastan.** 1992. The product of the mouse Xist gene is a 15 kb inactive X-specific transcript containing no conserved ORF and located in the nucleus. *Cell* **71**:515-26.
27. **Broday, L., Y. W. Lee, and M. Costa.** 1999. 5-azacytidine induces transgene silencing by DNA methylation in Chinese hamster cells. *Mol Cell Biol* **19**:198-204.
28. **Brown, C. J., A. Ballabio, J. L. Rupert, R. G. Lafreniere, M. Grompe, R. Tonlorenzi, and H. F. Willard.** 1991. A gene from the region of the human X inactivation centre is expressed exclusively from the inactive X chromosome. *Nature* **349**:38-44.
29. **Brown, C. J., B. D. Hendrich, J. L. Rupert, R. G. Lafreniere, Y. Xing, J. Lawrence, and H. F. Willard.** 1992. The human XIST gene: analysis of a 17 kb inactive X-specific RNA that contains conserved repeats and is highly localized within the nucleus. *Cell* **71**:527-42.
30. **Brown, C. J., R. G. Lafreniere, V. E. Powers, G. Sebastio, A. Ballabio, A. L. Pettigrew, D. H. Ledbetter, E. Levy, I. W. Craig, and H. F. Willard.** 1991. Localization of the X inactivation centre on the human X chromosome in Xq13. *Nature* **349**:82-4.
31. **Brown, C. J., and H. F. Willard.** 1994. The human X-inactivation centre is not required for maintenance of X-chromosome inactivation. *Nature* **368**:154-6.
32. **Buschhausen, G., B. Wittig, M. Graessmann, and A. Graessmann.** 1987. Chromatin structure is required to block transcription of the methylated herpes simplex virus thymidine kinase gene. *Proc Natl Acad Sci U S A* **84**:1177-81.
33. **Busslinger, M., J. Hurst, and R. A. Flavell.** 1983. DNA methylation and the regulation of globin gene expression. *Cell* **34**:197-206.
34. **Cameron, E. E., K. E. Bachman, S. Myohanen, J. G. Herman, and S. B. Baylin.** 1999. Synergy of demethylation and histone deacetylase inhibition in the re-expression of genes silenced in cancer. *Nat Genet* **21**:103-7.
35. **Cameron, E. E., S. B. Baylin, and J. G. Herman.** 1999. p15(INK4B) CpG island methylation in primary acute leukemia is heterogeneous and suggests density as a critical factor for transcriptional silencing. *Blood* **94**:2445-51.
36. **Carmen, A. A., P. R. Griffin, J. R. Calaycay, S. E. Rundlett, Y. Suka, and M. Grunstein.** 1999. Yeast HOS3 forms a novel trichostatin A-insensitive homodimer with intrinsic histone deacetylase activity. *Proc Natl Acad Sci U S A* **96**:12356-61.

37. **Choi, Y. C., and C. B. Chae.** 1991. DNA hypomethylation and germ cell-specific expression of testis-specific H2B histone gene. *J Biol Chem* **266**:20504-11.
38. **Church, G. M., and W. Gilbert.** 1984. Genomic sequencing. *Proc Natl Acad Sci U S A* **81**:1991-5.
39. **Clemson, C. M., J. C. Chow, C. J. Brown, and J. B. Lawrence.** 1998. Stabilization and localization of Xist RNA are controlled by separate mechanisms and are not sufficient for X inactivation. *J Cell Biol* **142**:13-23.
40. **Clerc, P., and P. Avner.** 1998. Role of the region 3' to Xist exon 6 in the counting process of X- chromosome inactivation. *Nat Genet* **19**:249-53.
41. **Cole, H., B. Huang, B. A. Salbert, J. Brown, P. N. Howard-Peebles, S. H. Black, A. Dorfmann, O. R. Febles, C. A. Stevens, and C. Jackson-Cook.** 1994. Mental retardation and Ullrich-Turner syndrome in cases with 45,X/46X,+mar: additional support for the loss of the X-inactivation center hypothesis. *Am J Med Genet* **52**:136-45.
42. **Cooper, D. W., P. G. Johnston, W. J. M., and J. A. M. Graves.** 1993. X-inactivation in marsupials and monotremes. *Semin. Dev. Biol.* **4**:117-28.
43. **Costanzi, C., and J. R. Pehrson.** 1998. Histone macroH2A1 is concentrated in the inactive X chromosome of female mammals. *Nature* **393**:599-601.
44. **Courtier, B., E. Heard, and P. Avner.** 1995. Xce haplotypes show modified methylation in a region of the active X chromosome lying 3' to Xist. *Proc Natl Acad Sci U S A* **92**:3531-5.
45. **Davey, C., S. Pennings, and J. Allan.** 1997. CpG methylation remodels chromatin structure in vitro. *J Mol Biol* **267**:276-88.
46. **Disteche, C. M.** 1995. Escape from X inactivation in human and mouse. *Trends Genet* **11**:17-22.
47. **Driscoll, D. J., and B. R. Migeon.** 1990. Sex difference in methylation of single-copy genes in human meiotic germ cells: implications for X chromosome inactivation, parental imprinting, and origin of CpG mutations. *Somat Cell Mol Genet* **16**:267-82.

48. **Duthie, S. M., T. B. Nesterova, E. J. Formstone, A. M. Keohane, B. M. Turner, S. M. Zakian, and N. Brockdorff.** 1999. Xist RNA exhibits a banded localization on the inactive X chromosome and is excluded from autosomal material in cis. *Hum Mol Genet* **8**:195-204.
49. **Eden, S., and H. Cedar.** 1994. Role of DNA methylation in the regulation of transcription. *Curr Opin Genet Dev* **4**:255-9.
50. **Ellis, N., E. Keitges, S. M. Gartler, and M. Rocchi.** 1987. High-frequency reactivation of X-linked genes in Chinese hamster X human hybrid cells. *Somat Cell Mol Genet* **13**:191-204.
51. **Epstein, C. J., S. Smith, B. Travis, and G. Tucker.** 1978. Both X chromosomes function before visible X-chromosome inactivation in female mouse embryos. *Nature* **274**:500-3.
52. **Fedor, M. J., N. F. Lue, and R. D. Kornberg.** 1988. Statistical positioning of nucleosomes by specific protein-binding to an upstream activating sequence in yeast. *J Mol Biol* **204**:109-27.
53. **Gartler, S. M., K. A. Dyer, and M. A. Goldman (ed.).** 1992. Mammalian X chromosome inactivation, vol. 2. Academic Press, New York.
54. **Gartler, S. M., and M. A. Goldman.** 1994. Reactivation of inactive X-linked genes. *Dev Genet* **15**:504-14.
55. **Gartler, S. M., and A. D. Riggs.** 1983. Mammalian X-chromosome inactivation. *Annu Rev Genet* **17**:155-90.
56. **Gasser, S. M., and U. K. Laemmli.** 1987. A glimpse at chromosomal order. *Trends in Genetics* **3**:16-22.
57. **Gilbert, S. L., and P. A. Sharp.** 1999. Promoter-specific hypoacetylation of X-inactivated genes. *Proc Natl Acad Sci U S A* **96**:13825-30.
58. **Glenn, C. C., D. J. Driscoll, T. P. Yang, and R. D. Nicholls.** 1997. Genomic imprinting: potential function and mechanisms revealed by the Prader-Willi and Angelman syndromes. *Mol Hum Reprod* **3**:321-32.
59. **Godde, J. S., Y. Nakatani, and A. P. Wolffe.** 1995. The amino-terminal tails of the core histones and the translational position of the TATA box determine TBP/TFIIA association with nucleosomal DNA. *Nucleic Acids Res* **23**:4557-64.
60. **Gold, J. D., and R. A. Pedersen.** 1994. Mechanisms of genomic imprinting in mammals. *Curr Top Dev Biol* **29**:227-80.

61. **Goldman, M. A., K. R. Stokes, R. L. Idzerda, G. S. McKnight, R. E. Hammer, R. L. Brinster, and S. M. Gartler.** 1987. A chicken transferrin gene in transgenic mice escapes X-chromosome inactivation. *Science* **236**:593-5.
62. **Goto, T., and M. Monk.** 1998. Regulation of X-chromosome inactivation in development in mice and humans. *Microbiol Mol Biol Rev* **62**:362-78.
63. **Goyon, C., J. L. Rossignol, and G. Faugeron.** 1996. Native DNA repeats and methylation in *Ascobolus*. *Nucleic Acids Res* **24**:3348-56.
64. **Grant, M., M. Zuccotti, and M. Monk.** 1992. Methylation of CpG sites of two X-linked genes coincides with X-inactivation in the female mouse embryo but not in the germ line. *Nat Genet* **2**:161-6.
65. **Grant, S. G., and V. M. Chapman.** 1988. Mechanisms of X-chromosome regulation. *Annu Rev Genet* **22**:199-233.
66. **Groudine, M., R. Eisenman, and H. Weintraub.** 1981. Chromatin structure of endogenous retroviral genes and activation by an inhibitor of DNA methylation. *Nature* **292**:311-7.
67. **Gutekunst, K. A., F. Kashanchi, J. N. Brady, and D. P. Bednarik.** 1993. Transcription of the HIV-1 LTR is regulated by the density of DNA CpG methylation. *J Acquir Immune Defic Syndr* **6**:541-9.
68. **Hansen, R. S., T. K. Canfield, A. D. Fjeld, and S. M. Gartler.** 1996. Role of late replication timing in the silencing of X-linked genes. *Hum Mol Genet* **5**:1345-53.
69. **Hata, K., and Y. Sakaki.** 1997. Identification of critical CpG sites for repression of L1 transcription by DNA methylation. *Gene* **189**:227-34.
70. **Heard, E., P. Clerc, and P. Avner.** 1997. X-chromosome inactivation in mammals. *Annu Rev Genet* **31**:571-610.
71. **Heard, E., F. Mongelard, D. Arnaud, and P. Avner.** 1999. Xist yeast artificial chromosome transgenes function as X-inactivation centers only in multicopy arrays and not as single copies. *Mol Cell Biol* **19**:3156-66.
72. **Hejnar, J., J. Plachy, J. Geryk, O. Machon, K. Trejbalova, R. V. Guntaka, and J. Svoboda.** 1999. Inhibition of the rous sarcoma virus long terminal repeat-driven transcription by in vitro methylation: different sensitivity in permissive chicken cells versus mammalian cells. *Virology* **255**:171-81.

73. **Hoeben, R. C., A. A. Migchielsen, R. C. van der Jagt, H. van Ormondt, and A. J. van der Eb.** 1991. Inactivation of the Moloney murine leukemia virus long terminal repeat in murine fibroblast cell lines is associated with methylation and dependent on its chromosomal position. *J Virol* **65**:904-12.
74. **Holliday, R., and T. Ho.** 1991. Gene silencing in mammalian cells by uptake of 5-methyl deoxycytidine-5'-triphosphate. *Somat Cell Mol Genet* **17**:537-42.
75. **Hornstra, I. K., and T. P. Yang.** 1994. High-resolution methylation analysis of the human hypoxanthine phosphoribosyltransferase gene 5' region on the active and inactive X chromosomes: correlation with binding sites for transcription factors. *Mol Cell Biol* **14**:1419-30.
76. **Hornstra, I. K., and T. P. Yang.** 1993. In vivo footprinting and genomic sequencing by ligation-mediated PCR. *Anal Biochem* **213**:179-93.
77. **Hornstra, I. K., and T. P. Yang.** 1992. Multiple in vivo footprints are specific to the active allele of the X-linked human hypoxanthine phosphoribosyltransferase gene 5' region: implications for X chromosome inactivation. *Mol Cell Biol* **12**:5345-54.
78. **Hsieh, C. L.** 1994. Dependence of transcriptional repression on CpG methylation density. *Mol Cell Biol* **14**:5487-94.
79. **Imbalzano, A. N., H. Kwon, M. R. Green, and R. E. Kingston.** 1994. Facilitated binding of TATA-binding protein to nucleosomal DNA. *Nature* **370**:481-5.
80. **Jablonka, E., R. Goitein, M. Marcus, and H. Cedar.** 1985. DNA hypomethylation causes an increase in DNase-I sensitivity and an advance in the time of replication of the entire inactive X chromosome. *Chromosoma* **93**:152-6.
81. **Jaenisch, R.** 1983. Retroviruses and mouse embryos: a model system in which to study gene expression in development and differentiation. *Ciba Found Symp* **98**:44-62.
82. **Jeppesen, P., and B. M. Turner.** 1993. The inactive X chromosome in female mammals is distinguished by a lack of histone H4 acetylation, a cytogenetic marker for gene expression. *Cell* **74**:281-9.
83. **Jin, S., and K. W. Scotto.** 1998. Transcriptional regulation of the MDR1 gene by histone acetyltransferase and deacetylase is mediated by NF-Y. *Mol Cell Biol* **18**:4377-84.

84. **Johnston, C. M., T. B. Nesterova, E. J. Formstone, A. E. Newall, S. M. Duthie, S. A. Sheardown, and N. Brockdorff.** 1998. Developmentally regulated Xist promoter switch mediates initiation of X inactivation. *Cell* **94**:809-17.
85. **Jones, P. A., W. M. d. Rideout, J. C. Shen, C. H. Spruck, and Y. C. Tsai.** 1992. Methylation, mutation and cancer. *Bioessays* **14**:33-6.
86. **Jones, P. L., G. J. Veenstra, P. A. Wade, D. Vermaak, S. U. Kass, N. Landsberger, J. Strouboulis, and A. P. Wolffe.** 1998. Methylated DNA and MeCP2 recruit histone deacetylase to repress transcription. *Nat Genet* **19**:187-91.
87. **Kadonaga, J. T.** 1998. Eukaryotic transcription: an interlaced network of transcription factors and chromatin-modifying machines. *Cell* **92**:307-13.
88. **Kaslow, D. C., and B. R. Migeon.** 1987. DNA methylation stabilizes X chromosome inactivation in eutherians but not in marsupials: evidence for multistep maintenance of mammalian X dosage compensation. *Proc Natl Acad Sci U S A* **84**:6210-4.
89. **Kass, S. U., D. Pruss, and A. P. Wolffe.** 1997. How does DNA methylation repress transcription? *Trends Genet* **13**:444-9.
90. **Keohane, A. M., O. n. LP, N. D. Belyaev, J. S. Lavender, and B. M. Turner.** 1996. X-Inactivation and histone H4 acetylation in embryonic stem cells. *Dev Biol* **180**:618-30.
91. **Keshet, I., J. Lieman Hurwitz, and H. Cedar.** 1986. DNA methylation affects the formation of active chromatin. *Cell* **44**:535-43.
92. **Keshet, I., J. Yisraeli, and H. Cedar.** 1985. Effect of regional DNA methylation on gene expression. *Proc Natl Acad Sci U S A* **82**:2560-4.
93. **Kim, S. H., J. C. Moores, D. David, J. G. Respass, D. J. Jolly, and T. Friedmann.** 1986. The organization of the human HPRT gene. *Nucleic Acids Res* **14**:3103-18.
94. **Klages, S., B. Mollers, and R. Renkawitz.** 1992. The involvement of demethylation in the myeloid-specific function of the mouse M lysozyme gene downstream enhancer. *Nucleic Acids Res* **20**:1925-32.
95. **Knoepfler, P. S., and R. N. Eisenman.** 1999. Sin meets NuRD and other tails of repression. *Cell* **99**:447-50.
96. **Kochanek, S., D. Renz, and W. Doerfler.** 1995. Transcriptional silencing of human Alu sequences and inhibition of protein binding in the box B regulatory elements by 5'-CG-3' methylation. *FEBS Lett* **360**:115-20.

97. **Kontaraki, J., H. Chen, A. D. Riggs, and C. Bonifer.** 2000. Chromatin fine structure profiles for a developmentally regulated gene: reorganization of the lysozyme locus before trans-activator binding and gene expression. *Genes and Development* **14**:2106-2122.
98. **Kornberg, R. D., and Y. Lorch.** 1999. Twenty-five years of the nucleosome, fundamental particle of the eukaryote chromosome. *Cell* **98**:285-94.
99. **Kornberg, R. D., and L. Stryer.** 1988. Statistical distributions of nucleosomes: nonrandom locations by a stochastic mechanism. *Nucleic Acids Res* **16**:6677-90.
100. **Krebs, J. E., and C. L. Peterson.** 2000. Understanding "active" chromatin: a historical perspective of chromatin remodeling. *Crit Rev Eukaryot Gene Expr* **10**:1-12.
101. **Lee, H., and T. K. Archer.** 1994. Nucleosome-Mediated Disruption of Transcription Factor-Chromatin Initiation Complexes at the Mouse Mammary Tumor Virus Long Terminal Repeat In Vivo. *Mol Cell Biol* **14**:32-41.
102. **Lee, J. T., L. S. Davidow, and D. Warshawsky.** 1999. Tsix, a gene antisense to Xist at the X-inactivation centre. *Nat Genet* **21**:400-4.
103. **Lee, J. T., and R. Jaenisch.** 1997. Long-range cis effects of ectopic X-inactivation centres on a mouse autosome. *Nature* **386**:275-9.
104. **Lee, J. T., and N. Lu.** 1999. Targeted mutagenesis of Tsix leads to nonrandom X inactivation. *Cell* **99**:47-57.
105. **Lee, J. T., N. Lu, and Y. Han.** 1999. Genetic analysis of the mouse X inactivation center defines an 80-kb multifunction domain. *Proc Natl Acad Sci U S A* **96**:3836-41.
106. **Lee, J. T., W. M. Strauss, J. A. Dausman, and R. Jaenisch.** 1996. A 450 kb transgene displays properties of the mammalian X-inactivation center. *Cell* **86**:83-94.
107. **Lesch, M., and W. L. Nyhan.** 1964. A familial disorder of uric acid metabolism and central nervous system function. *Am. J. Med.* **36**:561-570.
108. **Levine, A., G. L. Cantoni, and A. Razin.** 1992. Methylation in the preinitiation domain suppresses gene transcription by an indirect mechanism. *Proc Natl Acad Sci U S A* **89**:10119-23.
109. **Lewis, J., and A. Bird.** 1991. DNA methylation and chromatin structure. *FEBS Lett* **285**:155-9.

110. **Li, B., C. C. Adams, and J. L. Workman.** 1994. Nucleosome binding by the constitutive transcription factor Sp1. *J Biol Chem* **269**:7756-63.
111. **Li, E., C. Beard, and R. Jaenisch.** 1993. Role for DNA methylation in genomic imprinting. *Nature* **366**:362-5.
112. **Li, E., T. H. Bestor, and R. Jaenisch.** 1992. Targeted mutation of the DNA methyltransferase gene results in embryonic lethality. *Cell* **69**:915-26.
113. **Li, G., S. P. Chandler, A. P. Wolffe, and T. Hall.** 1998. Architectural specificity in chromatin structure at the TATA box *in vivo*: Nucleosome displacement upon β -phaseolin gene activation. *Proc. Natl. Acad. Sci. USA* **95**:4772-4777.
114. **Li, Q., and O. Wrangé.** 1995. Accessibility of a glucocorticoid response element in a nucleosome depends on its rotational positioning. *Mol Cell Biol* **15**:4375-84.
115. **Li, Q., and O. Wrangé.** 1993. Translational positioning of a nucleosomal glucocorticoid response element modulates glucocorticoid receptor affinity. *Genes Dev* **7**:2471-82.
116. **Li, Q., O. Wrangé, and P. Eriksson.** 1997. The role of chromatin in transcriptional regulation. *Int J Biochem Cell Biol* **29**:731-42.
117. **Lin, D., and A. C. Chinault.** 1988. Comparative study of DNase I sensitivity at the X-linked human HPRT locus. *Somat Cell Mol Genet* **14**:261-72.
118. **Lingenfelter, P. A., D. A. Adler, D. Poslinski, S. Thomas, R. W. Elliott, V. M. Chapman, and C. M. Disteche.** 1998. Escape from X inactivation of *Smcx* is preceded by silencing during mouse development. *Nat Genet* **18**:212-3.
119. **Litt, M. D., R. S. Hansen, I. K. Hornstra, S. M. Gartler, and T. P. Yang.** 1997. 5-Azadeoxycytidine-induced chromatin remodeling of the inactive X-linked HPRT gene promoter occurs prior to transcription factor binding and gene reactivation. *J Biol Chem* **272**:14921-6.
120. **Litt, M. D., I. K. Hornstra, and T. P. Yang.** 1996. *In vivo* footprinting and high-resolution methylation analysis of the mouse hypoxanthine phosphoribosyltransferase gene 5' region on the active and inactive X chromosomes. *Mol Cell Biol* **16**:6190-9.
121. **Lock, L. F., N. Takagi, and G. R. Martin.** 1987. Methylation of the *Hprt* gene on the inactive X occurs after chromosome inactivation. *Cell* **48**:39-46.
122. **Loebel, D. A. F., and P. G. Johnston.** 1996. Methylation analysis of a marsupial X-linked CpG island by bisulfite genomic sequencing. *Genome Res* **6**:114-23.

123. **Lorch, Y., J. W. LaPointe, and R. D. Kornberg.** 1987. Nucleosomes inhibit the initiation of transcription but allow chain elongation with the displacement of histones. *Cell* **49**:203-10.
124. **Lu, Q., L. L. Wallrath, and S. C. Elgin.** 1995. The role of a positioned nucleosome at the *Drosophila melanogaster* hsp26 promoter. *Embo J* **14**:4738-46.
125. **Luo, S., J. C. Robinson, A. L. Reiss, and B. R. Migeon.** 1993. DNA methylation of the fragile X locus in somatic and germ cells during fetal development: relevance to the fragile X syndrome and X inactivation. *Somat Cell Mol Genet* **19**:393-404.
126. **Lyon, m.** 1961. Gene action in the X chromosome of the mouse (*Mus musculus L.*). *Nature* **190**:372.
127. **Lyon, M. F.** 1998. X-chromosome inactivation: a repeat hypothesis. *Cytogenet Cell Genet* **80**:133-7.
128. **Marahrens, Y., J. Loring, and R. Jaenisch.** 1998. Role of the Xist gene in X chromosome choosing. *Cell* **92**:657-64.
129. **Marahrens, Y., B. Panning, J. Dausman, W. Strauss, and R. Jaenisch.** 1997. Xist-deficient mice are defective in dosage compensation but not spermatogenesis. *Genes Dev* **11**:156-66.
130. **Maxam, A. M., and W. Gilbert.** 1980. Sequencing end-labeled DNA with base-specific chemical cleavages. *Methods Enzymol* **65**:499-560.
131. **McKay, L. M., J. M. Wrigley, and J. A. Graves.** 1987. Evolution of mammalian X-chromosome inactivation: sex chromatin in monotremes and marsupials. *Aust J Biol Sci* **40**:397-404.
132. **McPherson, C. E., E. Y. Shim, D. S. Friedman, and K. S. Zaret.** 1993. An active tissue-specific enhancer and bound transcription factors existing in a precisely positioned nucleosomal array. *Cell* **75**:387-98.
133. **Mermoud, J. E., C. Costanzi, J. R. Pehrson, and N. Brockdorff.** 1999. Histone macroH2A1.2 relocates to the inactive X chromosome after initiation and propagation of X-inactivation. *J Cell Biol* **147**:1399-408.
134. **Michelotti, E. F., S. Sanford, and D. Levens.** 1997. Marking of active genes on mitotic chromosomes. *Nature* **388**:895-9.
135. **Migeon, B. R.** 1994. X-chromosome inactivation: molecular mechanisms and genetic consequences. *Trends Genet* **10**:230-5.

136. **Migeon, B. R., S. Luo, M. Jani, and P. Jeppesen.** 1994. The severe phenotype of females with tiny ring X chromosomes is associated with inability of these chromosomes to undergo X inactivation. *Am J Hum Genet* **55**:497-504.
137. **Migeon, B. R., M. Schmidt, J. Axelman, and C. R. Cullen.** 1986. Complete reactivation of X chromosomes from human chorionic villi with a switch to early DNA replication. *Proc Natl Acad Sci U S A* **83**:2182-6.
138. **Migeon, B. R., S. F. Wolf, J. Axelman, D. C. Kaslow, and M. Schmidt.** 1985. Incomplete X chromosome dosage compensation in chorionic villi of human placenta. *Proc Natl Acad Sci U S A* **82**:3390-4.
139. **Miller, A. P., K. Gustashaw, D. J. Wolff, S. H. Rider, A. P. Monaco, B. Eble, D. Schlessinger, J. L. Gorski, G. J. van Ommen, J. Weissenbach, and et al.** 1995. Three genes that escape X chromosome inactivation are clustered within a 6 Mb YAC contig and STS map in Xp11.21-p11.22. *Hum Mol Genet* **4**:731-9.
140. **Miller, A. P., and H. F. Willard.** 1998. Chromosomal basis of X chromosome inactivation: identification of a multigene domain in Xp11.21-p11.22 that escapes X inactivation. *Proc Natl Acad Sci U S A* **95**:8709-14.
141. **Miyashita, T., H. Yamamoto, Y. Nishimune, M. Nozaki, T. Morita, and A. Matsushiro.** 1994. Activation of the mouse cytokeratin A (endo A) gene in teratocarcinoma F9 cells by the histone deacetylase inhibitor Trichostatin A. *FEBS Lett* **353**:225-9.
142. **Mohandas, T., R. S. Sparkes, and L. J. Shapiro.** 1981. Reactivation of an inactive human X chromosome: evidence for X inactivation by DNA methylation. *Science* **211**:393-6.
143. **Nan, X., H. H. Ng, C. A. Johnson, C. D. Laherty, B. M. Turner, R. N. Eisenman, and A. Bird.** 1998. Transcriptional repression by the methyl-CpG-binding protein MeCP2 involves a histone deacetylase complex. *Nature* **393**:386-9.
144. **Ng, H. H., and A. Bird.** 1999. DNA methylation and chromatin modification. *Curr Opin Genet Dev* **9**:158-63.
145. **Ng, H. H., P. Jeppesen, and A. Bird.** 2000. Active repression of methylated genes by the chromosomal protein MBD1. *Mol Cell Biol* **20**:1394-406.
146. **Ng, H. H., Y. Zhang, B. Hendrich, C. A. Johnson, B. M. Turner, H. Erdjument-Bromage, P. Tempst, D. Reinberg, and A. Bird.** 1999. MBD2 is a transcriptional repressor belonging to the MeCP1 histone deacetylase complex. *Nat Genet* **23**:58-61.

147. **Noll, M.** 1974. Internal structure of the chromatin subunit. *Nucleic Acids Res* **1**:1573-8.
148. **Nyce, J.** 1991. Gene silencing in mammalian cells by direct incorporation of electroporated 5-methyl-2'-deoxycytidine 5'-triphosphate. *Somat Cell Mol Genet* **17**:543-50.
149. **Okano, M., S. Xie, and E. Li.** 1998. Cloning and characterization of a family of novel mammalian DNA (cytosine-5) methyltransferases. *Nat Genet* **19**:219-20.
150. **Park, J. G., and V. M. Chapman.** 1994. CpG island promoter region methylation patterns of the inactive-X-chromosome hypoxanthine phosphoribosyltransferase (Hprt) gene. *Mol Cell Biol* **14**:7975-83.
151. **Patel, P. I., P. E. Framson, C. T. Caskey, and A. C. Chinault.** 1986. Fine structure of the human hypoxanthine phosphoribosyltransferase gene. *Mol Cell Biol* **6**:393-403.
152. **Patel, S. A., D. M. Graunke, and R. O. Pieper.** 1997. Aberrant silencing of the CpG island-containing human O6-methylguanine DNA methyltransferase gene is associated with the loss of nucleosome-like positioning. *Mol Cell Biol* **17**:5813-22.
153. **Pazin, M. J., P. Bhargava, E. P. Geiduschek, and J. T. Kadonaga.** 1997. Nucleosome mobility and the maintenance of nucleosome positioning. *Science* **276**:809-12.
154. **Pazin, M. J., J. W. Hermann, and J. T. Kadonaga.** 1998. Promoter structure and transcriptional activation with chromatin templates assembled in vitro. A single Gal4-VP16 dimer binds to chromatin or to DNA with comparable affinity. *J Biol Chem* **273**:34653-60.
155. **Pazin, M. J., R. T. Kamakaka, and J. T. Kadonaga.** 1994. ATP-dependent nucleosome reconfiguration and transcriptional activation from preassembled chromatin templates. *Science* **266**:2007-11.
156. **Pazin, M. J., P. L. Sheridan, K. Cannon, Z. Cao, J. G. Keck, J. T. Kadonaga, and K. A. Jones.** 1996. NF-kappa B-mediated chromatin reconfiguration and transcriptional activation of the HIV-1 enhancer in vitro. *Genes Dev* **10**:37-49.
157. **Penny, G. D., G. F. Kay, S. A. Sheardown, S. Rastan, and N. Brockdorff.** 1996. Requirement for Xist in X chromosome inactivation. *Nature* **379**:131-7.

158. **Pfeifer, G. P., and A. D. Riggs.** 1991. Chromatin differences between active and inactive X chromosomes revealed by genomic footprinting of permeabilized cells using DNase I and ligation-mediated PCR. *Genes Dev* **5**:1102-13.
159. **Pfeifer, G. P., S. D. Steigerwald, R. S. Hansen, S. M. Gartler, and A. D. Riggs.** 1990. Polymerase chain reaction-aided genomic sequencing of an X chromosome-linked CpG island: methylation patterns suggest clonal inheritance, CpG site autonomy, and an explanation of activity state stability. *Proc Natl Acad Sci U S A* **87**:8252-6.
160. **Pfeifer, G. P., R. L. Tanguay, S. D. Steigerwald, and A. D. Riggs.** 1990. In vivo footprint and methylation analysis by PCR-aided genomic sequencing: comparison of active and inactive X chromosomal DNA at the CpG island and promoter of human PGK-1. *Genes Dev* **4**:1277-87.
161. **Pina, B., D. Baretino, M. Truss, and M. Beato.** 1990. Structural features of a regulatory nucleosome. *J Mol Biol* **216**:975-90.
162. **Pina, B., U. Bruggemeier, and M. Beato.** 1990. Nucleosome positioning modulates accessibility of regulatory proteins to the mouse mammary tumor virus promoter. *Cell* **60**:719-31.
163. **Plenge, R. M., B. D. Hendrich, C. Schwartz, J. F. Arena, A. Naumova, C. Sapienza, R. M. Winter, and H. F. Willard.** 1997. A promoter mutation in the XIST gene in two unrelated families with skewed X-chromosome inactivation. *Nat Genet* **17**:353-6.
164. **Prestridge, D. S., and C. Burks.** 1993. The density of transcriptional elements in promoter and non-promoter sequences. *Hum Mol Genet* **2**:1449-53.
165. **Rhodes, K., R. A. Rippe, A. Umezawa, M. Nehls, D. A. Brenner, and M. Breindl.** 1994. DNA methylation represses the murine alpha 1(I) collagen promoter by an indirect mechanism. *Mol Cell Biol* **14**:5950-60.
166. **Riggs, A. D., and G. P. Pfeifer.** 1992. X-chromosome inactivation and cell memory. *Trends Genet* **8**:169-74.
167. **Riggs, A. D., Z. Xiong, L. Wang, and J. M. LeBon.** 1998. Methylation dynamics, epigenetic fidelity and X chromosome structure. *Novartis Found Symp* **214**:214-25.
168. **Rincon Limas, D. E., D. A. Krueger, and P. I. Patel.** 1991. Functional characterization of the human hypoxanthine phosphoribosyltransferase gene promoter: evidence for a negative regulatory element. *Mol Cell Biol* **11**:4157-64.

169. **Rothnie, H. M., K. J. McCurrach, L. A. Glover, and N. Hardman.** 1991. Retrotransposon-like nature of Tp1 elements: implications for the organisation of highly repetitive, hypermethylated DNA in the genome of *Physarum polycephalum*. *Nucleic Acids Res* **19**:279-86.
170. **Russell, L. B.** 1963. Mammalian X-chromosome action: inactivation limited in spread and in region of origin. *Science* **140**:975-978.
171. **Russell, L. B.** 1983. Part A: Basic mechanisms of X chromosome behavior., p. 205-250. *In* A. A. Sandberg (ed.), *Cytogenetics of the mammalian X chromosome*. Alan R. Liss, New York.
172. **Russell, L. B., and C. S. Montgomery.** 1970. Comparative studies on X-autosome translocations in the mouse. II. Inactivation of autosomal loci, segregation, and mapping of autosomal breakpoints in five T (X;1) S. *Genetics* **64**:281-312.
173. **Sambrook, J., E. F. Fritsch, and T. Maniatis.** 1989. *Molecular cloning : a laboratory manual*, 2nd / ed. Cold Spring Harbor Laboratory Press, Cold Spring Harbor.
174. **Sasaki, T., R. S. Hansen, and S. M. Gartler.** 1992. Hemimethylation and hypersensitivity are early events in transcriptional reactivation of human inactive X-linked genes in a hamster x human somatic cell hybrid. *Mol Cell Biol* **12**:3819-26.
175. **Schild, C., F. X. Claret, W. Wahli, and A. P. Wolffe.** 1993. A nucleosome-dependent static loop potentiates estrogen-regulated transcription from the *Xenopus vitellogenin B1* promoter in vitro. *Embo J* **12**:423-33.
176. **Schwemmler, S., K. Mehnert, and W. Vogel.** 1989. How does inactivation change timing of replication in the human X chromosome? *Hum Genet* **83**:26-32.
177. **Selker, E. U.** 1990. Premeiotic instability of repeated sequences in *Neurospora crassa*. *Annu Rev Genet* **24**:579-613.
178. **Selker, E. U., and P. W. Garrett.** 1988. DNA sequence duplications trigger gene inactivation in *Neurospora crassa*. *Proc Natl Acad Sci U S A* **85**:6870-4.
179. **Sewack, G. F., and U. Hansen.** 1997. Nucleosome positioning and transcription-associated chromatin alterations on the human estrogen-responsive pS2 promoter. *J Biol Chem* **272**:31118-29.

180. **Sheardown, S. A., S. M. Duthie, C. M. Johnston, A. E. Newall, E. J. Formstone, R. M. Arkell, T. B. Nesterova, G. C. Alghisi, S. Rastan, and N. Brockdorff.** 1997. Stabilization of Xist RNA mediates initiation of X chromosome inactivation. *Cell* **91**:99-107.
181. **Shemer, R., Y. Birger, A. D. Riggs, and A. Razin.** 1997. Structure of the imprinted mouse Snrpn gene and establishment of its parental-specific methylation pattern. *Proc Natl Acad Sci U S A* **94**:10267-72.
182. **Shim, E. Y., C. Woodcock, and K. S. Zaret.** 1998. Nucleosome positioning by the winged helix transcription factor HNF3. *Genes Dev* **12**:5-10.
183. **Singer-Sam, J., L. Goldstein, A. Dai, S. M. Gartler, and A. D. Riggs.** 1992. A potentially critical Hpa II site of the X chromosome-linked PGK1 gene is unmethylated prior to the onset of meiosis of human oogenic cells. *Proc Natl Acad Sci U S A* **89**:1413-7.
184. **Solage, A., and H. Cedar.** 1978. Organization of 5-methylcytosine in chromosomal DNA. *Biochemistry* **17**:2934-8.
185. **Stein, R., A. Razin, and H. Cedar.** 1982. In vitro methylation of the hamster adenine phosphoribosyltransferase gene inhibits its expression in mouse L cells. *Proc Natl Acad Sci U S A* **79**:3418-22.
186. **Szabo, P. E., and J. R. Mann.** 1995. Biallelic expression of imprinted genes in the mouse germ line: implications for erasure, establishment, and mechanisms of genomic imprinting. *Genes Dev* **9**:1857-68.
187. **Takagi, N., O. Sugawara, and M. Sasaki.** 1982. Regional and temporal changes in the pattern of X-chromosome replication during the early post-implantation development of the female mouse. *Chromosoma* **85**:275-86.
188. **Tan, S. S., E. A. Williams, and P. P. Tam.** 1993. X-chromosome inactivation occurs at different times in different tissues of the post-implantation mouse embryo. *Nat Genet* **3**:170-4.
189. **Tate, P. H., and A. P. Bird.** 1993. Effects of DNA methylation on DNA-binding proteins and gene expression. *Curr Opin Genet Dev* **3**:226-31.
190. **Taylor, I. C., J. L. Workman, T. J. Schuetz, and R. E. Kingston.** 1991. Facilitated binding of GAL4 and heat shock factor to nucleosomal templates: differential function of DNA-binding domains. *Genes Dev* **5**:1285-98.
191. **Taylor, J. H.** 1960. Asynchronous duplication of chromosomes in cultured cells of chinese hamster. *J. Biophysic. and Biochem.* **7**:455-463.

192. **Tommasi, S., J. M. LeBon, A. D. Riggs, and J. Singer Sam.** 1993. Methylation analysis by genomic sequencing of 5' region of mouse P_{gk}-1 gene and a cautionary note concerning the method. *Somat Cell Mol Genet* **19**:529-41.
193. **Toniolo, D., M. Filippi, R. Dono, T. Lettieri, and G. Martini.** 1991. The CpG island in the 5' region of the G6PD gene of man and mouse. *Gene* **102**:197-203.
194. **Toniolo, D., G. Martini, B. R. Migeon, and R. Dono.** 1988. Expression of the G6PD locus on the human X chromosome is associated with demethylation of three CpG islands within 100 kb of DNA. *Embo J* **7**:401-6.
195. **Tormanen, V. T., P. M. Swiderski, B. E. Kaplan, G. P. Pfeifer, and A. D. Riggs.** 1992. Extension product capture improves genomic sequencing and DNase I footprinting by ligation-mediated PCR. *Nucleic Acids Res* **20**:5487-8.
196. **Travers, A., and H. Drew.** 1997. DNA recognition and nucleosome organization. *Biopolymers* **44**:423-33.
197. **Truss, M., J. Bartsch, A. Schelbert, R. J. Hache, and M. Beato.** 1995. Hormone induces binding of receptors and transcription factors to a rearranged nucleosome on the MMTV promoter in vivo. *Embo J* **14**:1737-51.
198. **Truss, M., R. Candau, S. Chavez, and M. Beato.** 1995. Transcriptional control by steroid hormones: the role of chromatin. *Ciba Found Symp* **191**:7-17.
199. **Vardimon, L., A. Kressmann, H. Cedar, M. Maechler, and W. Doerfler.** 1982. Expression of a cloned adenovirus gene is inhibited by in vitro methylation. *Proc Natl Acad Sci U S A* **79**:1073-7.
200. **Venter, U., J. Svaren, J. Schmitz, A. Schmid, and W. Horz.** 1994. A nucleosome precludes binding of the transcription factor Pho4 in vivo to a critical target site in the PHO5 promoter. *Embo J* **13**:4848-55.
201. **Vettese-Dadey, M., P. Walter, H. Chen, L. J. Juan, and J. L. Workman.** 1994. Role of the histone amino termini in facilitated binding of a transcription factor, GAL4-AH, to nucleosome cores. *Mol Cell Biol* **14**:970-81.
202. **Walsh, C. P., and T. H. Bestor.** 1999. Cytosine methylation and mammalian development. *Genes Dev* **13**:26-34.
203. **Walsh, C. P., J. R. Chaillet, and T. H. Bestor.** 1998. Transcription of IAP endogenous retroviruses is constrained by cytosine methylation. *Nat Genet* **20**:116-7.

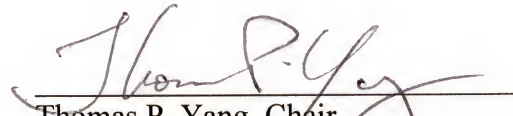
204. **Warshawsky, D., N. Stavropoulos, and J. T. Lee.** 1999. Further examination of the Xist promoter-switch hypothesis in X inactivation: evidence against the existence and function of a P(0) promoter. *Proc Natl Acad Sci U S A* **96**:14424-9.
205. **Weiss, A., I. Keshet, A. Razin, and H. Cedar.** 1996. DNA demethylation in vitro: involvement of RNA. *Cell* **86**:709-18.
206. **White, W. M., H. F. Willard, D. L. Van Dyke, and D. J. Wolff.** 1998. The spreading of X inactivation into autosomal material of an x;autosome translocation: evidence for a difference between autosomal and X-chromosomal DNA. *Am J Hum Genet* **63**:20-8.
207. **Widlak, P., R. B. Gaynor, and W. T. Garrard.** 1997. In vitro chromatin assembly of the HIV-1 promoter. ATP-dependent polar repositioning of nucleosomes by Sp1 and NFkappaB. *J Biol Chem* **272**:17654-61.
208. **Wolf, S. F., S. Dintzis, D. Toniolo, G. Persico, K. D. Lunnen, J. Axelman, and B. R. Migeon.** 1984. Complete concordance between glucose-6-phosphate dehydrogenase activity and hypomethylation of 3' CpG clusters: implications for X chromosome dosage compensation. *Nucleic Acids Res* **12**:9333-48.
209. **Wolff, D. J., C. J. Brown, S. Schwartz, A. M. Duncan, U. Surti, and H. F. Willard.** 1994. Small marker X chromosomes lack the X inactivation center: implications for karyotype/phenotype correlations. *Am J Hum Genet* **55**:87-95.
210. **Wong, J., Q. Li, B. Z. Levi, Y. B. Shi, and A. P. Wolffe.** 1997. Structural and functional features of a specific nucleosome containing a recognition element for the thyroid hormone receptor. *Embo J* **16**:7130-45.
211. **Workman, J. L., and K. R. E.** 1998. Alteration of Nucleosome Structure as a Mechanism of Transcriptional Regulation. *Ann Rev Biochem* **67**:545-79.
212. **Wutz, A., and R. Jaenisch.** 2000. A Shift, from Reversible to Irreversible X inactivation is Triggered during ES Cell Differentiation. *Molecular Cell* **5**:695-705.
213. **Yang, T. P., and C. T. Caskey.** 1987. Nuclease sensitivity of the mouse HPRT gene promoter region: differential sensitivity on the active and inactive X chromosomes. *Mol Cell Biol* **7**:2994-8.
214. **Yaniv, M., and S. Cereghini.** 1986. Structure of transcriptionally active chromatin. *CRC Crit Rev Biochem* **21**:1-26.
215. **Yisraeli, J., D. Frank, A. Razin, and H. Cedar.** 1988. Effect of in vitro DNA methylation on beta-globin gene expression. *Proc Natl Acad Sci U S A* **85**:4638-42.

216. **Yoder, J. A., C. P. Walsh, and T. H. Bestor.** 1997. Cytosine methylation and the ecology of intragenomic parasites. *Trends Genet* **13**:335-40.


BIOGRAPHICAL SKETCH

Chien Chen was born in Keelung, Taiwan, R.O.C., on December 26, 1969, one of three children including an older sister and a twin brother. In 1973, his family immigrated to the United States where they settled in Tampa, FL. He attended Harvard University from which he graduated magna cum laude in 1991. Subsequently he entered the MD/PhD program at the University of Florida, College of Medicine, in 1992. He began his PhD studies in the Department of Biochemistry and Molecular Biology at the University of Florida, College of Medicine, in 1994 and will graduate in December of 2000. He will return to the University of Florida, School of Medicine, to complete the MD portion of the MD/ PhD program.

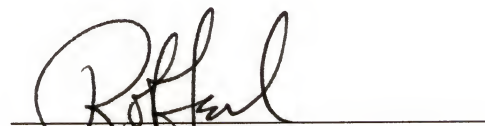
I certify that I have read this study and that in my opinion it conforms to acceptable standards of scholarly presentation and is fully adequate, in scope and quality, as a dissertation for the degree of Doctor of Philosophy.


Thomas P. Yang, Chair
Professor of Biochemistry and
Molecular Biology

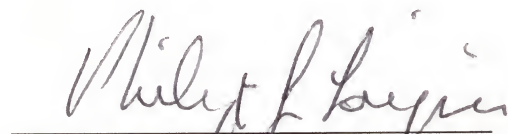
I certify that I have read this study and that in my opinion it conforms to acceptable standards of scholarly presentation and is fully adequate, in scope and quality, as a dissertation for the degree of Doctor of Philosophy.


Henry V. Baker
Associate Professor of Molecular
Genetics and Microbiology

I certify that I have read this study and that in my opinion it conforms to acceptable standards of scholarly presentation and is fully adequate, in scope and quality, as a dissertation for the degree of Doctor of Philosophy.


Robert J. Fern
Professor of Horticultural Science

I certify that I have read this study and that in my opinion it conforms to acceptable standards of scholarly presentation and is fully adequate, in scope and quality, as a dissertation for the degree of Doctor of Philosophy.


Philip J. Laipis
Professor of Biochemistry and
Molecular Biology

I certify that I have read this study and that in my opinion it conforms to acceptable standards of scholarly presentation and is fully adequate, in scope and quality, as a dissertation for the degree of Doctor of Philosophy.



Michael S. Kilberg
Professor of Biochemistry and
Molecular Biology

This dissertation was submitted to the Graduate Faculty of the College of Medicine and to the Graduate School and was accepted as partial fulfillment of the requirements for the degree of Doctor of Philosophy.

December 2000



Dean, College of Medicine



Dean, Graduate School